UMTRI-2005-3

Work Zone Safety ITS

Smart Barrel for an Adaptive Queue-Warning System

John M. Sullivan
Christopher B. Winkler
Michael R. Hagan

February 2005

UMTRI-2005-3

Work Zone Safety ITS

Smart Barrel for an Adaptive Queue-Warning System

John M. Sullivan
Christopher B. Winkler
Michael R. Hagan

The University of Michigan
Transportation Research Institute
Ann Arbor, MI 48109-2150
U.S.A.

February 2005

Technical Report Documentation Page

1. Report No.	2. Government Accession No.	3. Recipient's Catalog No.
UMTRI-2005-3		

4. Title and Subtitle	5. Report Date
Work Zone Safety ITS Smart-Barrel for an Adaptive Queue-Warning System	February 2005
	6. Performing Organization Code
7. Author(s)	8. Performing Organization Report No.
Sullivan, J.M.; Winkler, C.B.; Hagan, M.R.	UMTRI-2005-3
9. Performing Organization Name and Address	10. Work Unit no. (TRAIS)
The University of Michigan Transportation Research Institute 2901 Baxter Road Ann Arbor, Michigan 48109-2150 U.S.A.	
	11. Contract or Grant No.
12. Sponsoring Agency Name and Address	13. Type of Report and Period Covered
Federal Highway Administration U.S. Department of Transportation 400 7th Street S.W. Washington, D.C. 20590	Final Technical Report
	14. Sponsoring Agency Code FHWA

15. Supplementary Notes

16. Abstract

A broad concept has been developed for a Work-Zone Safety ITS System that would provide a distributed, queue-warning system that automatically adapts to the current traffic-flow situation in and upstream of the work zone. The core element of the system is be a *smart barrel*—an ordinary appearing traffic-control barrel containing an inexpensive speed sensor and equipped with a simple, adjustable signaling system and the necessary equipment for communication to a central controller. The study focused on initial investigations of two critical elements of such a system: (1) an inexpensive, but sufficiently capable speed sensor and (2) a simple but effective signaling system.

Three prototype speed sensors were developed and evaluated in a limited field study. They used active infrared, passive infrared, and magnetic sensor technologies, respectively. The active infrared system was found to be the most accurate but consumed the most power: an important factor for a device that will be battery-power in the field. The passive infrared system was nearly as accurate and required the least power of the three approaches.

Simple signaling schemes were also prototyped and presented to drivers in a pilot experiment using a driving simulator. Both subjective opinions about the utility of the system and objective measures of driving performance were collected. Results suggest that drivers find the adaptive systems more helpful than static road signs and there is evidence for systematic change in their driving performance indicative of enhanced safety.

17. Key Words	18. Distribution Statement
speed sensors, work zone, queue warning, speed differential, safety	Unlimited

19. Security Classification (of this report)	20. Security Classification (of this page)	21. No. of Pages	22. Price
None	None	118	

SI* (MODERN METRIC) CONVERSION FACTORS

APPROXIMATE CONVERSIONS TO SI UNITS

Symbol	When You Know	Multiply By	To Find	Symbol
		LENGTH		
in	inches	25.4	millimeters	mm
ft	feet	0.305	meters	m
yd	yards	0.914	meters	m
mi	miles	1.61	kilometers	km
		AREA		
in^2	square inches	645.2	square millimeters	mm^2
ft^2	square feet	0.093	square meters	m^2
yd^2	square yard	0.836	square meters	m^2
ac	acres	0.405	hectares	ha
mi^2	square miles	2.59	square kilometers	km^2
		VOLUME		
fl oz	fluid ounces	29.57	milliliters	mL
gal	gallons	3.785	liters	L
ft^3	cubic feet	0.028	cubic meters	m^3
yd^3	cubic yards	0.765	cubic meters	m^3
	NOTE: volumes greater than 1000 L shall be shown in m^3			
		MASS		
oz	ounces	28.35	grams	g
lb	pounds	0.454	kilograms	kg
T	short tons (2000 lb)	0.907	megagrams (or "metric ton")	Mg (or "t")
		TEMPERATURE (exact degrees)		
^oF	Fahrenheit	5 (F-32)/9 or (F-32)/1.8	Celsius	^oC
		ILLUMINATION		
fc	foot-candles	10.76	lux	lx
fl	foot-Lamberts	3.426	$candela/m^2$	cd/m^2
		FORCE and PRESSURE or STRESS		
lbf	poundforce	4.45	newtons	N
lbf/in^2	poundforce per square inch	6.89	kilopascals	kPa

APPROXIMATE CONVERSIONS FROM SI UNITS

Symbol	When You Know	Multiply By	To Find	Symbol
		LENGTH		
mm	millimeters	0.039	inches	in
m	meters	3.28	feet	ft
m	meters	1.09	yards	yd
km	kilometers	0.621	miles	mi
		AREA		
mm^2	square millimeters	0.0016	square inches	in^2
m^2	square meters	10.764	square feet	ft^2
m^2	square meters	1.195	square yards	yd^2
ha	hectares	2.47	acres	ac
km^2	square kilometers	0.386	square miles	mi^2
		VOLUME		
mL	milliliters	0.034	fluid ounces	fl oz
L	liters	0.264	gallons	gal
m^3	cubic meters	35.314	cubic feet	ft^3
m^3	cubic meters	1.307	cubic yards	yd^3
		MASS		
g	grams	0.035	ounces	oz
kg	kilograms	2.202	pounds	lb
Mg (or "t")	megagrams (or "metric ton")	1.103	short tons (2000 lb)	T
		TEMPERATURE (exact degrees)		
^oC	Celsius	1.8C+32	Fahrenheit	^oF
		ILLUMINATION		
lx	lux	0.0929	foot-candles	fc
cd/m^2	$candela/m^2$	0.2919	foot-Lamberts	fl
		FORCE and PRESSURE or STRESS		
N	newtons	0.225	poundforce	lbf
kPa	kilopascals	0.145	poundforce per square inch	lbf/in^2

*SI is the symbol for the International System of Units. Appropriate rounding should be made to comply with Section 4 of ASTM E380.
(Revised March 2003)

Executive Summary

The first phase of a research study entitled "Work Zone Safety ITS" has been conducted by the Transportation Research Institute of the University of Michigan (UMTRI) for the Federal Highway Administration (FHWA) of the US Department of Transportation under contract DTH61-01-C-00049. The purpose of this research is to investigate potential countermeasures to reduce crash risk within work zones.

Accident data show that crash risk is higher in work zones than in other roadway areas. Estimates of this increase range from 26% to 168%, depending on the circumstances. Major factors contributing to work-zone crashes include speed differences between vehicles, irregular maneuvers, and excessive speed in challenging roadway conditions. For example, rear-end collisions make up about 40% of work zone crashes, but only 30% of all other crashes. Rear end collisions occur whenever a stopped or slow-moving lead vehicle is struck from behind by a faster moving following vehicle. In a work zone, this can happen when lane closures in areas of high traffic volume cause traffic to slow down and backup away from the merge point of a work zone. The resulting roving transition point, between slow-moving traffic around the work zone and upstream traffic moving at posted speeds, creates uncertain dynamic conditions which apparently take drivers by surprise. The objective of the Work Zone Safety ITS project is to develop technology to directly address these (and other) problems in order to reduce work-zone related crashes.

An Adaptive Queue-Warning System Using Smart barrels

The Work Zone Safety ITS project aims to develop an *adaptive* speed-advisory system for work zones based on a *distributed* system of traffic speed sensors and traffic signaling devices. Such a system would sense traffic speeds in, and upstream, of the work zone and adjust speed-advisory signals appropriately for changing conditions *along the length of the system* and *in real time*. The core element of the system would be a *smart barrel*—an ordinary appearing traffic control barrel containing an inexpensive traffic speed sensor and equipped with a simple, adjustable signaling system and the necessary equipment for communication to a central controller.

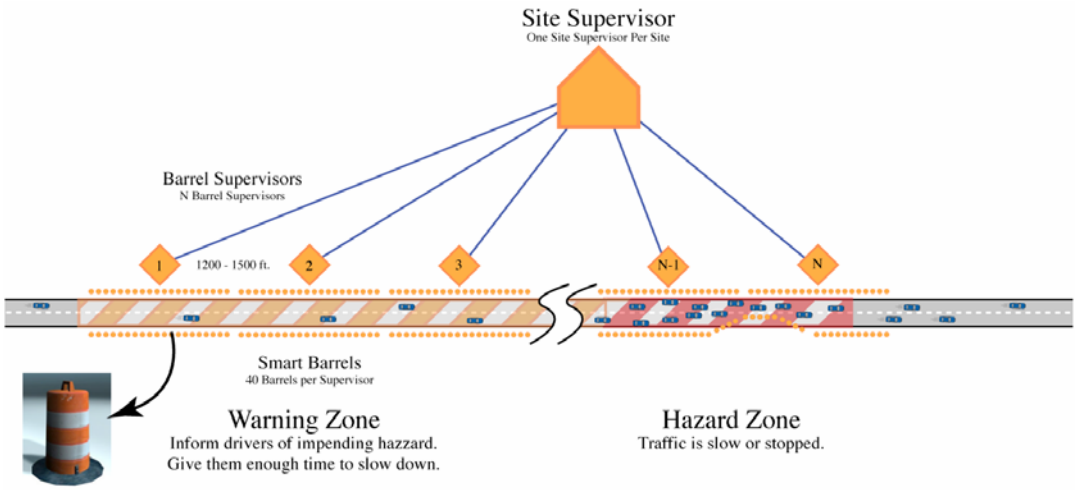

System concept for an adaptive Work Zone Safety ITS warning system using Smart Barrels

Whether or not a viable system of this concept can be produced depends on whether the two key components of the smart barrel can be developed. They are:

- a sufficiently capable traffic speed sensor, and
- a simple but effective signally system.

Both must be sufficiently inexpensive to allow the deployment of many smart barrels at a single work zone, and both must operate on sufficiently little electrical power to make battery-powered operation feasible.

This first phase of the Work Zone Safety ITS project concentrated on the initial development issues for these two elements.

Speed-sensor technologies

A preliminary list of seven sensor technologies that might be used in an inexpensive vehicle speed was narrowed down to three prime candidates:

- Passive infrared. All objects whose temperature is above absolute zero radiate infrared energy. *Pyroelectric* sensors react to this radiation and produce a signal related to the temperature of the object in their field of view. Passive infrared sensors require the least amount of power of the three technologies.
- Magnetometers. Magnetometers measure the earth's magnetic field at their own position. A passing object containing iron distorts this magnetic field, thereby indicating its presence to the magnetometer. The magnetometers make three separate measures along three sensitive axes: in the direction of travel (X), across the direction of travel (Y), and vertically (Z).

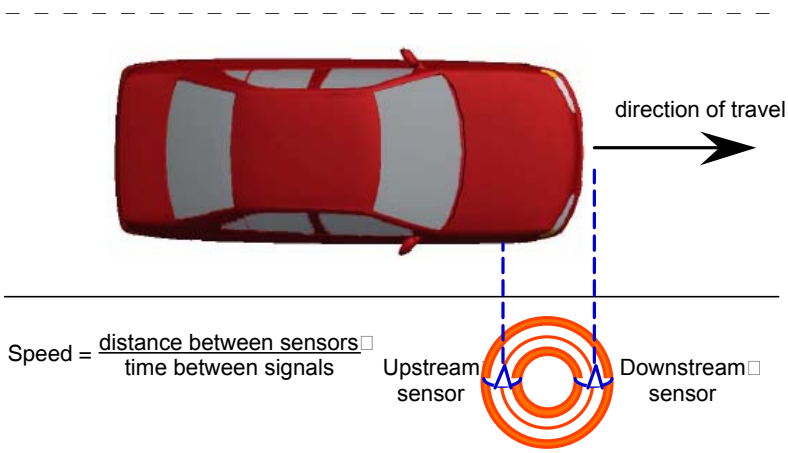

Vehicle speed is proportional to the time between signals from the two sensors in a smart barrel

- Active infrared. These *optical* sensors produce a focused beam of infrared light that, when reflected back is sensed by a photosensitive receiver, indicating the presence of an object. Active infrared sensors require the most amount of power of the three technologies.

In the application of each of these sensor technologies, the basic approach was to mount two identical sensors at diametrically opposed positions on a traffic-control barrel and deploy the barrel at a work zone with the sensors aimed across the travel lane of interest. Passing vehicles would produce a similar signal from each sensor, but with a time delay between them. The spacing between the sensors divided by this time delay would indicate vehicle speed.

Prototype speed sensors based on these three technologies were evaluated in a limited field test. Speeds measured by the experimental sensors were compared to speeds determined by a sophisticated radar system. Data were gathered from two sites on public roads, one urban and one rural. After making some adjustments, approximately nine hours of data including a total of 1627 vehicle passes were used for the comparative evaluation of the three sensors.

Of the three technologies examined in the field test, the active infrared, optical technology clearly performed the best in this limited test. The speed sensor based on this technology detected 97 % of the vehicles passing through the site and produced less than 4 % additional false detections. Two data processing methods developed for this sensor were about equally successful, one having a standard deviation of error in speed measurement of about 3.7 mph and the other, about 4.0 mph.

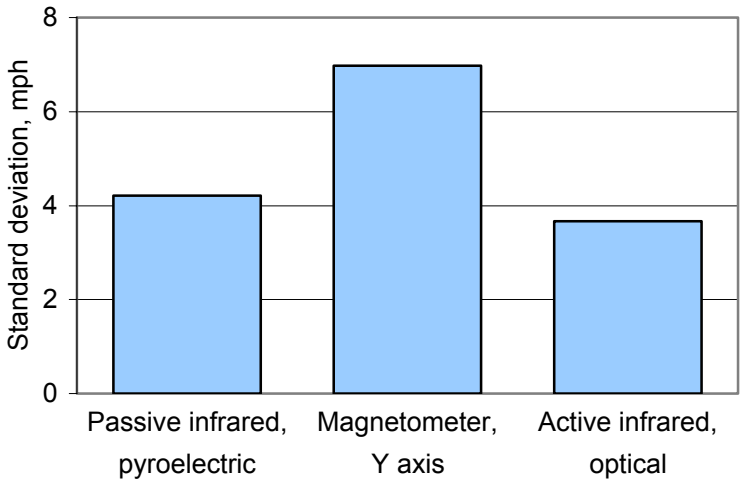

Standard deviations of the speed measurement errors of the three types of sensors. Low values are desirable.

The speed sensor based on the passive infrared, pyroelectric technology performed nearly as well but required a more computationally-expensive data processing method to do so. The standard deviation of the speed errors was about 4.2 mph with 96% of vehicles sensed. This method's biggest shortcoming was a false-positive rate approaching 20 %.

Sensing speed with the magnetometers was the least successful. The best data-processing method investigated had a standard deviation of the errors of about 7 mph, a missed-vehicle rate of about 17 % and a false-positive rate of about 21 %.

In hindsight, it seems probable that the relative performance of these three approaches to speed sensing derives largely from the frequency response qualities of the three systems. The faster responding systems naturally produce higher quality results. It appears likely that further development of the physical sensors and of the data-processing algorithms will improve the performance of the two infrared systems. The low power requirements of the passive infrared sensor make it appear most attractive. Further development and broader field testing of both infrared systems is recommended.

Speed-advisory signaling

Several versions of the speed-advisory system were prototyped independently of the speed sensor investigations using a vehicle simulator to quickly "breadboard" different schematic configurations of the system. In the simulation study, drivers passed a series of post-mounted warning lights placed on the right side of a straight section of roadway. Stopped traffic was located at an unpredictable forward location and was hidden from direct view by imposed sight limits. As drivers approached the

View of simulator-controlled roadway on which post-mounted warning lights advised drivers to decrease their speed when approaching stopped traffic.

stopped traffic ahead, the post-mounted warning lights flashed at different rates to indicate the magnitude of deceleration required to successfully avoid a collision with the forward traffic. In one version of the warning system, three blink rates were used to indicate the severity of stopping condition—0.5 Hz for the lowest severity, followed by 1 Hz, and 2 Hz for increasing severity. An alternate version of the system that used just one blink rate was also investigated. The two versions of the warning system were compared to a condition in which static signs were placed on the roadway, similar to current practice for work-zone sign placement.

The purpose of the human factors pilot study was to assess:

- drivers' subjective perception of the utility of the system, and
- the effect of such a system on objective driving performance.

The results of the study provide evidence that drivers find the adaptive systems more helpful than static road signs, and there is evidence for systematic change in their driving performance that is indicative of enhanced safety—drivers produced lower peak decelerations as they stopped before reaching the end of a line of stopped traffic.

Table Of Contents

Document Page i

SI Conversion Factors iii

Executive Summary v

Table Of Contents xi

List Of Figures xiii

List Of Tables xvi

Introduction 1

The Work-zone Crash Problem 3

Concept of the Work-zone Safety ITS System 7
- System Configuration 7
  - Smart Barrel 7
  - Barrel Supervisor 9
  - Site Supervisor 10
- Setup and Calibration 10
- Operation 11
  - Determining Signal Intensity Based On Distributed Speed Measurements 11
  - Data-Collection And Processing 12

Technological Feasibility 17
- Available Detection Technologies 17
  - Active Infrared 17
  - Passive Infrared 17
  - Passive Acoustic 18
  - Ultrasonic 18
  - Magnetic 19
  - Microwave 19
  - Video 19
- Initial Evaluation of Detection Technologies 20
  - Selected Sensors 22
  - Reference Speed System 29
- The Field Test 31
  - Methodology 31
  - Data Analysis 36
  - Results: Comparing Speeds Measured By The Three Sensors 51

Human Factors Requirements for a Speed-Differential Warning System 61
- Practical Considerations 61
- What Kind of Warning 62
- Format of Warning 63
- Credibility of Warning 64

Pilot Simulator Study of Queue-warning Countermeasure 67

Overview 67
Method 68
Simulator roadway environment 68
Post Mounted Warning System Operation 72
Subjects 72
Procedure 73
Dependent Measures 74
Results 75
Discussion 79
Conclusions and Recommendations 83
Speed-Senor Technologies 83
Human Factors Conclusions 87
References 89
Appendix A 91
Appendix B 93

List Of Figures

Figure 1. Total work-zone fatalities reported in FARS between 1984 and 2002 3

Figure 2. System concept 7

Figure 3. Configuration of a smart-barrel 8

Figure 4. Configuration of a barrel supervisor 9

Figure 5. Configuration of the site supervisor 10

Figure 6. Generalized flow diagram of speed-data collection and signal-intensity calculations 13

Figure 7. Nomenclature 15

Figure 8. Test fixture on Baxter Road 21

Figure 9. Vehicle speed measurement using paired proximity sensors 21

Figure 10. Pyroelectric detector and fresnel lens and assembled sensor 22

Figure 11. Differential Sensor Configuration 23

Figure 12. Pyroelectric Detectors on a barrel 23

Figure 13. Honeywell HMC2003 3-axis magnetic sensor hybrid 24

Figure 14. Magnetometers mounted inside a barrel 25

Figure 15. Left and right X-axis magnetometer signals for gravel hauler 25

Figure 16. Banner Engineering Corp. photoelectric sensor 26

Figure 17. Photoelectric sensors mounted to barrel 27

Figure 18. Eleven-axle gravel hauler and corresponding optical outputs 28

Figure 19. Speed measurement with pulsed Doppler ultrasound 28

Figure 20. Reference system barrel with video and radar 30

Figure 21. Vehicle identification and classification tool 31

Figure 22. Locations and satellite-views of the two test sites 32

Figure 23. Photographs of the two test sites 32

Figure 24. Instrumentation layout at test site #1 is typical of both sites 33

Figure 25. Stills from video taken at test site #2 34

Figure 26. Histogram of vehicle speeds measured by radar 36

Figure 27. Method 1 for the optical sensor speed estimation 40

Figure 28. Method 2 for the optical sensor speed estimation 41

Figure 29. Signals from the pyroelectric sensors for a passenger car and a tractor-semitrailer combination 43

Figure 30. Identifying a passing-vehicle event from the pyroelectric signals 44

Figure 31. Correlation function for the data of figure 30 45

Figure 32. Differentials of the pyroelectric signals used to identify the characteristic time shift between signals 46

Figure 33. Magnetometer data for a passenger car, a tractor-semitrailer combination and a double-bottom combination 48

Figure 34. Comparison of signals from the magnetometers and from the passive infrared sensors in response to a passing passenger car 50

Figure 35. Identifying a passing-vehicle event using the magnetometers signals 51

Figure 36. Comparison of matched measured and reference speeds: test site #1, optical sensors, method 1 reduction, with and without gain correction 53

Figure 37. Standard deviations of speed-measurement errors based on uncorrected measured speeds 55

Figure 38. Standard deviations of speed-measurement errors based on corrected measured speeds 55

Figure 39. Comparison of signals from the three types of sensors generated by the passing of a passenger car 57

Figure 40. Percent of vehicles missed by the speed sensors by test site and data-reduction method 58

Figure 41. False positive speed measurements by the sensor type, test site and data-reduction method 59

Figure 42. COMPANION post-mounted queue-warning system and photograph of sample post 61

Figure 43. Illustration of lane closure configuration prescribed in the 2003 edition of the *Manual on Uniform Traffic Control Devices* (MUTCD) 69

Figure 44. Simulator roadway layout in the static-road-sign condition..... 69

Figure 45. Simulator layout in the dynamic warning post conditions 70

Figure 46. Simulator roadway with sight-distance-limiting screen 71

Figure 47. Detail of sight-distance-limiting screen and post-mounted warning lights.... 71

Figure 48. Minimum time to collision for each roadway condition. 75

Figure 49. Minimum time to collision for each approach speed. 76

Figure 50. Three-way interaction observed between approach speed, gender, and age group. 76

Figure 51. Peak deceleration for each roadway condition. 77

Figure 52. Main effect of upstream distance of stopped vehicle on peak deceleration. .. 77

Figure 53. Main effect of driver age on observed peak deceleration..... 78

Figure 54. Two-way interaction of speed and roadway condition on peak deceleration. 78

Figure 55. Average subjective rating by roadway condition for each of the three survey questions posed. 79

Figure 56. Vehicle speed is proportional to the time lag between signals from the upstream and downstream sensors..... 84

Figure B1. Active infrared corrected and non-corrected results versus the reference speed for method 1, first and last transition 93

Figure B2. Active infrared corrected and non-corrected results versus the reference speed for method 2, all transitions 94

Figure B3. Passive infrared corrected and non-corrected results vs. the reference speed for correlation method..... 95

Figure B4. Passive infrared corrected and non-corrected results vs. the reference speed for maximum slope method 96

Figure B5. Magnetometer X signal corrected and non-corrected results vs. the reference speed 97

Figure B6. Magnetometer Y signal corrected and non-corrected results vs. the reference speed 98

Figure B7. Magnetometer Z signal corrected and non-corrected results vs. the reference speed 99

Figure B8. Magnetometer magnitude signal corrected and non-corrected results vs. the reference speed..... 100

List Of Tables

Table 1. Field test data runs 35

Table 2. Review of the statistics of measured speeds 54

Introduction

This document is the *Final Technical Report* on the first phase of a research study entitled "Work Zone Safety ITS." The study is being conducted by the Transportation Research Institute of the University of Michigan (UMTRI) for the Federal Highway Administration (FHWA) of the US Department of Transportation under contract DTH61-01-C-00049.

Accident data show that work zones increase crash risk. Estimates of this increase range from 26% to 168% depending on the circumstances. The main objective of the Work Zone Safety ITS project is to develop a technology that directly addresses this problem of elevated crash risk in work zones. Unlike other work zone ITS technologies devised to promote efficient traffic flow in work zones, the key objective for this technology is to directly reduce the incidence of work-zone crashes.

Major factors contributing to work-zone crashes include the speed differential between two vehicles, irregular maneuvers, and speeding in challenging locations. Of these, speed differential is the most obvious explanation for the prevalence of rear-end collisions in work zones. A simple theory of work-zone risk suggests that as traffic density in a work zone increases, traffic slows down in the heavily congested areas causing a backup of slow-moving traffic. The speed differential between slow-moving traffic and the traffic moving at posted speeds farther upstream becomes a hazard because of the driver's uncertainty about *where* the differential occurs, the *magnitude* of the speed differential, and the *span* of roadway over which the differential is observed.

The Work Zone Safety ITS projects aims to develop an *adaptive* speed-advisory system for work zones based on a *distributed* system of traffic speed sensors and traffic signaling devices. Such a system would sense traffic speeds in, and upstream, of the work zone and adjust speed-advisory signals appropriately *in real time*. The core element of the system would be a *smart barrel*—an ordinary appearing traffic control barrel containing an inexpensive traffic speed sensor and equipped with a simple, adjustable signaling system and the necessary equipment for communication to a central controller.

This document reports on the first phase of the development of such a system. The work has concentrated on three primary tasks:

- development of the broad concept and general scheme for implementation of the adaptive speed-advisory system;
- initial development and evaluation of an inexpensive traffic speed sensor for installation in smart barrels;
- initial development and evaluation of adaptive traffic signalling schemes applicable to the smart-barrel concept.

Six main sections follow this *Introduction* in this report. Respectively, they address

- *The work-zone crash problem*. This section presents background information on the nature and statistics of the work-zone safety problem and reviews some of the previous research on the subject.
- *The concept of the work zone ITS system*. This section describes the configuration, setup and calibration methods, and general operation of an adaptive system for speed-advisory signaling at work zones.
- *Traffic speed sensors for a smart barrel*. Development of a sufficiently inexpensive but capable speed sensor for installation in individual barrels is seen as the key technological challenge to the development of the system. This section reviews and evaluates available technologies, and describes and presents results from a limited field test of three prototype speed sensors.
- *Human-factors requirements for a queue-warning system*. This section discusses practical considerations for deployment and the issues related to objectives, format, and credibility of the warning signals.
- *Pilot simulator study*. The conduct and findings of a driving-simulator study of prototype signaling methods are presented.
- *Conclusions and recommendations*. The technological and human-factors findings of the study are reviewed and recommendations for future work are presented.

The Work-zone Crash Problem

The national rise in highway work-zone activity along with a national rise in traffic volumes have produced a rise in work-zone fatalities. The trend, illustrated by data from the Fatality Analysis Reporting System (FARS) presented in figure 1, underscores an increasing need to develop a substantive understanding of how to manage driver behavior within the work-zone driving environment. Besides the increase in overall fatalities, the change in the distribution of these fatalities suggests that the most severe problems involve multi-vehicle collisions: fatal rear-end collisions comprised about 15% of work-zone fatalities in 2002, versus 10% in 1987; angle collisions comprised 21% of work-zone fatalities in 2002, versus 12% in 1987. Among traffic fatalities not related to work zones in 2002 (and 1987), rear-end collisions comprised 5% (5%) of total fatalities, and angle collisions comprised 24% (18%), suggesting that fatalities from rear-end collisions are especially overrepresented in work zones.

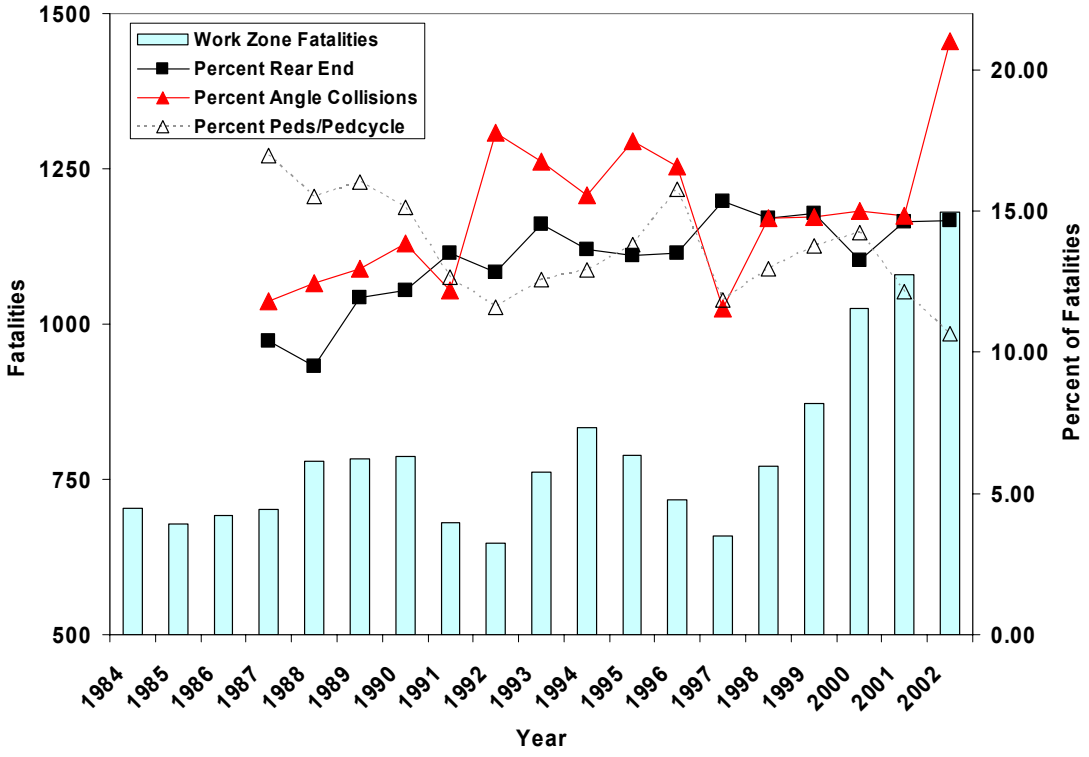

Figure 1. Total work-zone fatalities reported in FARS between 1984 and 2002 along with percentage of work-zone fatalities attributable to rear-end collisions, angle collisions, and pedestrian/pedalcycle collisions.

Estimates of both fatal and non-fatal crashes also confirm that rear-end collisions are overrepresented in work zones. According to the National Automotive Sampling System (NASS) 2001 General Estimates System (GES), there were approximately 1.9 million police-reported rear-end crashes in the United States, comprising about 30% of all crashes. In contrast, 40% of work-zone-related crashes were rear-end collisions.

Work-zone-related fatalities from rear-end collisions primarily occur on interstate roadways where speeds are high. In 2002, about 60% (100) of rear-end collision fatalities occurred on interstates. A comparative analysis of work-zone crashes and non work-zone crashes (Chambless, Lindly, Ghadiali, & McFadden, 2002) found work-zone crashes are overrepresented:

- on interstates, U.S., and state roads (63% in work zones, versus 37% outside);
- in speed zones between 45 and 55 mph (48% vs. 34%);
- involving misjudgment of stopping distance or close following (27% vs. 15%).

Detailed studies of crash locations within work zones (Garber & Zhao, 2002; Raub, Sawaya, Schofer, & Ziliaskopoulos, 2001) report that most crashes occur in the activity area (60%-70%), typically after a lane merge. The next most frequent number of crashes occur in the merge taper and advance warning areas (combined range from 23%-40%), although systematic biases in reporting work-zone crashes may underestimate these figures (J. Wang, Hughes, Council, & Paniati, 1996). For example, crashes that occur at the end of a traffic queue located far upstream of a work zone are less likely to be reported as work-zone related. The above work-zone analyses also do not make adjustments for exposure differences associated with each area. Depending on the particulars of the work zone, the length of the activity area, the transition area, and the advance warning area all vary widely. To assess real differences in risk between the different work-zone areas, it would be necessary to report crashes per million miles of travel.

Despite the above limitations, the preponderance of rear-end collisions and cited contributing factors in crash datasets (e.g., following too closely, driving too fast) support the idea that large speed differentials between two vehicles play a major role in work-zone crashes. A simple theory of work-zone crash risk suggests that as traffic density in a work zone increases, traffic slows down in the heavily congested areas, causing a backup of slow-moving traffic upstream of the congested area. The speed differential between slow-moving traffic and the traffic moving at posted speeds

becomes a hazard because of the driver's uncertainty about the *location* of the differential, the *magnitude* of the speed differential, and the *span* of roadway over which the differential is observed. This uncertainty appears to surprise drivers, leaving them ill-prepared to take the necessary evasive action to avoid a crash.

Substantial effort has been placed on the development of roadside warning and advisory systems to help reduce the speed of vehicles approaching areas of stopped or slower-moving traffic. A recent research report by Wiles, Cooner, Walters, and Pultorak (2003) provides a comprehensive review of the problem of traffic-queue propagation, as well as numerous ITS countermeasures applied to help mitigate the problem. Among the special concerns cited in the report is the problem of rapid fluctuations in the length of a traffic queue. In one instance, the queue tail was reported to grow upstream at a rate of 30 mph. As a queue tail lengthens and moves upstream of traffic, the tail overruns the upstream warning signs so that drivers may reach the queue before seeing a single warning sign. As the queue shortens, the gap between signs warning of the "*slow moving traffic ahead*" and the actual start of the queue lengthens. When the *actual* start of the queue and the *expected* start of the queue (implied by the fixed warning sign) do not correspond, drivers may become confused, uncertain, and even skeptical about the reliability of work-zone signs. Confusion and uncertainty may delay detection of stopped traffic; perceived unreliability may induce drivers to pay less attention to the roadway signs, and, instead, rely more on prior experience with the work zone. As a result, drivers may be unprepared to stop when they reach the tail of the traffic queue (Tudor, Meadors, & Plant, 2003). The speed of the tail movement also precludes manual intervention by a traffic controller (Wiles et al., 2003).

Several studies have noted drivers' disregard for posted warnings and speed limits around work zones, reporting better compliance when variable/changeable message signs, which measure and report the driver's actual speed are posted (e.g., Fontaine & Carlson, 2001; Garber & Patel, 1995 ; Garber & Srinivasan, 1998; C. Wang, Dixon, & Jared, 2003). The effectiveness of variable message signs advising drivers about upcoming roadway speeds also appears to be related to their proximity to the actual work-zone area (McCoy & Pesti, 2002). Perhaps this is related to the driver's confidence that the message reflects actual conditions around the work zone (i.e., seeing *is* believing). When a driver repeatedly passes warning signs which do not match actual conditions observed in a work zone, it seems natural that the driver might come to rely more on past experience than on the posted signs for guidance.

Reliance on past experience is particularly hazardous in a roadway environment in which the queue location can move rapidly and unpredictably over large distances. Drivers may be confronted with stopped or slowed traffic sooner (or later) than expected.

The length of a few work-zone queues have been examined in empirical work evaluating the accuracy of analysis tools used to predict queue length (Schnell, Mohror, & Aktan, 2002). Depending on changes in traffic volume, concentration of heavy trucks, and the number of lanes closed, queue tails have been reported to migrate as much as six miles upstream of the activity area for short periods of time. The large distance makes it particularly difficult to effectively position warning information for drivers.

These facts about work zones suggest that an effective work-zone-queue-warning system (QWS) should do the following:

- It should accurately detect the queue-tail location, defined by a large speed differential over relatively short distances.
- It should track the queue tail automatically and with sufficient responsiveness to follow upstream migration speeds of up to 30 mph.
- It should follow the migration of the queue tail over the plausible maximum extent of a queue.
- It should present useful queue advice or status to approaching drivers in a credible fashion.
- It should be suitable for temporary traffic control.

Concept of the Work-zone Safety ITS System

The work-zone safety ITS system outlined here is intended to provide distributed speed-advisory signaling which automatically adapts to the current traffic flow situation in the work zone. As shown in figure 2, the system is primarily based on the notion of a *smart barrel*, a device similar in appearance to today's work-zone traffic-control barrel but containing a short-range traffic speed sensor, a simple but adjustable signaling device and short-range communication equipment for interfacing with supervisory computers. Such smart barrels would be distributed in large numbers and at relatively short intervals throughout the work zone—as ordinary traffic-control barrels are distributed. The distributed traffic-speed data would be received and processed by the supervisory computers to provide rapid, real-time adaptation of the distributed signals as appropriate for the existing speed differential throughout the work zone.

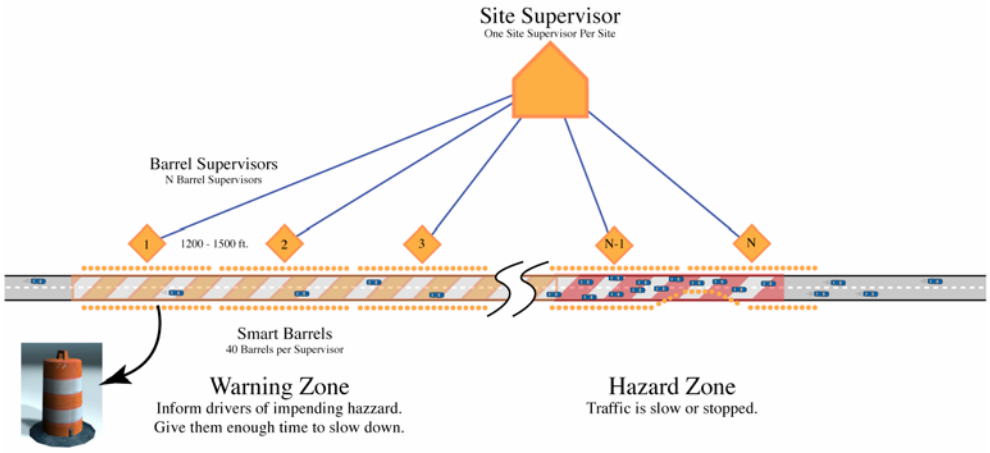

Figure 2. System concept

System Configuration

The system consists of *smart barrels*, *barrel supervisors*, and a *site supervisor*.

Smart Barrel

Figure 3 shows the major elements that comprise a smart barrel. A low-power microcontroller contains a local clock that is synchronized to GPS time via inputs from the barrel supervisor. It has program logic and hardware interface elements to derive speed from the detector(s) and control the on/off state of the signals (LEDs). It should also be able to go into a low-power sleep mode when low traffic density

permits. A message containing the barrel identification, time, and vehicle speed is sent when a vehicle (or portion of a vehicle) is first detected. Closely spaced vehicles may not require a new communication.

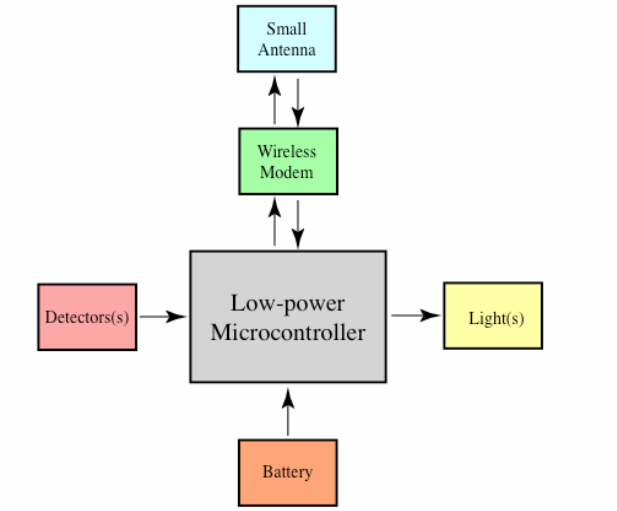

Figure 3. Configuration of a smart-barrel

Individual barrels will not include GPS hardware. However, each barrel's LAT/LON will be determined during set up (see the section entitled *Setup and Calibration* below). A "tilt" sensor will be contained in each barrel to warn the supervisor if the barrel has moved since setup.

Each barrel would be powered by its own battery providing long-term operation on a single charge. Low-power communications ability is essential for this to succeed. For purposes of explanation, an actual radio module will be described here even though a fully communicating system was beyond the scope of this phase of the project.

The Wi.232DTS (Radiotronix) embedded wireless module combines a high-performance DTS spread-spectrum transceiver and a protocol controller to create a transparent wireless solution to replace conventional RS-232/422/485 wiring. It can be used in point-to-point, point-to-multipoint, or multipoint-to-multipoint applications. Its footprint is less than one square inch and cost is estimated at $20 in production quantities. The module is designed to interface directly with standard UART signals from a microcontroller. It can use a printed-circuit board antenna or an external 1/4-wave whip antenna. In this application, the set of barrels "attached" to a *barrel supervisor* would share a single data channel and part of the maximum data rate of approximately 150 K Baud. The set of barrels and their supervisor should be in

line of sight within a maximum range of 1000 to 1500 feet. Thus the number of barrel supervisors is determined by barrel spacing and the terrain.

The detectors should reliably sense the speed of vehicles in the immediately adjacent lane. Stopped vehicles are not directly transduced but are deduced (see the section entitled *Operation* below). Detectors should also consume as little power as possible and be immune to variations in weather, vibration, and other disruptive influences as found in a typical roadside application.

Barrel Supervisor

The barrel supervisor acts as a gateway between its barrels and the site supervisor. It could be attached to the back of a sign that is also used to signal drivers. The main parts are diagrammed in figure 4. The heart of this system is a low-powered embedded PC chosen because of the experimental nature of the system development and ease of programming. A final product might use a simple microcontroller. The system contains one or two of the same wireless modules that are in the smart barrels. In addition, it needs a higher-power (longer-range) radio modem to talk to the site supervisor. The higher power consumption of this system will probably require a solar panel to charge the battery.

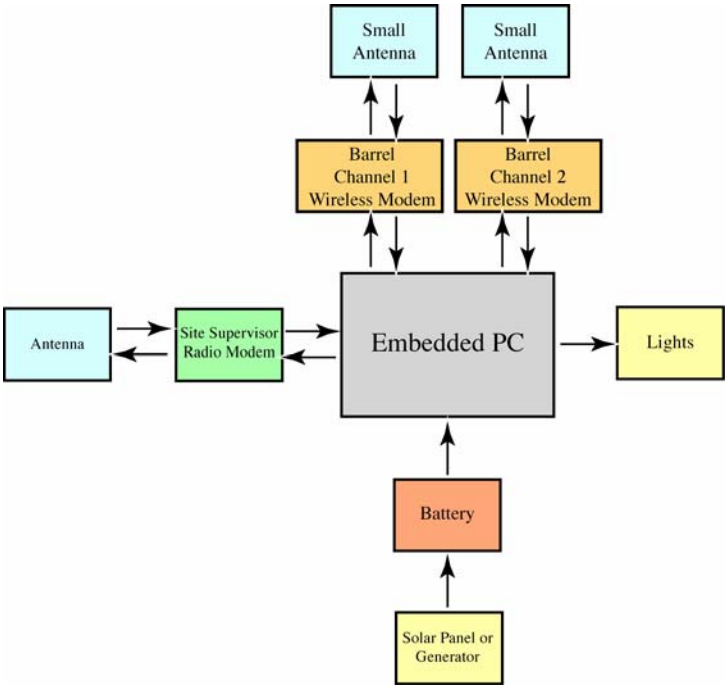

Figure 4. Configuration of a barrel supervisor

The barrel supervisor collects speed readings from the barrels and forwards them to the site supervisor. It also receives signal commands and time synchronization messages from the site supervisor and relays those to its barrels. It would also participate in setting the barrels to a low-power standby state and then reawakening them when traffic approaches.

Site Supervisor

The site supervisor is the brains of the system. A possible hardware configuration is shown in figure 5. It has a GPS receiver to synchronize its clock and to locate it and the smart barrels. A GPRS cellular modem is provided for reporting to funding or managing agencies. Since the latitude and longitude of each barrel is known, automatic reporting of work-zone location, extent, and traffic conditions is possible.

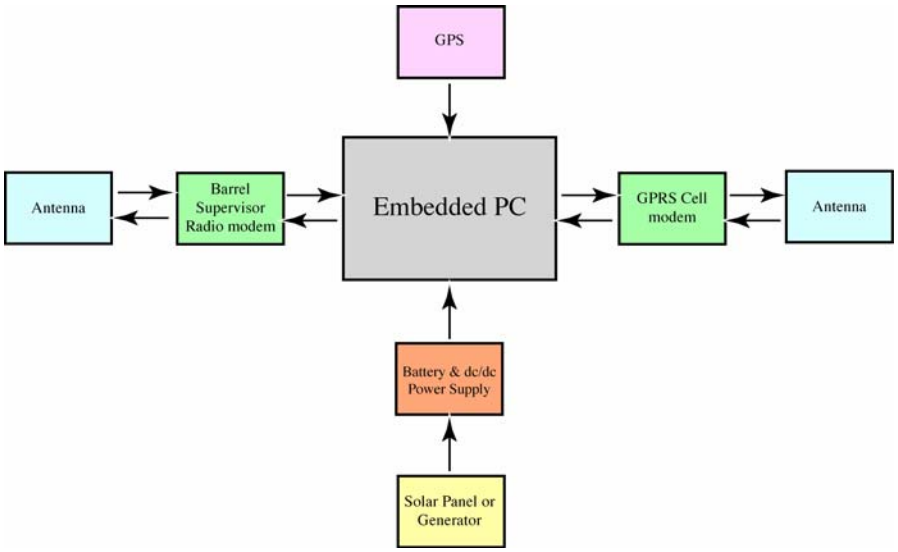

Figure 5. Configuration of the site supervisor

The site supervisor receives time-stamped, ID'ed speed readings from the barrels via the barrel supervisors. The algorithms described in the next section create signaling commands that are sent out to the barrel supervisors and then to the barrels or other connected driver-warning or communication devices.

Setup and Calibration

Barrels are turned on and placed along the lane(s) of travel with attention paid to proper alignment relative to the traffic lane of interest. When a set of barrels has been placed, a configuration box is used to send an initialization message to the barrels to tell them to switch their radios to the proper channel and then to enter a low-power

active standby mode. After the barrel supervisors and site supervisors are powered and initialized, the barrels are switched to active mode and begin speed sampling.

Next the barrels need to be located. A laptop computer with a 10 or 20 Hz differential GPS is placed in a suitable vehicle. The vehicle is driven three times (in each lane of interest) over the length of the deployment. GPS time, altitude, latitude, and longitude are collected and written to file or files on the laptop hard disk. The files are then transferred to the site supervisor computer via an ethernet connection. The site computer imports these files and uses the times in the file to connect the vehicle path to the time-stamped speed data collected from the barrels. Thus "the barrels" are located on the map. (Note that, more precisely, it is the position of the *vehicle* at the moment the barrel senses its speed that is actually determined. This, in fact, is the more desirable location information.) Distances and grades between barrels are then calculated and stored for use in system operation (see the section entitled *Operation* below). The site supervisor can now start its normal operating algorithms.

Operation

Determining Signal Intensity Based On Distributed Speed Measurements

Actual development of full system software was beyond the scope of this phase of the Work Zone Safety ITS project. Nevertheless, it was necessary to "develop" system algorithms at least at the conceptual level in order to have a basis for design of the hardware elements discussed above. The following discussion presents the structure of the core algorithms at this basic level. For the moment, these concepts are limited to single-lane traffic, although we believe they will be readily adaptable to multilane situations.

Signal intensities (presumably to be manifest as blink rates) to be displayed at each individual signaling device are expected to be set primarily on the basis of the deceleration required of faster-moving traffic to avoid collision with slower-moving traffic ahead, but with additional adjustment based on over-speeding relative to the posted speed limit.

Addressing the deceleration basis first, signals would not be activated unless the required deceleration exceeded a minimum threshold. When required deceleration did exceed the minimum, signal intensity would be adjusted, either proportionately or in steps, to progressively higher levels up to a maximum associated with an upper

deceleration threshold. Although the specific thresholds of deceleration remain a matter of study (in the simulator) and would, at any rate, be adjustable in a final system, our expectation would be for a minimum threshold of about 0.05 g (0.5 m/sec^2) and an upper threshold of about 0.15 g (1.5 m/s^2). This expectation derives from recognizing that (1) the deceleration capability of heavy trucks, not passenger cars, is the more important reference and (2) our understanding of the distribution of braking deceleration of trucks in real use. It also should be noted that, in practice, deceleration thresholds would be adjusted for the grade. That is, on descending road segments, the thresholds would be reduced in accordance with the downward grade and, similarly, increased on ascending road segments.

A similar adjustment of intensity would be based on over speeding relative to the posted speed limit. In a fashion analogous to the deceleration procedure, this calculation would define a minimum and an upper threshold of over speed and vary intensity in proportionately (or step wise) across the range they define.

Finally, of course, the actual intensity setting used would be the higher of the respective results of the deceleration and the over-speed criterion.

Data-Collection And Processing

Figure 6 presents a highly generalized flow diagram of the data-collection and calculation process envisioned for the site supervisor. The process is shown as a continuous loop whose cycle time would be on the order of 10 Hz or more.

As the first step of the process at the top of the figure, speed data is collected from each of the distributed speed sensors. These data include the speed value, the sensor ID (providing location) and a time stamp. Note that if traffic speed and density are relatively high, a given sensor may well have made more than one measurement in the preceding cycle period. On the other hand, other sensors may have had no vehicles pass by during the cycle period, in which case they would transfer no new data.

Following data input, each new data point is checked for validity. This is primarily a “reality check” to remove spurious data. Each new data point would be compared with current and recent data from neighboring sensors and “impossible” readings would be discarded. Valid data would be added to the data record.

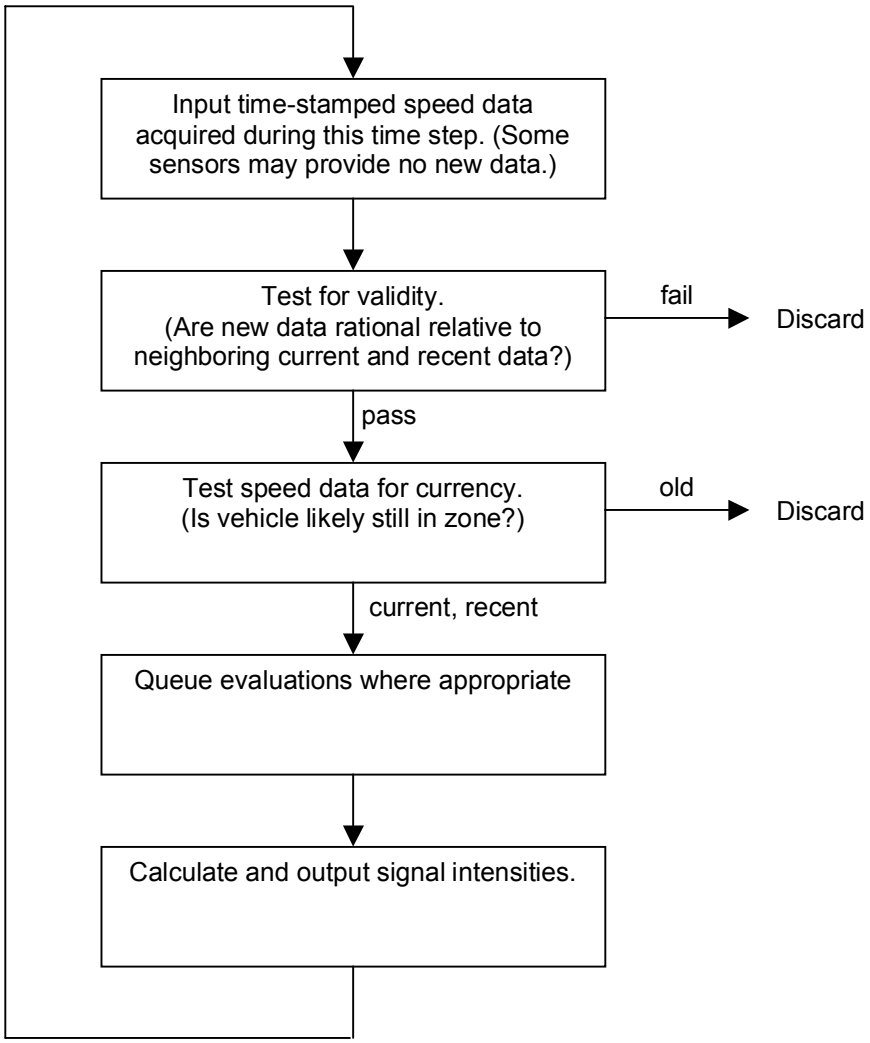

Figure 6. Generalized flow diagram of speed-data collection and signal-intensity calculations

The data is then checked for "currency." That is, given the measured speed, the distance between sensors, and the time elapsed since the measurement, is the vehicle which generated the measurement likely still in the measurement zone. Where traffic is moving slowly or stopped, a measurement taken by a given sensor would stay current for a substantial time and many process cycles. Where traffic is moving rapidly, a measurement may derive from a vehicle which passed completely through the measurement zone within a single cycle period. Data for vehicles still in the zone of measurement would be designated as "current" in that zone. New data would be current in either the zone of measurement or a down-stream zone where the vehicle is predicted to be. Where multiple data are current for a single zone, the maximum (or perhaps average) speed would be used to represent the zone. The data record would also retain at least several "recent" readings from each sensor zone (primarily for use

in the validity check). Finally, if there is no "current" speed value for the first barrel (upstream) of the system, an "expected" speed, based on the recent history of speeds of entering vehicles would be assigned as the current speed for the first zone.

The data can then be further processed to evaluate queue growth where this is appropriate. The complexity of this undertaking is largely determined by the spacing of sensors. Where sensors are relatively closely spaced (on the order of the stopping distance of vehicles at the nominal speed of travel, or less), growth of the queue can essentially just be observed. For example, with sensors in every smart barrel, and barrels spaced by the often-used rule of spacing in feet equal to two times the speed in miles per hour, projecting queue growth between barrels would not be needed. Where spacing between sensors approaches an order of magnitude greater than stopping distance, projecting queue growth between sensors may be necessary. In this case, queue evaluation is a conceptually simple process wherein vehicles entering the zone (i.e., passing the lead sensor) and leaving the zone (passing the second sensor) are counted in order to keep track of the increasing number of vehicles in the zone. Using a representative vehicle spacing in the queue, the tail of the queue relative to the second sensor can be estimated. A modest complication arises from estimating how many of the vehicles in the zone are still in relatively free motion prior to reaching the queue. In either case, whether queue growth is simply observed or it is calculated, when velocity of growth upstream is substantial, it can be used to modify the calculation of required decelerations of upstream traffic.

The final step in the processing cycle is the calculation and output of the signal intensities for each zone. Figure 7 presents the nomenclature used in the explanation of that calculation that follows which deals with areas of closely spaced sensors and signals without the complication of substantial queue growth. The figure shows that there are (n+1) smart barrels in the system, each here assumed to have a speed sensor and a signaling device and numbered from 0 through n, B_0 being the first barrel. A full matrix of the distances between barrels is known, a priori, the distance from the barrel i to barrel j (where $j > i$) being designated $d_{[i][j]}$. Each barrel also has an associated elevation (e_i), speed value (s_i), and signal intensity (r_i).

Assuming close spacing of the smart barrels, per the previous discussion, determining signal intensity proceeds as follows:

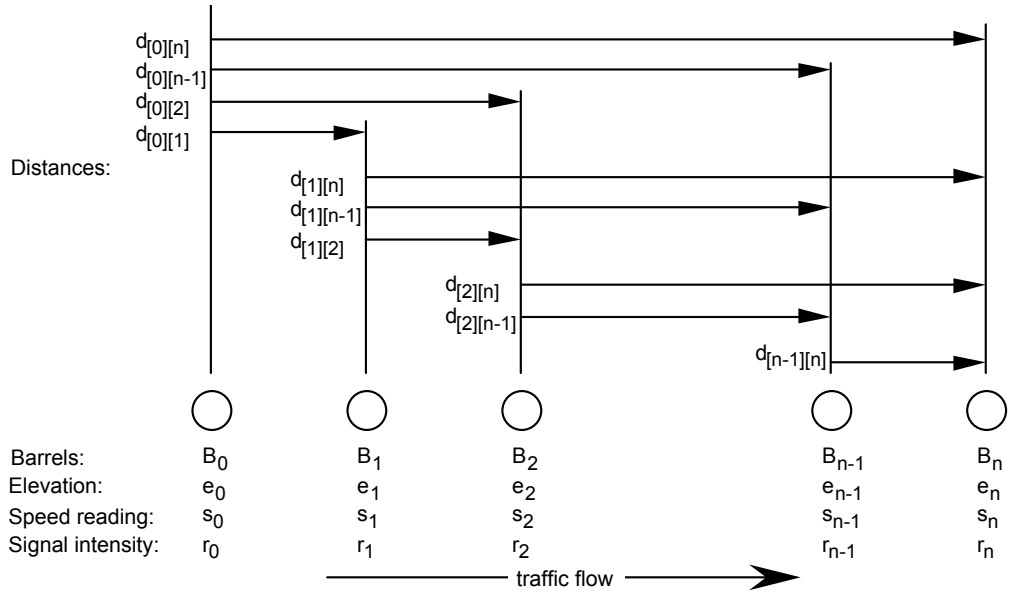

Figure 7. Nomenclature

For positions i = 0 through (n-2) *for which the speed readings* (s_i) *are current*, a matrix of decelerations ($dec_{[i][j]}$) can be calculated according to:

$$dec_{[i][j]} = 0.102\frac{\left(s_i - s_j\right)^2}{2\left(d_{[i][j]} - s_i t_{lag}\right)} + grd_{[i][j]} \qquad (1)$$

for all j > i and where:

$dec_{[i][j]}$ is the deceleration, in gravitational units (g),

$d_{[i][j]}$ is a constant (predetermined at the time of set up) and is the distance between barrels i and j, in meters,

s_i, s_j are the speeds at barrels i and j, in meters/second,

t_{lag} is a constant representing the total time lag (system latency and driver reaction), in seconds,

$grd_{[i][j]}$ = $(e_i-e_j)/d_{[i][j]}$, predetermined at the time of setup, is the average downgrade between barrels i and j,

e_i, e_j are the elevations at barrels i and j, in meters, and

0.102 is the conversion constant for deceleration, in g per m/s^2.

Note that in equation 1, the first term on the right side is the actual required deceleration and the second term on the right side is an adjustment for average road

grade, increasing the apparent acceleration demand on downgrades and decrease it on upgrades, thus providing the grade compensation discussed previously.

From these values, the "required deceleration" for the vehicle currently passing barrel i ($dec_{req[i]}$) is the maximum of the set $dec_{[i][j]}$, i.e.:

$$dec_{req[i]} = \max\left[dec_{[i][j]}\right]_{j=i+1}^{n} \qquad (2)$$

This required deceleration, along with the speed of the vehicle relative to the posted speed, would be used to establish the signal intensity *assigned to the next barrel*, $r_{[i+1]}$. As outlined previously, when dec_{req} exceeds a minimum threshold, the associated intensity would be adjusted, either proportionately or in steps, to higher levels up to a maximum intensity associated with an upper deceleration threshold. Also, the differential speed of the vehicle above the posted speed (i.e., s_i-s_{posted}) would be compared to a another set of thresholds to determine an intensity setting based on over-speed. The maximum of two intensities so determined would actually be used.

For barrels where the intensity is not calculated by the preceding procedure (i.e., the positions i+1 where s_i is not current), the signal intensity would be set equal to that of the preceding barrel. The process would be progressive such that a currently calculated intensity would propagate down the line until reaching a position where a different intensity had been calculated (i.e., a position where a different vehicle established the rate).

Finally, where it may be advantageous for paired sets of speed sensor and signaling device to be widely spaced, the "smart barrel" concept would require slight modification. Namely, where spacing is so wide that the next barrel is not readily visible, the signal device must be spaced downstream from its associated speed sensor in order that the adaptive signal, calculated on the measured speed, could actually be displayed to an isolated vehicle passing the station. Thus a widely-spaced "barrel" would actually have to be a pair of barrels, or perhaps a single barrel followed by an associated barrel supervisor with an incorporated signaling device. The calculation of signal intensity would, however, proceed on the same basis as indicated above, perhaps with the addition of queue evaluation in the intervening zone to the next "barrel."

Technological Feasibility

Available Detection Technologies

Most of the existing traffic detection and surveillance products are targeted to either signalized intersections or freeway applications. The intersection products detect vehicle presence and are used to activate traffic signals. Inductive loops buried in each lane are the most common detector. Direct speed sensing is not the primary measurement. Freeway applications emphasize vehicle counting and classification, and usually report average speeds.

The non-intrusive sensors are usually mounted on existing structures (signs, bridges, mast arms, and poles) and get their power from 110 or 230 volt connections to the power grid or use DC power supplied by traffic control cabinets. The power consumptions range from 1 to 160 watts. Large size, restrictive mounting requirements, or excessive power consumption preclude using many of the existing products examined below. Some of the sensor technology, however, can be adapted for use in this application.

Active Infrared

An active infrared sensor sends out infrared light generated by a LED or laser diode and measures the time required to reflect off an object and return to an infrared detector or array of detectors. The Autosense (Scwartz Electroptics) series of sensors scan across multiple lanes and can provide 3D imagery to classify vehicles. Speed can also be calculated by measuring the time it takes the vehicle to cross detection zones. The Traffic observation module (MBB Sens Tech) does not scan but uses two to six laser beams to create several detection zones. These sensors mount 20 to 25 ft above the road. They are very accurate but much higher in cost ($5000-$10000) and energy consumption (40 to 160 watts) than the other technologies.

A scaled-down solution that uses infrared emitters and detectors in a side-looking configuration is discussed in a later section (entitled *Field Test*.).

Passive Infrared

All matter above absolute zero emits radiation in the far infrared part of the spectrum. The amount of radiation is a function of the object's temperature, size, and structure. Passive infrared sensors measure this radiation. A non-imaging detector has a

relatively wide field of view and can detect a vehicle's presence or velocity (with more than one sensor or detection zone). An imaging sensor contains a two-dimensional array of detectors and so can indicate presence, speed, and classification. The IR 254 (ASIM Technologies Ltd) has four detection zones, mounts overhead to 33 ft, costs $955 and consumes just 0.3 watts.

Passive infrared is a promising technology for this application because of its low power consumption, cost, and an adaptability to a side viewing detector. Many security products use infrared motion detectors. A speed sensor is described later in the *Field Test* section.

Passive Acoustic

A passive acoustic sensor detects sound (primarily tire noise) from approaching vehicles with a two-dimensional array of microphones. The array is mounted on a pole 20 to 40 feet above the ground beside the road. SmartSonic and SAS-1 sensors are two passive acoustic products. They both have trouble with slow-moving vehicles and stop-and-go traffic. They are primarily recommended for measuring free-flow traffic at speeds above 30 mph and therefore are inappropriate for a work-zone application.

Ultrasonic

Ultrasonic air sensors emit a burst of sound pulses at a frequency between 25 and 50 KHz. Distance is calculated by measuring the time it takes the beam to return after reflecting off the target. Two closely spaced emitters can permit speed measurement. Sensors can be overhead or side mounted. The TC-30C (Microwave Sensors) is a an ultrasonic ranging sensor that indicates vehicle presence. It costs $559 and consumes 3 to 4 watts. There are dozens of ultrasonic emitter, transducer, and integrated sensor manufacturers whose products are used in object detection in commercial and industrial applications and are fairly inexpensive. An ultrasonic detector that also measures the Doppler frequency shift of a reflected signal also exists.

The two main problems with these types of detectors are high power consumption (relative to the passive technologies) and the challenge of running them at high enough burst rates to detect fast-moving vehicles.

Magnetic

Magnetic sensors use a dual-axis flux-gate magnetometer to measure the Earth's magnetic field. When a vehicle approaches the detector, the vehicle distorts the magnetic field and the sensor detects this change. Both the SPVD-2 (Self-Powered Vehicle Detector – Midian Electronics) and the Groundhog Permanent Count Station (Nu-Metrics) use this method. They are packed in plastic canisters and buried in the roadway. The SPVD-2 is powered by a 13.5 Volt, 17 amp hour alkaline D-cell pack that can last 4 to 5 years. The sensor sends vehicle arrival and departure messages to an above-ground receiver via a 47 MHz FM radio modem. This sensor technology is passive and consumes very little power which satisfies one of the primary requirements in the smart barrel application.

Banner Engineering Corp. has recently introduced the M-Gage S18M Vehicle Detection Sensor which sells for $209 in quantities of one. This product uses a 3-axis magnetometer and is targeted for both above- and below-grade installations. Background condition and sensitivity adjustments allow tailoring the sensor to the application's magnetic environment, object properties, and desired range. Several sensor manufactures (Honeywell, Crossbow, and Fraunhofer-Institut Photonsche Mikrosysteme) sell two- and three-axis magnetometers. This is another technology potentially available for the smart barrel.

Microwave

Continuous microwave devices use the Doppler principle —the change of frequency of a wave reflected from a moving object is proportional to the object's speed— to directly measure the speed of a vehicle. The available systems (TDN-30 by Whelen Engineering, TC-20 by Microwave Sensors, and DRS1000 by GMH Engineering), are configured to be used in an overhead mount or an elevated side mount. Typical power consumption is 2 to 6 watts and cost of a single unit is $1000 to $2000. It might be possible to mount a radar device on top of a barrel facing towards oncoming traffic. The high cost, high power consumption, and possible interference problems with multiple radars in the same location would make this only a fallback solution.

Video

Video image processing promises the richest data set of traffic measurements including vehicle detection, speed, classification, headway, density, and volume. A camera sends an image to a video processor which digitizes it and applies various

detection and tracking algorithms to extract the applicable measurements. Cameras can be side or overhead mounted. The Autoscope Solo (Econolite Control Products) even integrates the camera and processor into one package. Video systems are probably the hardest to install and calibrate correctly of all detector technologies. The lack of portability, high cost, and the high power consumption (20-50 watt range) make them unsuitable for this application. The dirty construction environment and changing road features might also prevent their use.

Initial Evaluation of Detection Technologies

Four technologies were initially selected for evaluation: passive infrared (pyroelectric), magnetic (magnetometer), active infrared (optical), and pulsed Doppler ultrasonic.[1] The initial evaluation process included identifying and purchasing candidate sensors, designing and fabricating mounts and electronic interface circuitry, laboratory examination and preliminary testing, parking-lot tests with instrumented vehicles, and testing on a nearby road with both instrumented vehicles and normal traffic. Finally, three of the sensors types were mounted on barrels and prepared for evaluation in a limited field test.

All of the sensors were interfaced to a general purpose UMTRI data acquisition system (DAS). The DAS contains an embedded PC, 12-bit A/D, 16 analog and 8 digital signal conditioning channels, and a differential GPS. Each analog signal conditioning channel provides for software programmable offsets and gains. The sensor data were sampled at a 1000 Hz rate and stored on disk with the start time of each test synchronized to GPS time. The data files were later loaded into a Microsoft SQL Server database to facilitate viewing and processing.

For preliminary checkout and testing, the sensors were mounted to a fixture with an adjustable aluminum bar as shown in figure 8. This facilitated exploring sensor heights, separations, and aiming angles and the simultaneous testing of the different technologies.

Three of the four sensor types, the ultrasonic sensor being the exception, were essentially used as paired, proximity detectors in order to measure speed. The concept

1 . Early in the process it was determined that appropriate ultrasconic sensors could not be purchased and so these were not subject to test. Nevertheless they will be included in this discussion of initial evaluation.

is depicted in figure 9. The idea, of course, is that there are two identical sensors, spaced apart from one another along the direction of travel and oriented with their sensitive directions parallel to one another and at right angles to the direction of travel. In this arrangement, a passing vehicle should produce similar responses from the two sensors, but with the responses of the downstream sensor occurring some time after the response of the upstream sensor. The speed of the vehicle can then be determined by dividing the distance between sensors by the time between signals.

This general approach was used for both infrared sensor types and for the magnetometers. The ultrasonic detector investigated measures speed directly using the principle of Doppler frequency shift. Only one unit would be required.

Figure 8. Test fixture on Baxter Road

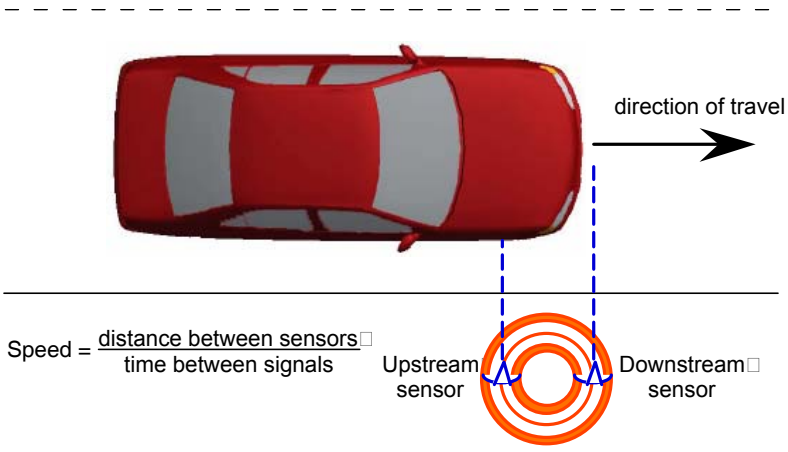

Figure 9. Vehicle speed measurement using paired proximity sensors

Selected Sensors

After accurate measurement of vehicle speed, low power consumption is the next most desirable feature of a battery-powered speed sensor. The following sections describe the evaluated technologies in the order of lowest to highest power usage: passive infrared, magnetic, active infrared, and ultrasonic.

Dual passive infrared

The pyroelectric detector is one of the most common types of passive infrared detector. It is commonly used in motion detectors for security products and in automatic door and lighting applications. It contains a crystalline element (e.g., lithium tantalite) whose ends become oppositely charged when heated and produces an output current proportional to the rate of change in the applied temperature.

An Infratec LME-345 (shown on the left side of figure 10) was chosen for this application. It contains two crystals connected in reverse polarity in parallel. One crystal is exposed to external radiation via a 2 mm square silicon window that passes light in the IR spectrum between 6000 and 15000 nm. The other crystal is blocked from outside radiation and is used to cancel out the effects of changing temperature due to self-heating and other ambient influences. A fresnel lens focuses the radiation on the window and is shown to the right of the detector. The assembled sensor (circuit board, detector, lens, and protective tube) is shown on the right side of figure 10. Many of the sensors used in human motion detection are configured in voltage mode and have electrical time constants in the 0.5 to 4 second range. For this application, the detector contained an embedded amplifier and operated in current mode with an electrical time constant around 20 ms.

Figure 10. Pyroelectric detector and fresnel lens and assembled sensor

Figure 11 illustrates how a dual sensor measures speed. The difference in the phase between the sensors is the quantity of interest. As a vehicle passes the barrel, the heat is detected first in sensor #1 and then in sensor #2. The sensor separation (nominally 0.5 m) divided by the time difference equals the vehicle speed. The actual output of the sensor is inverted, i.e., a positive change in temperature produces a negative voltage output. The time lag can be estimated by several different algorithms including, cross correlation, time between peak values, and time between peak rates of change.

Error! Objects cannot be created from editing field codes.

Figure 11. Differential Sensor Configuration

Figure 12 shows a barrel with two pyroelectric sensors aimed at a downward angle of approximately 24 degrees.

Figure 12. Pyroelectric Detectors on a barrel

Dual 3-axis magnetometer

Another way to detect a vehicle is by measuring the change in the earth's magnetic field due to the passage of the iron content in the vehicle. Figure 13 shows a 3-axis magnetic sensor hybrid (Honeywell HMC2003 – 3 permalloy magneto-resistive sensors with onboard signal conditioning) that was selected for this application. Each sensor (Wheatstone bridge and amplifier) can detect a field from less than 40 microgauss to ± 2 gauss. The sensors and amplifiers have high enough bandwidth for detection of ferrous objects (vehicles) at high speeds.

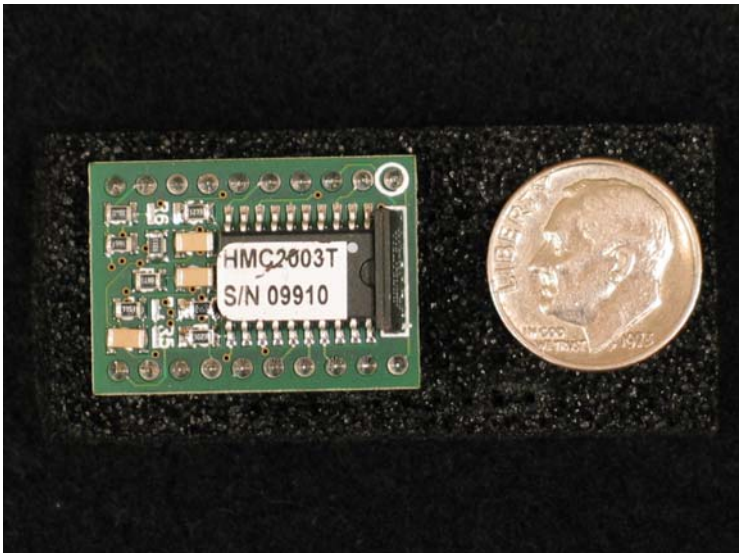

Figure 13. Honeywell HMC2003 3-axis magnetic sensor hybrid

Two issues complicate the use of this device. First, the semi-static earth's magnetic field must be removed from the sensor outputs so that the signals can be amplified 25-50 times to get enough resolution in the signal change caused by the vehicle. This bias is also a function of the orientation of the sensor axes relative to magnetic north. These biases were removed via the UMTRI DAS offset adjustments prior to each data collection period. Smaller normal fluctuations in the earth's magnetic field were not removed. Second, the sensors can be affected by momentarily high magnetic fields that can degrade the quality of the output (gain and crosstalk changes) in subsequent measurements. The sensor module includes a current strap to allow a strong restoring magnetic field to be applied to remove the effects of the upsetting field. A current pulse of 3-4 amps of approximately 2 microseconds in duration must be applied in both directions. The sensors were mounted to a prototyping circuit board and a pulse circuit (as suggested by the manufacturer's application notes) was wired. A DAS output triggered the pulses at five minute intervals. Figure 14 shows a close-up of a circuit board and the placement of the boards in a barrel.

Figure 14. Magnetometers mounted inside a barrel.

As with the pyroelectric sensors above, speed is calculated from the time lag between the first and second sensor. Signal strength falls rapidly as distance to the object increases. The z-axis signal and the magnitude (square root of the sum $x^2 + y^2 + z^2$) are the strongest presence detection indicators. The x-axis is nominally aligned tangential to the road and is used in the speed calculation. In the final application only one 3-axis sensor and one-single axis (x) sensor would be used to bring down the cost of the sensors and supporting circuitry.

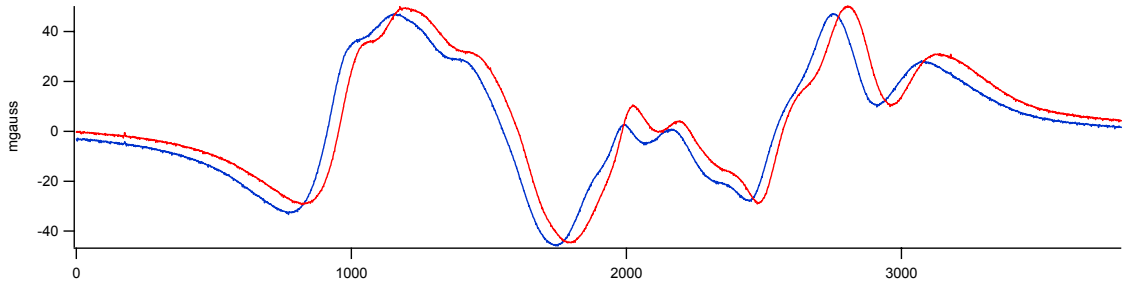

Figure 15. Left and right X-axis magnetometer signals for gravel hauler

A pair of the Banner Engineering M-Gage S18m detectors was also purchased. This detector has a 3-axis magnetometer and uses the magnitude to detect presence of a vehicle. It provides only a "vehicle detected" (yes/no) output. Two sensors were mounted to the test fixture about 18 inches apart. Passing vehicles were detected but, due to intrinsic filtering and use of the magnitude for detection, the time between detection activations could not reliably measure speed.

Dual active infrared

Because active photoelectric sensors react to light they emit, they see a more discrete (point source) target than a pyroelectric sensor responding to a large heat source or a magnetometer reacting to a distributed collection of ferrous material. They canproduce a binary signal: true, if a target is detected, and false otherwise.

Packaged active red or infrared sensors are available from several companies that target automated assembly or conditioning machines. A diffuse reflective sensor consists of an irradiating (usually infrared) element and an element photosensitive to the irradiated light in the same unit. The emitted light reaches the detector after being reflected from an object. Variation in the color and texture of the object will change the amount of reflected light and, hence, the detection range. Output light is modulated to differentiate it from external sources such as sunlight. Units are available with an output signal proportional to the distance to the object or a logical output that indicates an object is within a specified range. This technology consumes more power than the above two and also is more sensitive to ambient conditions. Speed is calculated from the time it takes an object to travel between the two sensor beams.

Two sets of different photoelectric sensors from Banner Engineering Corp were purchased and evaluated. The left picture in figure 16 shows the ruggedized housing and the transmit and receive lenses while the right picture shows the top view of the internal assembly. Both sensors are diffuse-mode models that use 880 nm infrared light.

Figure 16. Banner Engineering Corp. photoelectric sensor

The long-range Q45BB6DLQ5 model was examined first. It has a nominal current draw of 15 milliamps and has a beam pattern that is elliptical with a range of 6 feet and a maximum width of 2 inches. When mounted horizontally at a height of 20 inches it could pick up most vehicles in the closest lane but also reacted to reflectors on vehicles in the next lane. Next, it was pointed down about 7 degrees to eliminate objects from the next lane. This also caused heavy trucks to be missed because of the lack of sufficient reflection off of their dirty wheels.

The high-power Q45BB6DXQ5 model was examined next. It has a nominal current draw of 20 milliamps and has a beam pattern that is elliptical with a range of 10 feet and a maximum width of approximately 4 inches. It was judged to be acceptable for further testing, and so, two sensors were mounted to a barrel as pictured in figure 17.

Figure 17. Photoelectric sensors mounted to barrel

The mounting structure allowed the adjustment of the angle that the sensors were aimed with respect to the road. Figure 18 on the next page shows a picture of an eleven-axle tractor-trailer combination and the resulting outputs from the sensors.

Figure 18. Eleven-axle gravel hauler and corresponding optical outputs

Pulsed Doppler ultrasound

This solution is different from the side looking configurations already examined because it uses only one sensor mounted on the barrel that is focused towards oncoming traffic as shown in figure 19.

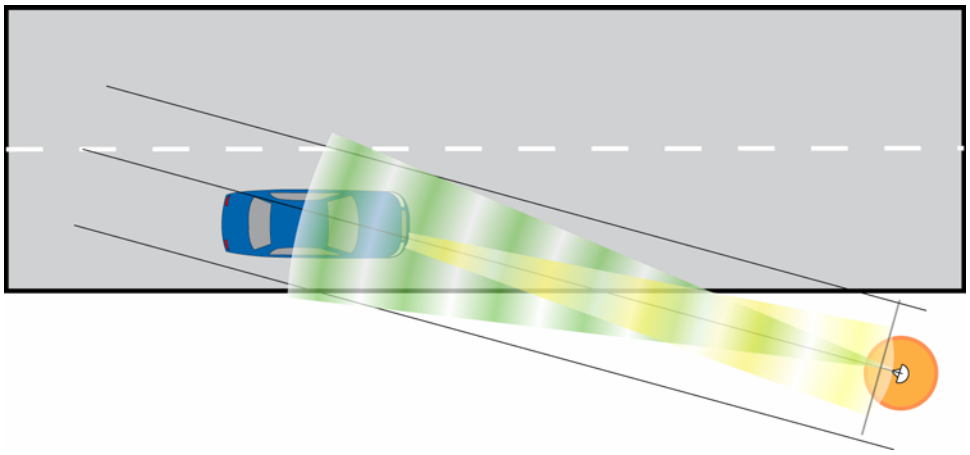

Figure 19. Speed measurement with pulsed Doppler ultrasound

A single piezoelectric transducer is used to transmit a series of pulses and then receive the reflected signal. Units are available with frequencies in the 30-50 KHz range, beam widths from 8 to 30 degrees, and ranges to 50 feet.

A microcontroller can calculate range by measuring the time lapse between the outgoing pulses and the reflected pulses. Speed can be calculated by measuring the frequency of the returning pulses and subtracting it from the outgoing frequency to yield the Doppler frequency. Because the speed of sound in air is a function of temperature, the ambient temperature must be measured and used to correct ranges.

The HE661 (Hexamite) signal conditioner interfaces with the company's line of ultrasonic sensors and outputs the range to the closest object and the speed of the object traveling at the maximum speed within the operating boundaries. After further consulting with the vendor, it was learned that the transducers had a narrow bandwidth and therefore would not reliably measure speeds above about 25 mph. Two ultrasonic development kits (sold by Airmar and SensComp) were purchased. A circuit to convert the return signal into digital form to estimate the return frequency was designed and wired. Reliable counting proved to be difficult because of missing pulses in tests performed in the parking lot. Further investigation and development was deemed beyond the scope of the project and so no ultrasonic solution was available for field testing.

A continuous ultrasonic Doppler solution would be more accurate and reliable but the power demand would be far too great for the battery-operated barrel system

Reference Speed System

To evaluate the accuracy of the above technologies an independent way of detecting vehicles and measuring their speed required a reference speed system to be developed. A Bosch ACC Radar was purchased. It measures and transmits range, range rate, transverse distance, and acceleration for up to eight targets on a controller area network (CAN) bus.

The radar sensor and a video camera were mounted in a barrel as shown in figure 20. An additional camera aimed perpendicular to the road was mounted on top of a barrel placed 15 to 20 feet from the roadway. The CAN bus and cameras were interfaced to an UMTRI FOT (field operational test) DAS. The DAS collected radar packets, JPEG compressed camera images and GPS timestamps.

Figure 20. Reference system barrel with video and radar

The radar data files were later loaded into a Microsoft, SQL Server database and synchronized to the sensor signals. A video viewing tool (see figure 21 on the next page) was modified to playback the video from the two cameras and show the radar targets. A researcher advanced the video at high speed to find vehicles directly positioned in front of the barrels. Manual detections were recorded and saved along with the automated detection data into the database.

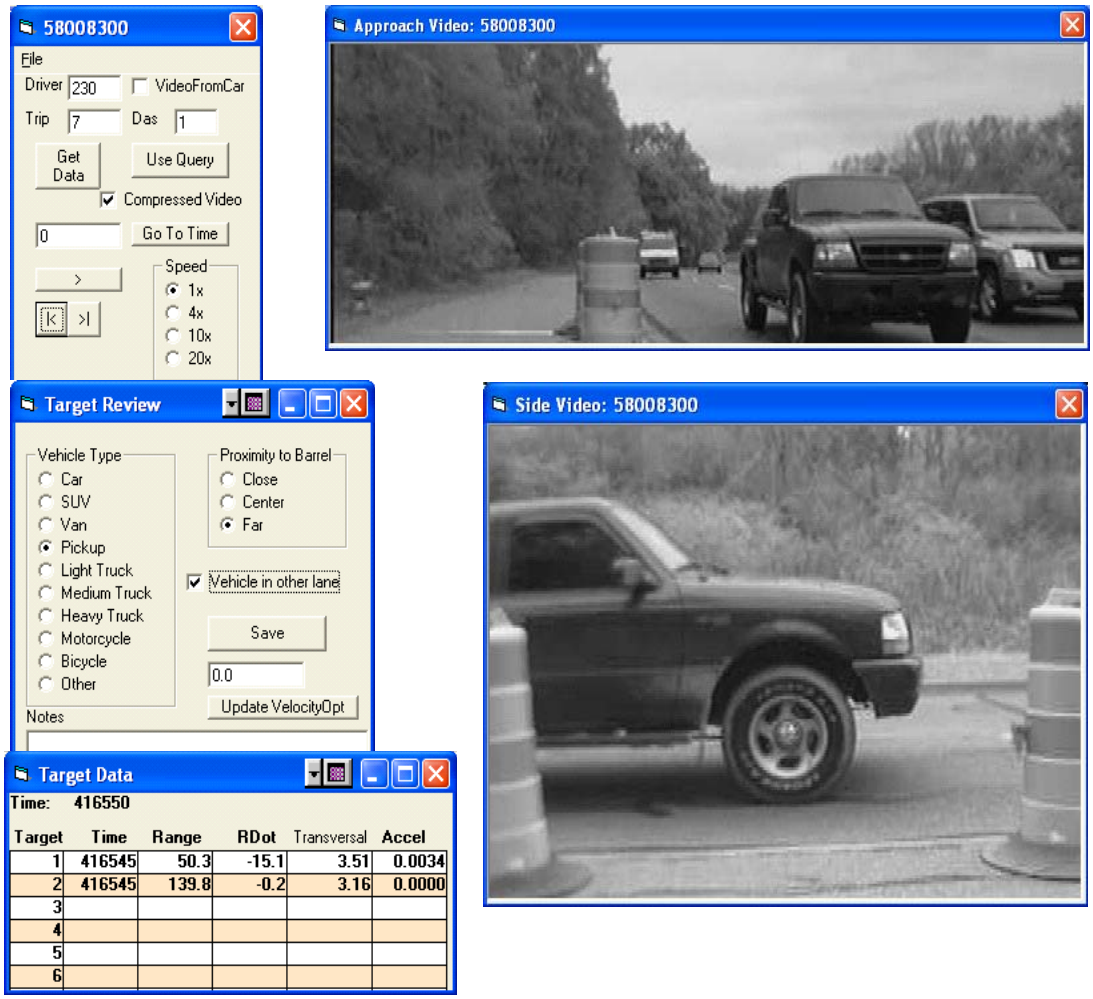

Figure 21. Vehicle identification and classification tool

The Field Test

Methodology

A limited field test of the three selected sensor types was conducted during October and November of 2004. The instrumentation setup for the field test was not autonomous nor secure, and thus required an attending technician. Consequently, the test was conducted at two sites relatively close to the UMTRI building and for short time periods.

The total time of data collection was just over eighteen hours. The locations and the qualities of the two test sites are shown in figures 22 and 23.

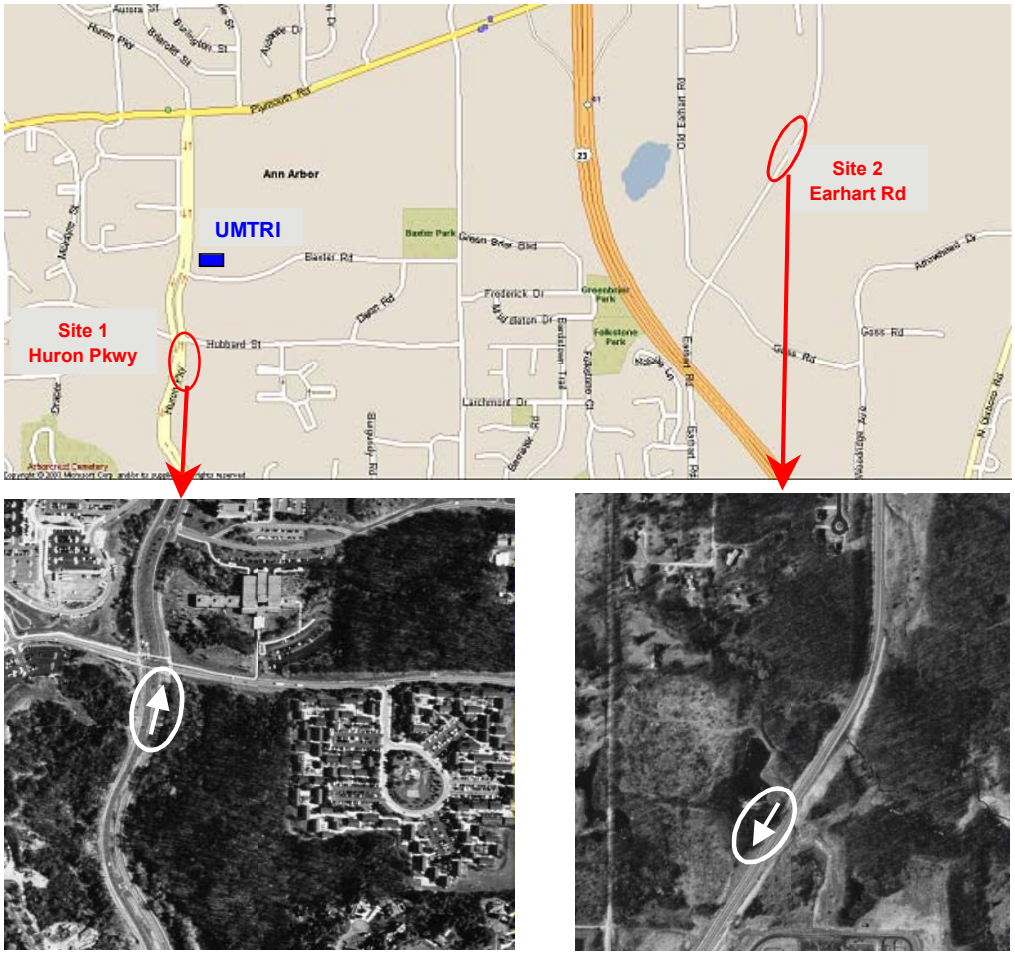

Figure 22. Locations and satellite-views of the two test sites

Test site #1 Test site #2

Figure 23. Photographs of the two test sites

Site #1 was located on the north-bound lane of Huron Parkway, south of the signalized intersection with Hubbard Road. This intersection is centrally located between the academic section of the University's North Campus to the southeast, a large area of student housing to the northwest, commercial research, retail, and private residential areas to the north and more university and private housing to the west. Huron Parkway is a major, four-lane surface road with average daily traffic (ADT) of approximately 8200 vehicles (Washtenaw Area Transportation Study, 1991-2000). Through traffic moved at a moderate speed (typically 25 to 40 mph). However, during stop signal phases, vehicles passed by slowly or even stopped in front of the sensors. Lengthy queues were typical at this site during morning and evening rush hours.

Site #2 was located a few miles east of UMTRI alone south-bound Earhart Road, a two-lane surface road. This site was in a much more rural setting than site 1 and was far removed from any intersecting roads. Traffic averaged about 50 mph through this site. This road was not as heavily traveled as Huron Parkway (ADT is about 2000 vehicles), but it serviced several industrial parks to the north and south, so that this site bore substantial traffic during the rush hours.

The nominal layout of instrumentation for both sites is shown in figure 24, using the specifics of site #1 as an example. There are five functional traffic barrels depicted in figure 24.[2]

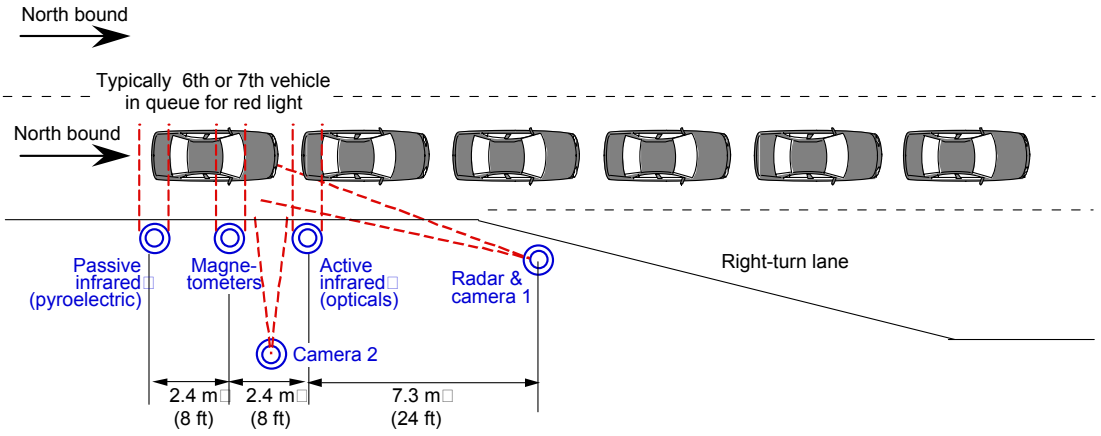

Figure 24. Instrumentation layout at test site #1 is typical of both sites

2. In figure 23, the picture at site #1 does not include the barrel with the passive infrared sensors. The barrels in the distance in the picture at site #2 are "real" traffic barrels associated with road repairs recently completed.

Farthest to the left (farthest upstream relative to the traffic flow) and next to the curb lane is the barrel containing the passive infrared sensors. Some 2.4 m (8 feet) downstream is the second barrel housing the magnetometers, followed by the third barrel with the active infrared sensors. (The details of sensor arrangement in these three barrels were described in the previous section.) Another 7.3 m (24 feet) downstream and near the curb is a fourth barrel housing a radar sensor and a video camera; both are aimed back at the traffic lane in front of the three sensor barrels. Finally, a fifth barrel, set back from the curb, holds a second video camera aimed at traffic passing the sensor barrels. The radar data and video from these latter two barrels provided the comparison standard (or "truth") speed data for evaluation of the sensors.

The data from all these barrels were captured using an adaptation of the UMTRI DAS developed for vehicle field testing. Objective data were collected at a sampling rate of 1 kHz under control of one CPU. A separate, but time-synchronized CPU managed collection of the video data at 10 frames per second.

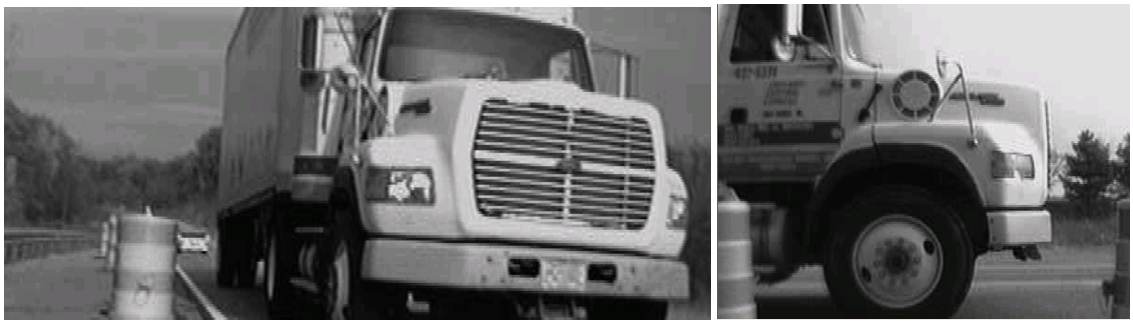

Camera #1 **Camera #2**

Figure 25. Stills from video taken at test site #2

As outlined in table 1, over 18 hours of data were gathered at these two sites. Numerous adjustments were made to the transducers and data acquisition system during the course of these tests (noted in the table).

Table 1. Field test data runs

Run ID		*Site*	*Date*	*Start*	*Duration, hrs*	*Notes*
120	1	Huron Pkwy	21-Oct-04	12:01:56 PM	0.84	1
121	1	Huron Pkwy	21-Oct-04	12:46:41 PM	0.74	
122	1	Huron Pkwy	21-Oct-04	1:52:29 PM	1.02	
123	1	Huron Pkwy	21-Oct-04	3:22:01 PM	1.47	
124	1	Huron Pkwy	27-Oct-04	12:16:07 PM	0.80	1,2
125	1	Huron Pkwy	27-Oct-04	2:07:58 PM	1.85	
126	1	Huron Pkwy	27-Oct-04	3:21:13 PM	1.14	
127	2	Earhart	28-Oct-04	3:25:02 PM	1.30	
145	2	Earhart	16-Nov-04	11:39:13 AM	1.40	3
146	2	Earhart	16-Nov-04	1:11:08 PM	1.51	
147	2	Earhart	16-Nov-04	2:41:11 PM	1.39	
148	1	Huron Pkwy	18-Nov-04	11:56:00 AM	0.92	4
149	1	Huron Pkwy	18-Nov-04	1:08:34 PM	1.14	
150	1	Huron Pkwy	18-Nov-04	2:17:25 PM	1.13	
151	2	Earhart	23-Nov-04	3:22:48 PM	1.44	5

Notes:
1. Adjust magnetometer gains.
2. Replace left active infrared (optical) sensor.
3. First runs with passive infrared (pyroelectric) sensors.
4. Adjust pyroelectric sensor gains.
5. Reposition optical sensors to top of barrel.

The adjustments were as follows:

- After runs 120 through 123, the amplifier gains on the x and y magnetometers were doubled to decrease the observed noise and to increase signal resolution.
- The left optical sensor missed many of the vehicle features detected by the right one. The sensors were examined in the laboratory and it was confirmed that the left sensor was significantly less sensitive than the right. A third sensor was substituted for the remaining tests.
- In runs 145 through 147, the pyroelectric sensors saturated a few times. The gains were halved (full scale doubled) for the remaining runs.
- The optical sensors were moved to the top of the barrel in run 151 to test a configuration that would be easier to manufacture than the mid-barrel configuration.
- The pyroelectric sensors were not introduced until the second half of the testing (run id 145).

The data analyses that follow in the next section of this report are therefore based these later runs only.

Data Analysis

As was noted in the previous section, data analysis focused on the final seven data runs of the field test. These runs provided a total of 8.9 hours of data, 3.2 hours at site #1 and 5.7 at site #2. Figure 26 presents histograms of the speeds of all the vehicles passing through the two sites, respectively, in these runs. The histograms show that, although data were collected for nearly twice as much time (1.8) at site 2 than at site 1, because of the higher traffic volumes at site 1, the ratio of the number of vehicles observed at the two sites was close to unity (845/782 = 1.1). The distributions of speeds are both asymmetric with larger tails at the lower velocities. The average speed at site 1 (29.0 mph) was less than that at site 2 (48.2 mph) and site 1 provided numerous samples at very low speeds (113 samples under 20 mph).

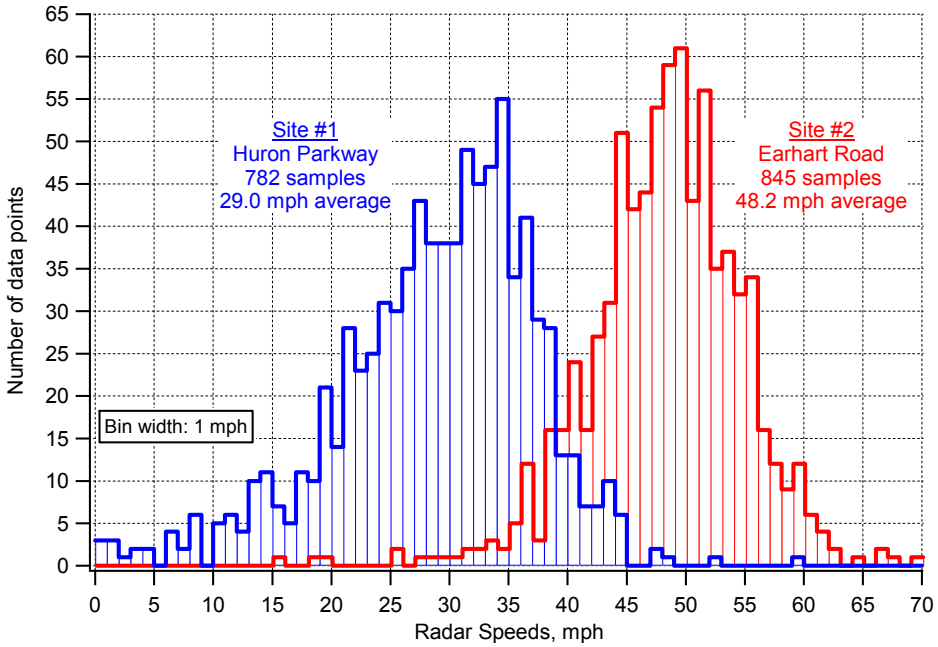

Figure 26. Histogram of vehicle speeds measured by radar during runs 145 through 151

Apart from the difference in average speed, the sites also differed in the degree of speed variation. At site 2, most vehicles passed through at a nearly constant speed. At site 1, however, because of the traffic signals, many vehicles were in the process of accelerating or decelerating as they passed through. This variation in speed caused some conceptual and practical difficulties in determining the appropriate speed of the vehicle measured by the various sensors. That is, not only does the measured speed vary as the vehicle passes from barrel to barrel, but appreciable change in speed may also occur within the view of a single sensor.

The reference speed measurements

The reference speed measurements that form the basis for figure 26 and provide the "truth" data for the analyses that follow were derived from the scanning radar sensor used at each of the test sites. These reference speed measurements were reduced from the data by individual inspection. A programmer/analyst, viewing both measurement and video data provided by cameras 1 and 2, developed a table of precise time marks identifying when each vehicle traveling in the nearest lane passed the sensor barrels. The radar data were then reviewed at and near these time marks to determine the best estimates of the speed of the vehicle as it passed each of the three sensor barrels. These measures can only be called estimates for the following reasons.

Speed measurements of fast-moving vehicles (e.g., 55 mph or 25 m/sec) were not always available in close proximity to each of the three sensor barrels. This was due to the fact that the scanning radar used for these measurements had an effective update rate of only 10 Hz. Moreover, the radar did not always report every target at every 0.1-second interval. However, for such fast-moving vehicles, it is typical that very little change in speed occurs between the time of the closest radar speed measurement and the time the vehicle passes an individual barrel. Consequently, the last radar speed measurement taken as the vehicle approached the barrel was used as the reference speed for that vehicle at all three barrels. This speed measurement, along with range measurements, were used to estimate when the vehicle passed each of the three barrels. (That is, for each vehicle, separate time marks were created for each sensor barrel in order to facilitate matching that particular radar speed measurement with the measurements of each sensor barrels.)

With slower moving vehicles (particularly at site #1), a vehicle's speed often changed substantially as it passed from barrel to barrel. Such vehicles were either decelerating, while stopping for a red light, or accelerating, when pulling away with a green light. In this case, although radar speed measurements were more likely to be available near each barrel, the rate of speed change was sufficient to justify interpolating between measurements to determine a vehicle's speed and time at which it passed each barrel.

Automated algorithms were developed to apply these approaches at each of the original time markers established from the initial review of the video. All of the results, however, were given a final review by the programmer/analyst and compared to the raw radar data to check their validity.

Speed measurements derived from the sensor data—general approach

The data provided by each of the three pairs of sensors were reduced to produce estimates of vehicle speed for comparison to the reference radar speed measurements. The basic philosophy of the data reduction method was similar for all three cases. That is, each measurement barrel housed two identical proximity sensors at a known, horizontal spacing and with their sensitive axes parallel to one another and perpendicular to the direction of their spacing. The barrels were placed at the site such that this spacing was parallel to, and the sensitive axes was perpendicular to, the direction of travel of the target vehicles. Ideally, as a vehicle passes a barrel the two sensors should produce identical signals, one delayed in time relative to the other such that:

$$(\text{vehicle speed}) = (\text{sensor spacing})/(\text{signal time shift}) \qquad (3)$$

Of course, the difficulty lies in the fact that this characterization is ideal and the reality is not. The two sensors are never precisely identical, the sensitive axes are never precisely parallel to each other, nor precisely perpendicular to the direction of travel—vehicles do not all travel in precisely the same direction. Thus, the resulting two signals are never identical. In addition, the sensors may detect more than just the position (proximity) of the target vehicle. That is, the signals contain substantial noise of various types.

Accordingly, specialized data reduction procedures were developed for each type of sensor. Each procedure had two basic tasks: to detect the presence of a passing vehicle (or group of closely spaced vehicles) and to determine its speed. The following subsections outline the approaches taken.

Over the many speed measurements made, each of the procedures occasionally produced obviously incorrect speeds (some very large negative as well as very large positive values). In addition, as will be described later, the magnetometers often sensed vehicles in the far lane, traveling in the opposite direction, and "correctly" reported a negative speed. Thus, for all methods, "reasonable" limits of 0 (or slightly above zero when required mathematically) and 80 mph were assumed, and measurements of speed (or equivalent measures of time shift) outside this range were discarded. (These discards are included in counts of "missed vehicles" to be reported.)

Processing data from the active infrared, optical sensors

Two methods were used to estimate vehicle speed based on the signals generated from the two optical sensors. The two sensors were mounted on the side of the construction barrel at the same height and nominally 0.55 m apart, as shown in figure 24. They were oriented such that their "lines of sight" (axis of the focused, sensitive beam) were parallel to one another and perpendicular to their spacing. They were also tilted such that the line of sight sloped downward away from the barrel with the intent that the sensitive beam was at the appropriate height for vehicles in the lane adjacent to the barrels, but would not sense vehicles in lanes farther from the barrel. (Some adjustments to mounting height and angle were made over the course of the test.)

The two sensors produced signals with only two states: zero and one, equivalent to "object not present" and "object present," respectively. Differences between the two signals, other than the nominal time lag, can derive from a variety of sources. For example, the leading face of many vehicles is sloped and irregular. Small differences in beam orientations or ride motions of the vehicle may result in different triggers for the two sensors. Reflectivity of different vehicles and different components on a vehicle can be radically different. A beam set nominally to bumper height for cars will see only the tires and wheels of large trucks. While both methods described below estimate the speed of a passing vehicle by dividing the distance between each sensor by the amount of time that elapses between the equivalent state change of each sensor, the difficulty, of course, is to properly find the correspondence between the two signals, given the types of inconsistencies noted.

Both methods developed divide the long-term signal stream into passing-vehicle events. Each such event is distinguished from other events by periods of no less than 500 ms during which no vehicle is sensed by the upstream sensor. That is, when the upstream sensor's signal first goes high, an event is started and continues until this same signal goes low for no less than 500 ms. Thereafter, an new event would begin on the next occurrence of a high state of this sensor.

The first analysis method compares the first and last transition times for each sensor during a passing-vehicle event, ignoring any "chatter" of the signals during the event. An example of this method is illustrated in figure 27.

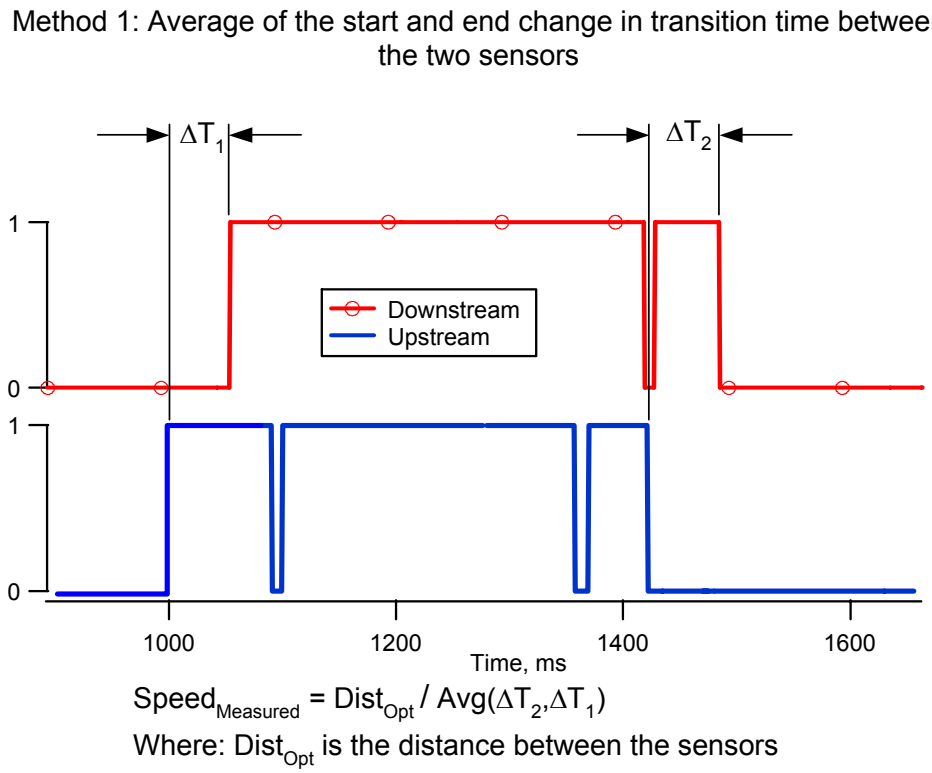

Figure 27. Method 1 for the optical sensor speed estimation

The figure shows the signal from each sensor (upstream and downstream, respectively) as a function of time, measured in milliseconds. The first elapsed time estimate, ΔT_1, is calculated by taking the difference in time when each of the two signals initially transition from a value of zero to a value of one. Similarly, the second change in time, ΔT_2, is derived by taking the difference in time when each of the two signals made their final transition from one to zero. Note that while there are other transitions from one to zero and from zero to one within this event, only the first rising and last falling transitions are used.

The two elapsed times determined are first compared to the acceptable range (in this case, 2 to 227 ms, corresponding to estimated speeds of 1 to 80 mph) and are discarded if they are outside the range. If both values are retained, they are averaged and the result used to determine speed according to equation 3 If only one is retained, it alone is used to calculate speed. If both values are rejected, no speed is calculated.

The second method considers all the observed transition times for each sensor during a passing-vehicle event and selects a "most likely" subset to characterize the event. Initially, the method obtained (1) elapsed times between each rising transition in the upstream data and all *subsequent* rising transitions in the downstream data and (2)

elapsed times between each falling transition in the upstream data and all *subsequent* falling transitions in the downstream data. The first step is illustrated in figure 28. (Note that this figure is based on the same time histories as were presented in figure 27.)

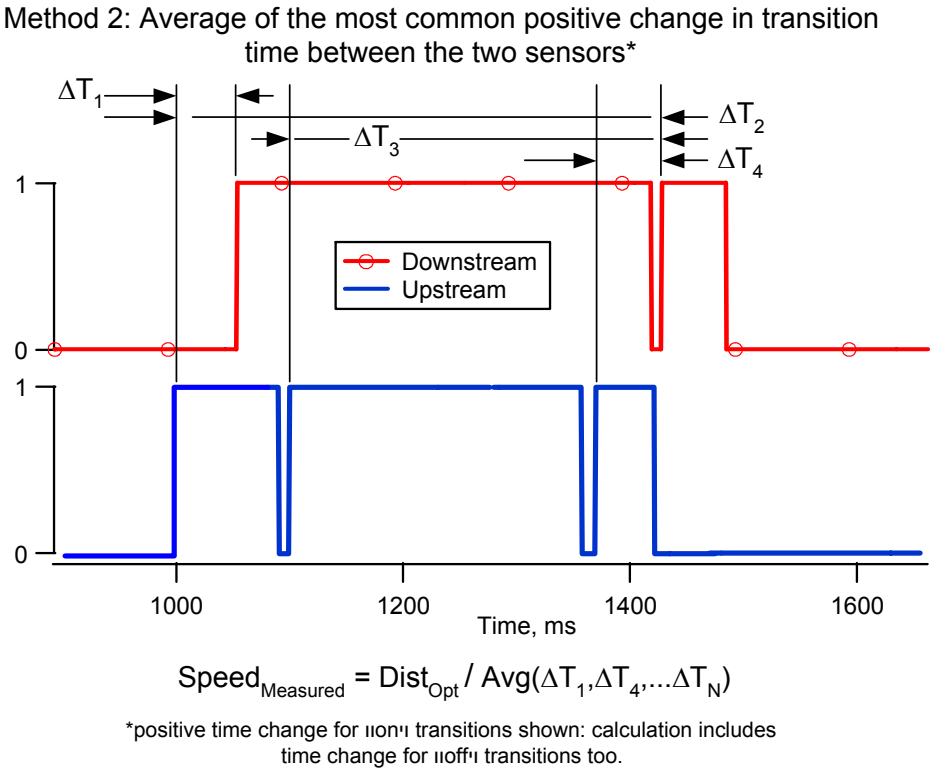

Figure 28. Method 2 for the optical sensor speed estimation

For these data, four elapsed times are determined for rising transitions. For the first rising transition of the upstream data, there are two subsequent rising transitions of the downstream data yielding ΔT_1 and ΔT_2. The second and third rising transitions in the upstream data each have just one subsequent rising transition in the downstream data yielding ΔT_3 and ΔT_4, respectively. Although not shown in the figure, the same process also applied to falling transitions yields five additional elapsed times, ΔT_5 through ΔT_9. Following this initial determination of "ΔT's," the tabulated values are grouped (using a ±3 ms tolerance) and the one set with the largest count of values is averaged and used in the calculation of estimated vehicle speed. If two or more of the grouped values have equal counts, then the smallest averaged ΔT is used in the speed estimation based on the assumption that it is more conservative to over-estimate speed. Similar to method 1, any individual ΔT with a value outside of the acceptable range is discarded before averaging.

Processing data from the passive infrared, pyroelectric sensors

Two methods were used to estimate vehicle speeds based on the signals generated from the two passive infrared, pyroelectric sensors. These two sensors were mounted on their barrel in a manner similar to that of the active infrared, optical sensors. That is, their focused fields of view were parallel to each other, perpendicular to the direction of vehicle travel, and sloped downward away from the barrel to select vehicles in the near adjacent lane, while ignoring vehicles in lanes further away.

These sensors essentially respond to the changes in temperature within their spatial field of view. They produce an analog signal proportional to the rate of change of sensed temperature. For these particular sensors, the signal is inverted such that rising temperature produces a negative signal. Since a passing vehicle can be seen as a time-series of multiple heat sources, including the front tires, engine, body, rear tires, and exhaust gas and wake turbulence, the resulting time history can be rather complex.

Figure 29 presents two sets of time histories from the pyroelectric sensors. The vertical scales in the graphs of this and other figures in this section are relative only, and show the fraction of "full scale" as determined by the gain settings of the DAS. The graph at the top of the figure presents data typical of a rather "clean" pass of a passenger car. The lower graph presents a more complex signature of a tractor-semitrailer combination.[3]

3. Note that the data from which all the figures in this section are made have been "zeroed" as the first step in post processing. In the field, there was appreciable low-rate, long-term drift of the signals that was only dealt with after the fact in this project.

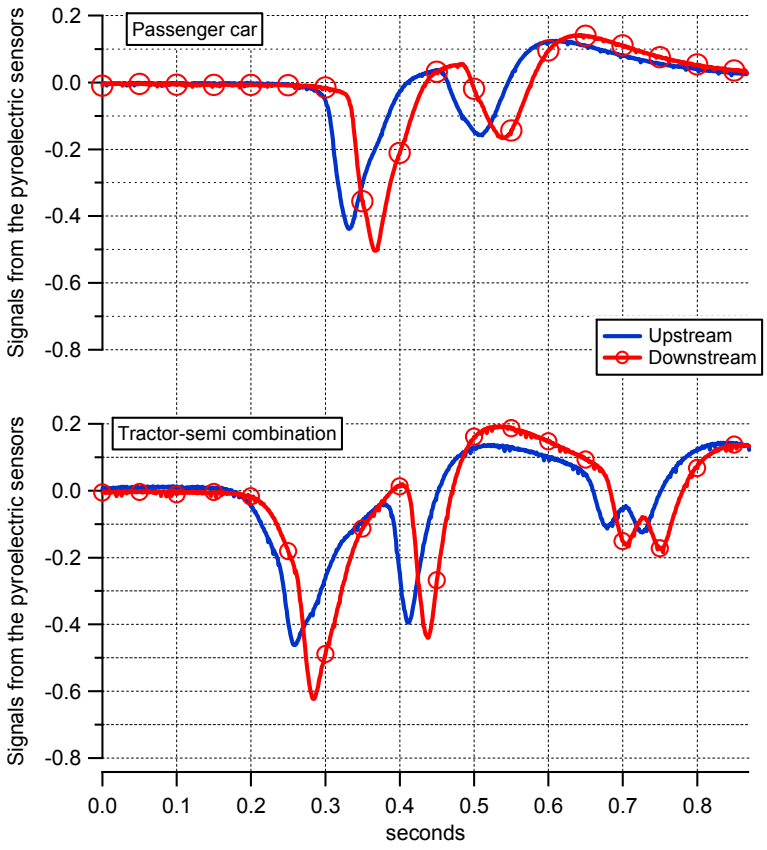

Figure 29. Signals from the pyroelectric sensors for a passenger car and a tractor-semitrailer combination

Nominally, we believe the first, large (negative) peak derives primarily from a combination of front tire and engine heat. Later negative peaks are likely from tires of the following axles while the tapering ends of the signals appear to be associated with wake disturbances. The time histories of the figure all derive from vehicles passing in the near lane. Traffic in the far lane may also produce noticeable, but lower level signals, presumably due to air turbulence. Occasionally, other disturbances were found in the data that were largely unexplainable.

The procedure used to identify a passing-vehicle event for the pyroelectric data is represented in figure 30. The procedure is similar in concept to that described for the optical sensors, but since the pyroelectric signals are analog in form (not binary), the details are different.

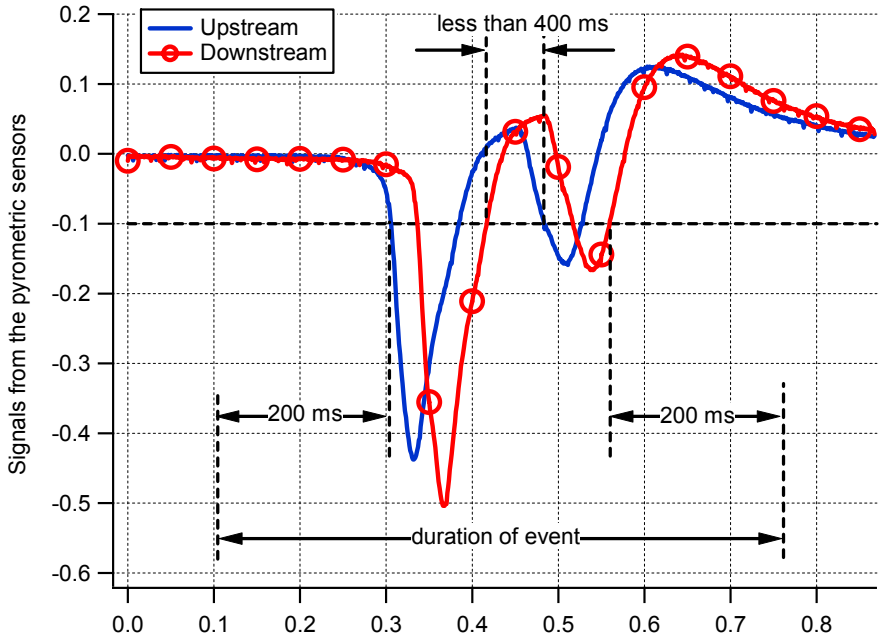

Figure 30. Identifying a passing-vehicle event from the pyroelectric signals

In this case, each event is distinguished from other events by periods of no less than 400 ms during which the signal strength does not exceed (negatively) an established minimum (negative) threshold. The threshold used was -0.1 (of full scale and with the signals "zeroed" as noted). Having established this initial identification of an event, additional periods of 200 ms each were added to the beginning and end of the event in order to more fully capture the initial and final transients (which typically contain important information for characterizing the time shift between signals). Data within the resulting time span were analyzed as a single vehicle-passing event (although, as with the other sensors, the event may include stimulation from multiple, closely grouped vehicles).

The first method used to evaluate these events applied a straightforward cross correlation of the two signals to determine the representative time shift between the upstream and downstream signal. The correlation process compares the two time histories in the frequency domain and produces a function describing the relative "strength" of time shifts between the signals. The correlation function that results

from the data of figure 30 is shown in figure 31. The peak of the function is seen to occur at a value of 0.032 seconds. This value would then be used as the characteristic time shift in the calculation of speed for this event.

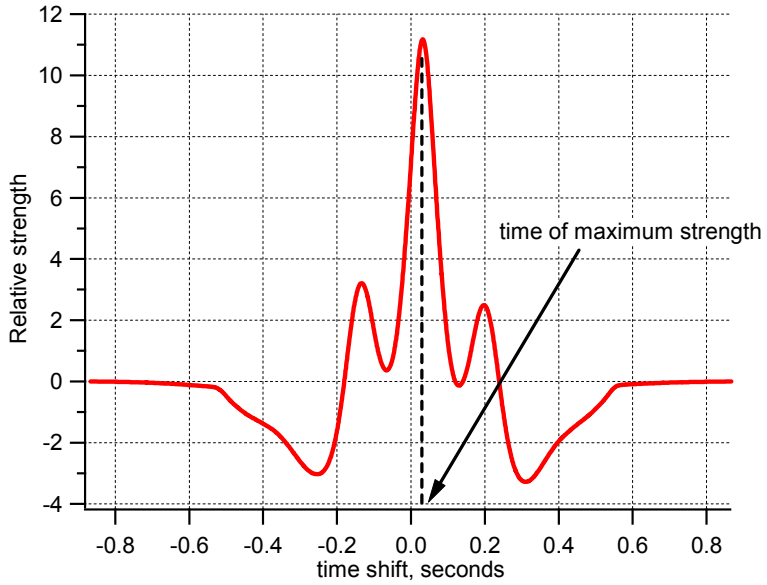

Figure 31. Correlation function for the data of figure 30

This method is computationally expensive and, therefore, may not be applicable in an actual device for use in the field (although, given the seemingly exponential improvement in inexpensive computing capability, it may very well become reasonable before such devices are actually produced for the field). Nevertheless, it may provide a good indication of "the best" that can reasonably be expected from the use of the sensor in a smart-barrel approach to speed measurement. Details of results will be presented in later sections, but this method proved sufficiently encouraging to warrant an attempt at a computationally simpler method.

The second method used to characterize the time shift between pyroelectric singles concentrated on the point of maximum rate of change of the signal.[4] Both signals are initially smoothed with a digital filter.[5] Subsequently, both signals are differentiated

4. Preliminary analyses also investigated using the time shift between the peak (negative) values of the two signals. However, in many cases these peaks were either noisy or relatively "flat" such that this was not a reliable method. On the other hand, the initial transients of an event was typically quite sharp.
5. A binomial function spanning 201 samples or 200 ms was used. This was the most computationally expensive portion of the procedure, but such an elaborate digital filter may not be required, particularly if electronic filtering of the signal were optimized.

and the time of the peak negative value of the differential time histories, which corresponds to the maximum negative rate of the primary signal, are identified. The time difference between these peaks is used as the characteristic time shift for this event. The approach is shown graphically in figure 32 where the lower graph shows the original sensor signals and the upper graph shows the derivative functions. ΔT is the characterizing time shift.

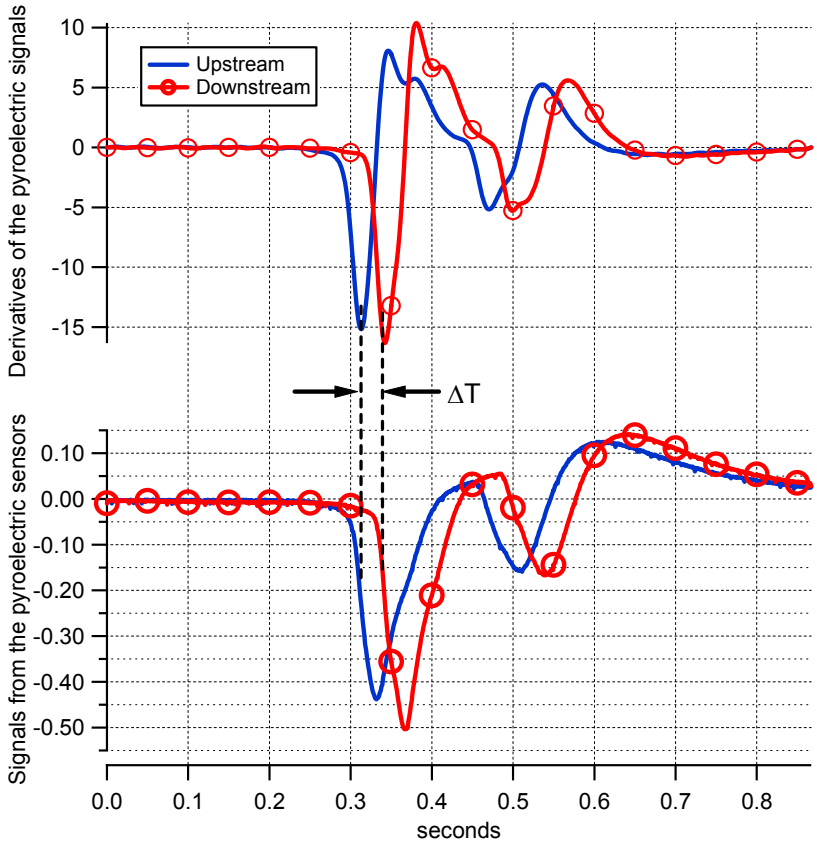

Figure 32. Differentials of the pyroelectric signals used to identify the characteristic time shift between signals

Processing data from the magnetometers

Data collected from the magnetometers were processed to determine several estimates of vehicle speed. All the procedures were similar to the correlation method applied to the pyroelectric data explained in the previous section, and differed only in the source data used. That is, the magnetometers used in this experiment measured and reported the change in magnetic field along three rectilinear axes (X, Y, and Z). The devices were oriented in the barrels such that X was in the direction of travel, Y was horizontal and perpendicular to the direction of travel and Z was vertical. In addition

to examining each of these signals separately, the three were combined to produce a "magnitude" signal, M, where

$$M = \sqrt{X^2 + Y^2 + Z^2} \tag{4}$$

This measure was also examined.

The magnetometers respond to changes in the magnetic field at their own position as generated by changes in surrounding conditions: in this case, passing vehicles. Consequently, they could not be "aimed," as was the case with both the active and passive infrared sensors. Specifically, these sensors respond to passing vehicle (actually passing ferrous material) in proportion to a combination of their distance from the sensor, speed, and mass. Figure 33 on the next page reveals some of the complicating consequences of this. The figure presents a total of twelve graphs, four graphs (arranged vertically) for each of three passing vehicles (arrange horizontally). From top to bottom, the graphs present the signals for the X, Y, Z and M measurements.[6] From left to right they present data from a passenger car, a tractor-semitrailer combination, and a double-bottom gravel train. The passenger car and tractor-semi are the same vehicles used in previous examples; they were both in the adjacent (near) lane and traveling in the intended direction for speed measurement. The double, however, was being driven in the far lane and was traveling in the opposite direction. (Note that despite the reversal of direction, the labels "upstream" and "downstream" remain applicable to the same sensors).

.

6. Like the pyroelectric signals, these magnetometer signals also have been "zeroed" during post processing.

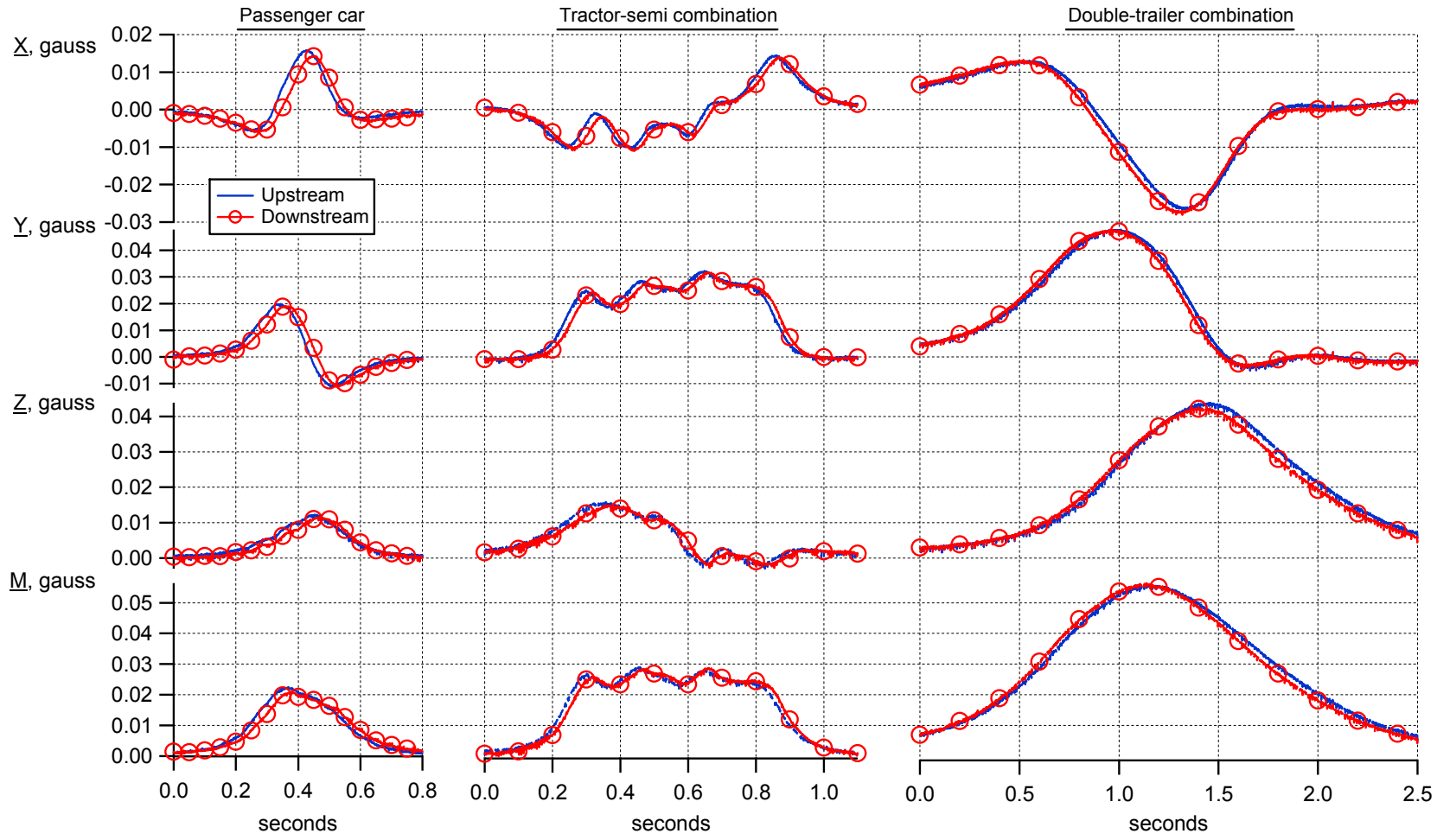

Figure 33. Magnetometer data for a passenger car, a tractor-semitrailer combination and a double-bottom combination

The figure shows that the signals generated by the tractor-semi are both longer in duration and somewhat stronger than those from the passenger car, although perhaps not as much stronger as might first be expected. The trailer of this vehicle was a common van, likely constructed largely of aluminum. The freight was apparently non-ferrous as well. In contrast, the double bottom combination was a gravel hauler and both of its trailers were likely constructed of steel. Consequently, even though it passed further from the barrels, it produced much stronger signals. In addition, two qualities also show that this vehicle was headed in the opposite direction: (1) the relationships between the signals of the "upstream" and "downstream" sensors are reversed in time, and (2) the form of the response of the X signal (along the direction of travel) is inverted (both along the ordinate and the abscissa). As a matter of interest, note that a similar reversal would take place in the Y signals were a vehicle to pass by on the opposite side of the barrel.

Figure 34 highlights another significant quality of the signals from the magnetometers by comparing them to the signals from the passive infrared, pyroelectric sensors. In this figure, the X, Y and Z signals from the magnetometers are presented in the top three graphs and the bottom graph shows the signals from the pyroelectric sensors. All signals are responses to the passing of the passenger car. (The signals from the two barrels have been shifted in time appropriately so that the time scales are all relative to the passing of the sensor's own barrel.) Most importantly the figure clearly shows that the transients of the magnetometers signals are much more gradual than those of the pyroelectric signals. The implication would be that precise time-phasing information may be more difficult to obtain from the magnetometer. Also of interest is the fact that the magnetometer's three signals have relative time shifts to one another. The Y response leads and the Z signal is last. The initial peaks of the Y signals are fairly well aligned with those of the pyroelectric signals.

Figure 35 again presents the data from the passing passenger car where the forth graph at the bottom of the figure presents the calculated magnitudes of the combined magnetometers signals. It is these magnitude signals that are used to identify passing-vehicle events. Given that the reference signal is the combined magnitude, the process

is virtually identical to that described for the pyroelectric sensors except that the threshold signal value is 0.014 gauss.[7]

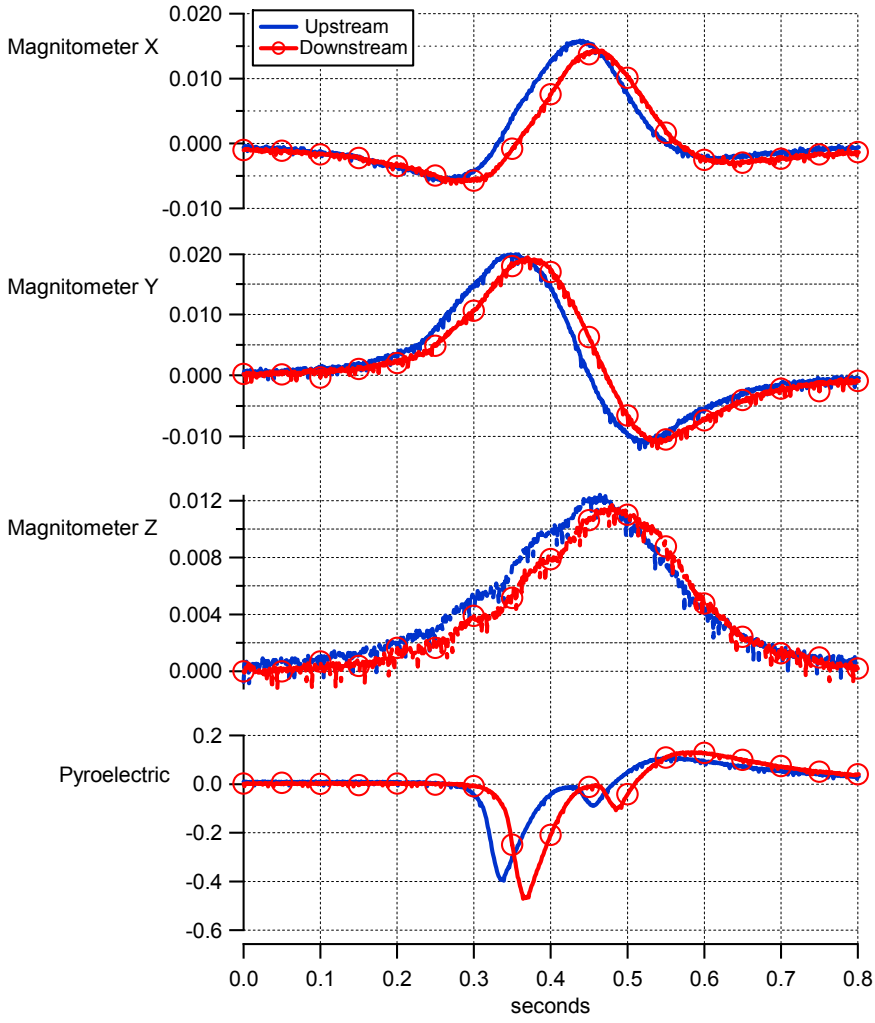

Figure 34. Comparison of signals from the magnetometers and from the passive infrared sensors in response to a passing passenger car

7. The actual process calculates and test M^2, not M, thus reducing calculation expense by avoiding the need for a square root operation. In this case, the threshold of 0.014 gauss depicted in the figure is equivalent to the actual threshold of 0.002 $gauss^2$.

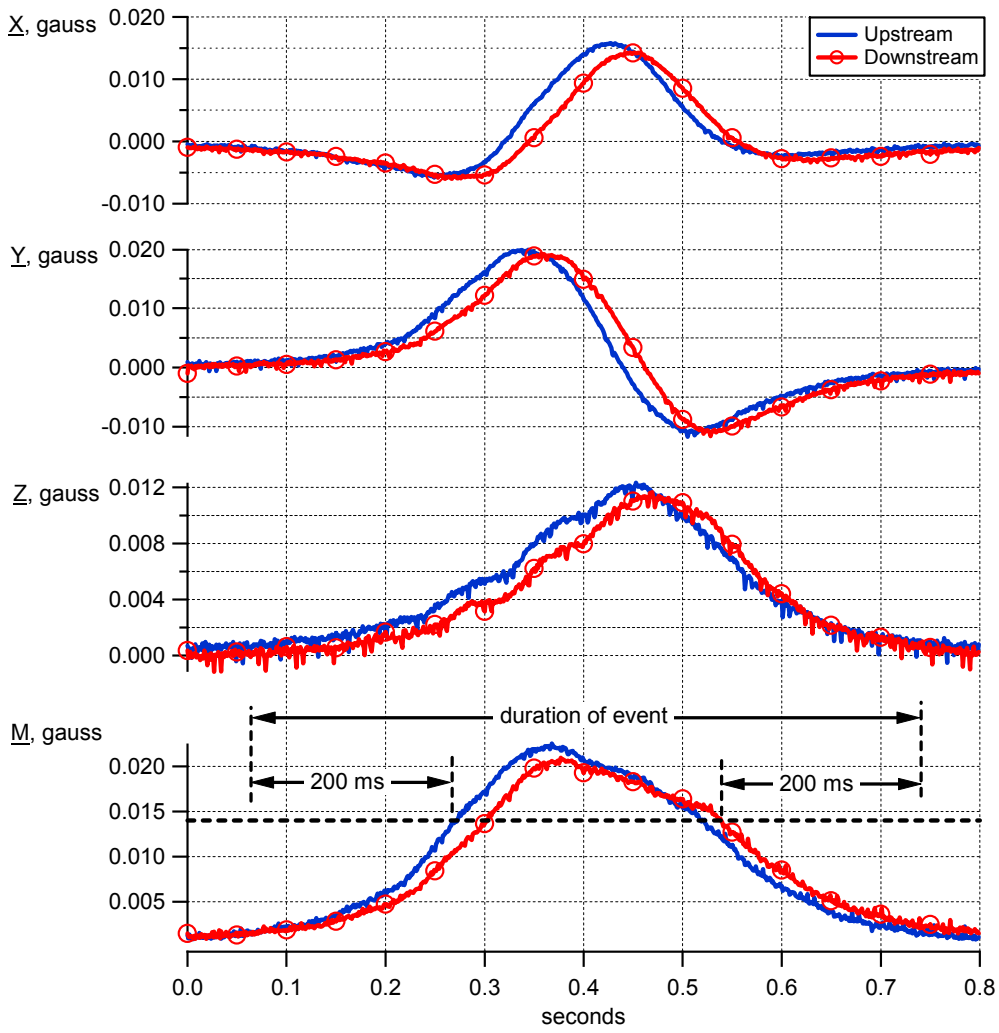

Figure 35. Identifying a passing-vehicle event using the magnetometers signals

Having identified passing-vehicle events, each of the four signal pairs (i.e., the X pair, Y pair, Z pair and M pair) were evaluated to obtain a characteristic time shift and each result was used to determine vehicle speed. In all, four time shifts were determined using the correlation procedure described as method 1 for the pyroelectric data. No other procedures were applied to the magnetometer data.

Results: Comparing Speeds Measured By The Three Sensors

The evaluation criteria for the each of the three sensor types is, of course, accuracy of the measured speeds. However, "accuracy," in this case, has several elements.

The primary measure of accuracy was the standard deviation of measurement error derived from comparing the speeds measured by the experimental sensor to the reference speeds measured using the radar system. The error was determined for each

individual measurement of the experimental sensors that could be matched to an individual radar-based measurement. The average and, most importantly, the standard deviation of those errors were calculated for each combination of sensor and data reduction method. Of these two measures, standard deviation of the error is seen as the most important measure, because, in practice, reducing the *average* error to zero is simply a matter of calibrating the system gain through appropriate adjustment of the value used to represent spacing between the two sensors. The standard deviation of error, on the other hand, can not be "adjusted away." Indeed, as an additional step in the analyses, each set of matched measured speeds were adjusted by the appropriate ratio to result in a set of measurements whose average was equal to the average of the matching radar speeds (i.e., the resulting *average* errors were zero) and the standard deviations of the errors were then recalculated.[8]

In addition to the set of experimental speed measurements that could be matched to reference measurements, each combination of sensor and reduction method also produced some false positive readings (i.e., produced "measured speeds" that could not be matched to radar speed data) and also failed to produce measurements for vehicles that were, indeed, present and whose speed was measured by radar (i.e., completely missed or produced out-of-range measurements). Thus, two additional important measures of "accuracy" are the percent of missed vehicles (i.e., percent of radar measurements not matched by experimental measurements) and the number of false positives (also expressed as a percent of radar measurements).

Throughout the following, the reader should keep in mind that the resolution of all of the experimental systems under evaluation was fundamentally limited by the spacing of the sensor in a single barrel (nominally 0.5 m) and the fixed sampling rate of 1 kHz used in these experiments. For such an approach (fixed spacing and fixed sampling rate), the resolution of speed measurement is proportional to the square of speed. Thus, at low speeds, the resolution of speed measurement is quite fine, but at high speeds it becomes rather coarse. The combination of 0.5-meter spacing and 1-kHz sampling results in a resolution of just 1.4 m/s or 3.2 mph at 60 mph. In actual

8. This amounts to a gain calibration of the system during post processing. It is justifiable in as much as the general plan for deploying smart barrels at real work zones involves calibration of individual barrels at the site through several passes of the a set-up/calibration vehicle(s) traveling through the site at known speeds.

application (i.e., with one, rather than three sensor pairs, and no radar and no video), either more rapid or interrupt-driven sampling could improve resolution substantially.

To help provide the reader with an intuitive sense of the results, figure 36 presents histograms comparing the speeds measured at site 1 (Huron Parkway) using the active infrared (optical) sensors and the first method of data reduction (first and last transitions) to the reference speeds; only the matched measurements from the experimental and reference speed data are used. (The data shown in figure 36 are among the best results of the study.

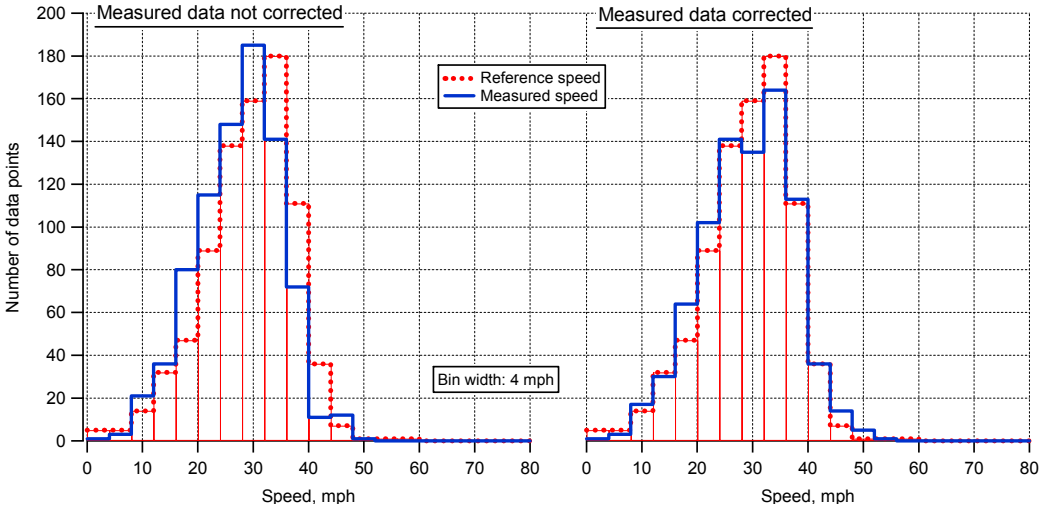

Figure 36. Comparison of matched measured and reference speeds: test site #1, optical sensors, method 1 reduction, with and without gain correction

Similar figures for each combination of the test site, sensor type, and reduction method are presented in appendix B. The bin widths in these histograms are a rather coarse, 4 mph, required because of the measurement resolution issue described above.) Two sets of superimposed histograms are presented. On the left, the measured speeds are not corrected for gain. In these data, the average speed values of the reference and measured speeds are 29.2 mph and 27.4 mph, respectively. On the right, the measured speeds have been "corrected" by multiplying each by 1.07 (29.2/27.4). Thus, on the right, both sets have an average value of 29.1 mph. The standard deviation of the error in measurement for the uncorrected data was 3.28 mph; after correcting the average, the standard deviation of error was 3.36 mph. Table 2 presents similar measures of averages and standard deviations for all sixteen combinations of sensor, reduction method, and test site.

Table 2. Review of the statistics of measured speeds

			Average speed, mph		Standard deviation of error, mph	
Sensor	*Reduction method*	*Test site*	*Uncorrected*	*Corrected**	*Uncorrected*	*Corrected*
Active infrared, Optical	first & last transitions	1. Huron Pkwy	27.41	29.24	3.28	3.36
		2. Earhart Rd	47.69	48.39	4.66	4.73
	all transitions	1. Huron Pkwy	28.21	29.24	4.19	4.28
		2. Earhart Rd	48.65	48.39	3.12	3.11
Passive infrared, Pyroelectric	correlation	1. Huron Pkwy	31.29	29.77	4.39	4.17
		2. Earhart Rd	47.67	48.25	4.20	4.25
	maximum slope	1. Huron Pkwy	26.67	29.72	6.89	7.56
		2. Earhart Rd	44.23	48.26	4.87	5.27
Magnetometer	correlation, X signal	1. Huron Pkwy	29.63	29.39	9.80	9.73
		2. Earhart Rd	54.97	48.05	8.02	7.09
	correlation, Y signal	1. Huron Pkwy	34.95	29.20	8.80	7.54
		2. Earhart Rd	55.58	48.03	7.36	6.45
	correlation, Z signal	1. Huron Pkwy	39.25	29.29	12.09	9.42
		2. Earhart Rd	62.25	47.03	10.00	8.00
	correlation, Magnitude	1. Huron Pkwy	34.80	29.43	12.94	11.17
		2. Earhart Rd	55.46	47.52	11.35	9.89

* Note: Average of the reference speeds is identical to the average of the corrected measured speeds

Figures 37 and 38 provide graphical comparisons of the standard deviation values presented in table 2. Figure 37 presents the values for the uncorrected speed measures, and figure 38 presents the values for the corrected measures.

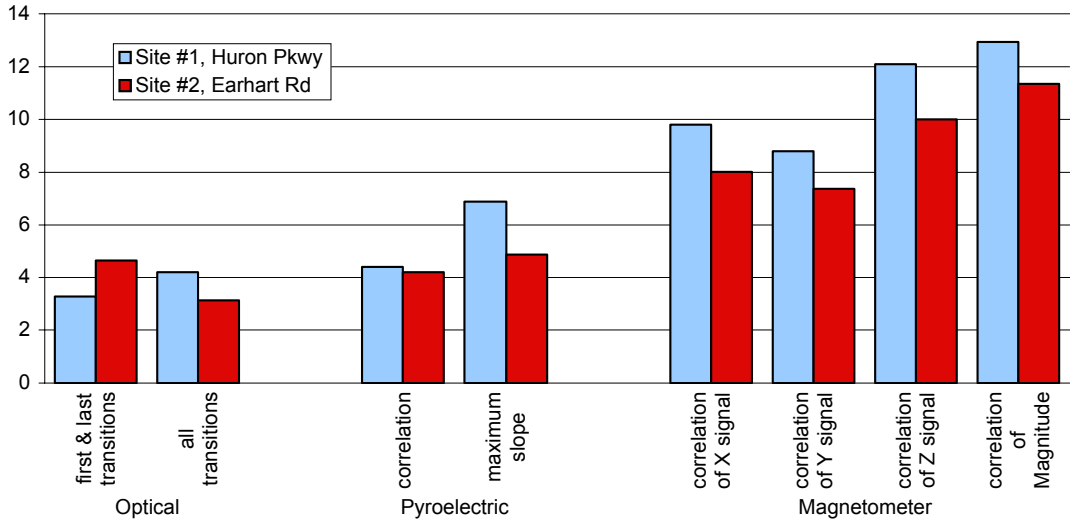

Figure 37. Standard deviations of speed-measurement errors based on uncorrected measured speeds

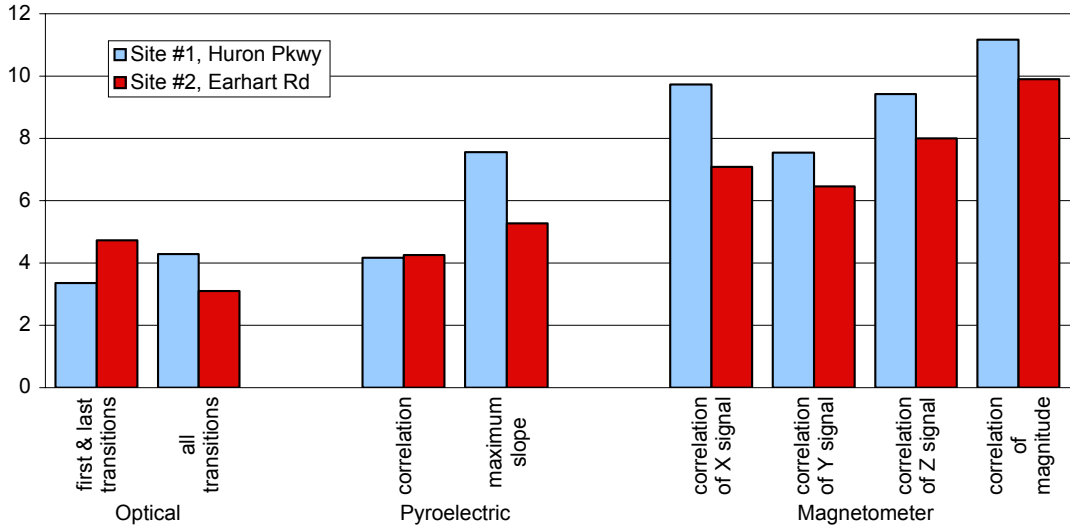

Figure 38. Standard deviations of speed-measurement errors based on corrected measured speeds

The figures reveal very similar results qualitatively with, a slight improvement (smaller standard deviations) overall for the corrected data. In either case, the best results were clearly obtained with the optical sensor, with little to choose from between the two reduction methods used for that sensor, although, overall, the

method using all transitions provided slightly better results. Standard deviations for this sensor range from a low of 3.1 mph to a high of 4.7 mph. Results from the pyroelectric sensors in combination with the data reduction method employing cross correlation, are nearly as good (from 4.2 to 4.4 mph), but degrade appreciably when the simpler, maximum-slope method is used (4.9 to 7.6 mph). All results for speeds measured with the magnetometer are poorer still, even though only the cross correlation method was used. The signal from the Y axis provides the best results from this device (standard deviations from 6.5 to 8.8 mph).

The relationships between the quality of speed measures (as indicated by standard deviation of the error) obtained from the different sensors are, we believe, largely explainable by one fundamental quality of those sensors signals, namely, frequency content. Figure 39 on the next page compares the time histories of signals generated by the three types of sensors. (The Y channel is chosen to represent the magnetometer here, as this channel produced the "quickest" responses of the three and produced the best speed measurements.) All the signals derive from a passenger car passing by at 59 mph. This figure shows, rather graphically, that the primary power of the signals resides at lower and lower frequency as one moves down the figure from optical to pyroelectric to magnetometer.

It has already been noted in the discussion above that, due to the 0.5-meter spacing of the paired sensors, a sampling rate of "only" 1 kHz limits the resolution of speed measurement to about 3 mph in the 60 mph range. That is to say, quality speed measurements in this range require the ability to discern time shifts between the two signals with at least millisecond accuracy. In figure 38, the rapid, edge-like rise and fall of the optical signals indicates that there is ample power in the 1-kHz frequency range and implies that this is a reasonable undertaking with this sensor. The major rise and fall of the signal from the pyroelectric sensor extends a bit over 0.01 seconds, however, implying that the primary content of this signal is in the 0.1 kHz range. This makes discerning time shifts to 1-milisecond resolution more difficult if the signals contain noise or other "imperfections," which they do. The time spanned by the signal from the magnetometer is greater still and makes accurate determination of time shift between the two signals proportionately more difficult.

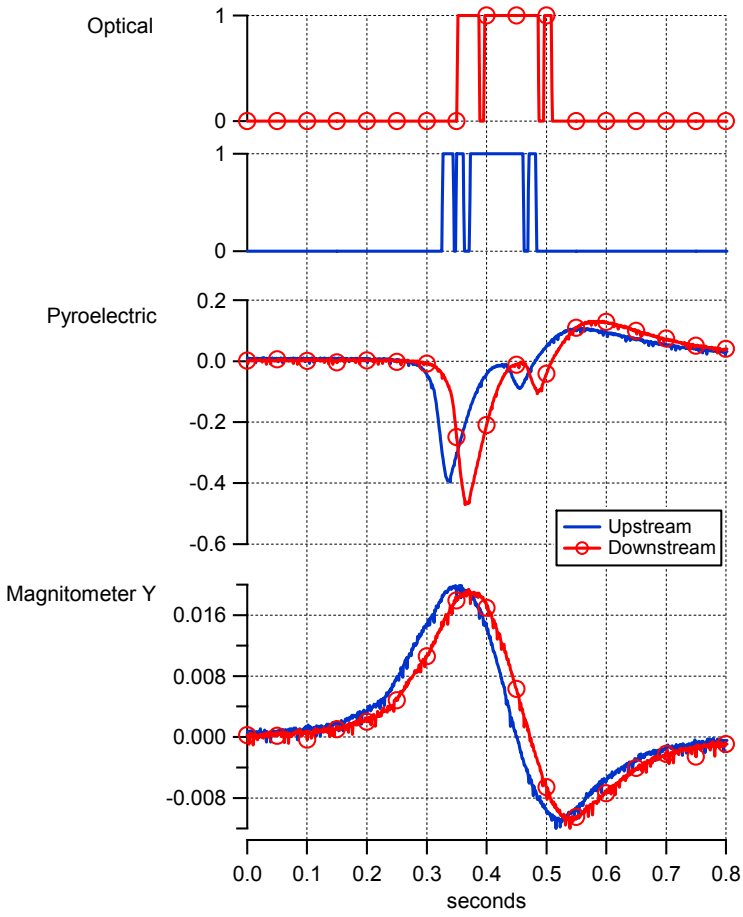

Figure 39. Comparison of signals from the three types of sensors generated by the passing of a passenger car

The frequency content of these signals are rather fundamental to the ways in which the sensors operate. The optical sensor uses a focused beam of infrared light which, when reflected back with sufficient power, results in a change of state of the output. The frequency response is essentially limited only by the internal electronics and, in our case, the data sampling rate. The pyroelectric sensor, on the other hand, receives infrared light indicative of the temperature of the source of that light within a limited field of view; it produces a signal proportional to the rate of change of that temperature. Accordingly, in this application, the frequency content of the signal depends on the size of the field of view, the speed at which a vehicle passes through the field of view, and how temperature varies over the length of the vehicle. Finally, the magnetometer senses change in the magnetic field at its own location brought about by the vehicles passing nearby. Again, frequency content of the signal depends on the speed of the vehicle and the distribution of field changes around the vehicle. Since the vehicle's influence on this field extends well beyond the length of the

vehicle itself the result is a physical influence that begins earlier and lasts longer producing a signal with similar properties.[9]

The secondary measures of speed-sensor performance characterizing the number of missed vehicles and the number of false positives are summarized graphically in figures 40 and 41, respectively.[10]

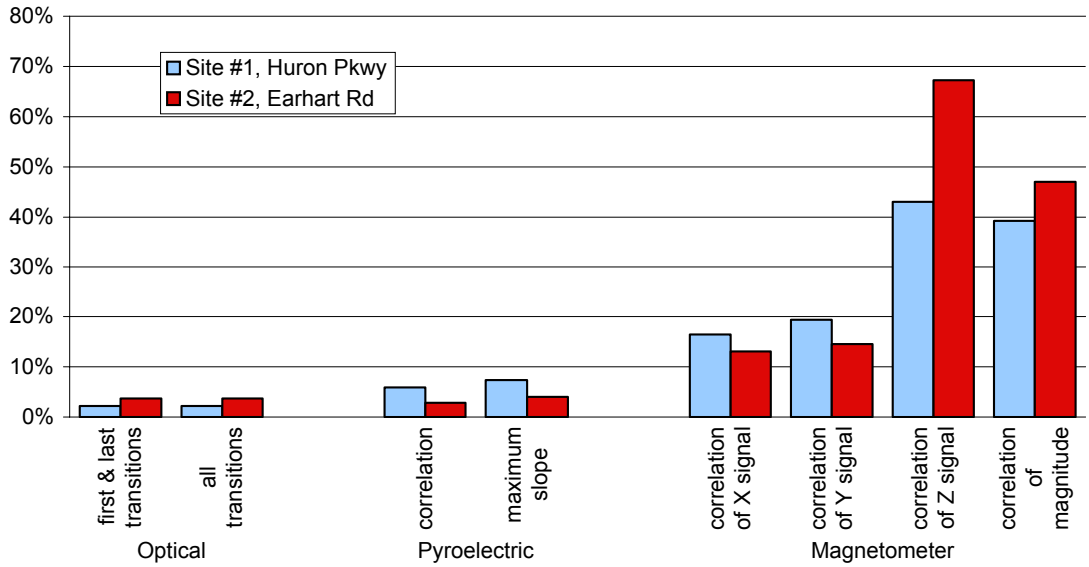

Figure 40. Percent of vehicles missed by the speed sensors by test site and data-reduction method

9. Magnetometers set beneath the road surface have been used to sense vehicle speed in a manner similar to that used in this study. This application has the advantage of locating the sensors closer to the vehicle. The ferrous elements of the vehicle can pass within perhaps 0.2 meters, or at the most within 0.4 meters, of the sensor as the vehicle passes over it. In the smart-barrel application, it is difficult to locate the magnetometers any closer than a meter from the vehicle and more typically it is farther still..
10. Note that these measures may both be slightly overstated. A few of the so-called missed vehicles result from two or more vehicles moving very close to one another and essentially moving at the same speed. Some false positive detections arise from sensing vehicles in the far lane. At the Earhart site, some of these are properly measured as having "negative" speed and are therefore discarded, but are included in the count of false positives.

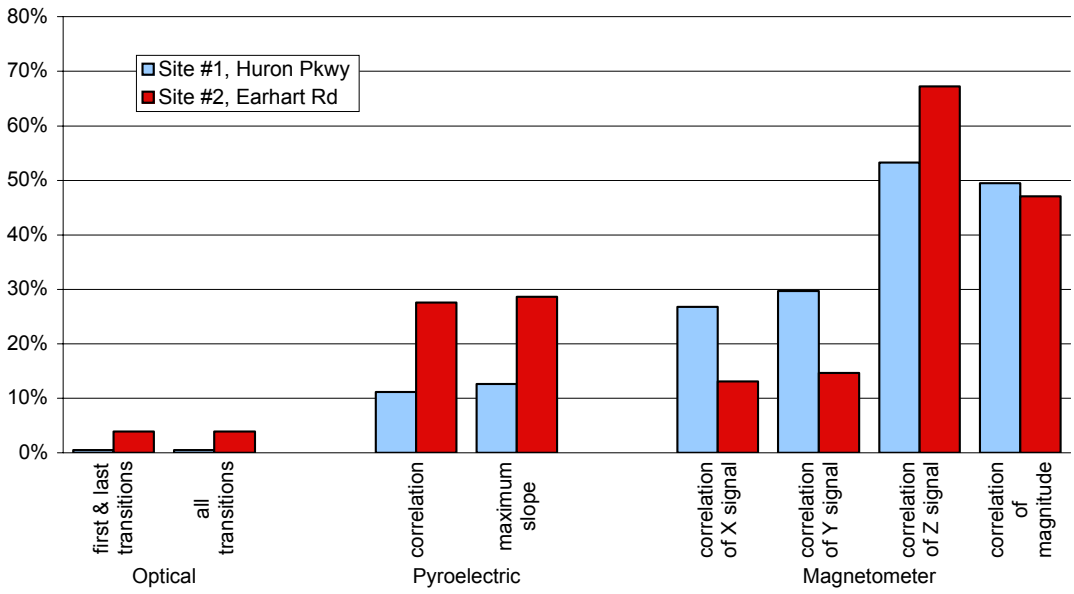

Figure 41. False positive speed measurements by the sensor type, test site and data-reduction method

These figures reveal that the sensors generally maintain the same relative ranking by both of these measures as they had according to the primary measure of standard deviation of the error of measured speed. Indeed, the optical sensors miss very few vehicles and generate very few false positives. The pyroelectric sensors also miss few vehicles, but generate more false positives. The magnetometers generally do poorly in both these measures. Much of the difficulty for both the pyroelectric sensors and the magnetometers lies in (1) the need to establish an arbitrary signal threshold for these analog-like sensors and (2) the fact that they can not be "aimed" as effectively as the optical sensors. A threshold level for reliably detecting all vehicles in the near lane invariably results in sensing some vehicles in the far lane.

In summary then, in this field test the optical sensors clearly provided the best method for sensing vehicle speed. They were best in terms of the accuracy of the measurements they made as well as in limiting the number of false positive measures and missed measurements. The pyroelectric sensors were second, and, when the correlation method of data reduction was used, their performance compared rather well with the optical sensors. The magnetometers were a relatively distant third. The X and Y signals produced much better results than the Z channel or the combination of channels in the form of magnitude.

THIS PAGE WAS LEFT BLANK INTENTIONALLY

Human Factors Requirements for a Speed-Differential Warning System

Practical Considerations

Because an effective warning about an approaching speed differential (e.g., the tail of a traffic queue) must cover a potentially large area, use of large numbers of conventional variable message signs is likely to be prohibitively expensive. Instead, a low-cost minimal display using a configuration of blinking lights is recommended. Permanently-installed warning systems of post-mounted LEDs (figure 42) have been used with some success in Scotland, Italy, and Germany to warn drivers of roadway incidents, fog, bad weather, and road work (Fum & Tognoni, 1999; Groves, Tarry, & Pyne, 2000; Hardie, Lavelle, & Fehl, 2001; Klassen et al., 1998; Klassen, Tarry, & Tognoni, 1997; Lerner, Huber, & Krause, 1997). In these systems, the warning message is conveyed to approaching drivers using either changes in the color of the light (orange/yellow), alternating flashing lights within a single post (up/down), or a sweeping (or *funneling*) effect in which lights blink in sequence down the roadway.

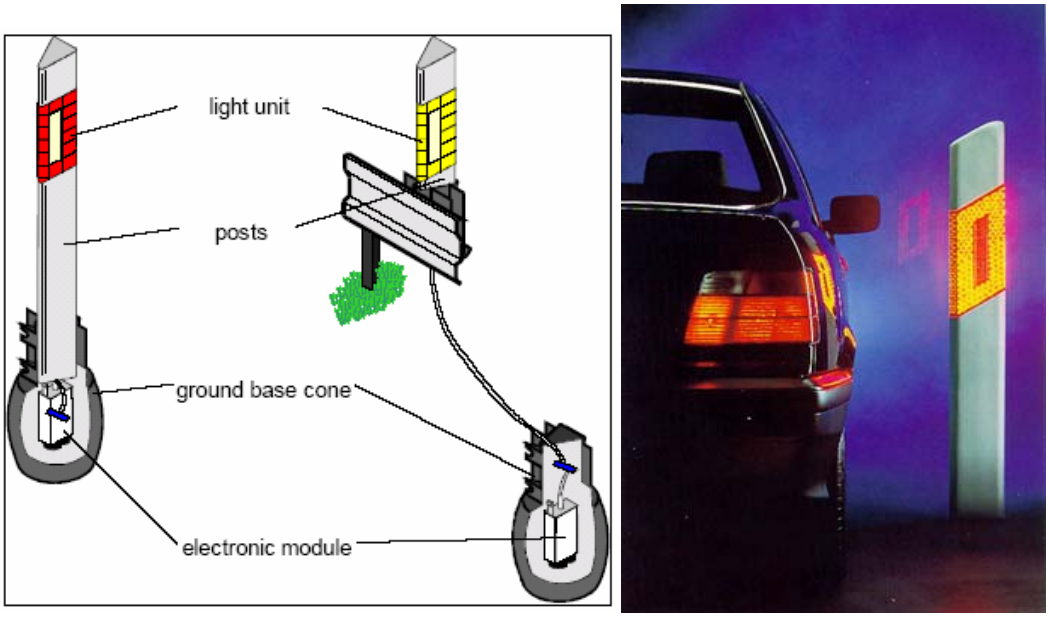

Figure 42. COMPANION post-mounted queue-warning system (from Klassen et al., 1998) and photograph of sample post (from http://www.ertico.com/its_basi/succstor/compacon.htm).

What Kind of Warning

A speed differential warning (or a queue-warning system [QWS]) can present several kinds of warning information to drivers approaching slower-moving traffic. For example, if the rear-end crash problem is produced by driver inattention to the roadway, as some have suggested, merely flashing a light toward a speeding driver could be sufficient to effectively warn a driver of the impending danger. This presumes that a driver, once advised of the danger ahead, will look down the road and accurately surmise that he or she is approaching slow-moving traffic. Although there is evidence suggesting that a driver's ability to detect closing distance is impaired using peripheral vision while looking away from the forward traffic scene (Summala, Lamble, & Laakso, 1998), rear-end crash reports do not contain sufficient detail to confirm that striking drivers were actually looking away from the roadway prior to the collision. Nevertheless, if work-zone rear-end collisions are indeed a consequence of glancing away from the road, then redirection of the driver's attention may be sufficient to improve safety.

If drivers have a special difficulty accurately judging their closing speed to slow-moving or stopped traffic while directly observing it, a simple *danger* flash may not be sufficient to avert a crash. Instead drivers may require more detailed and/or graded information about the approaching roadway conditions. This can be done with several kinds of information. For example, variable message signs have been used to warn drivers about their proximity to an area of slow-moving traffic (e.g., *Slow Traffic Ahead*), to estimate the speed of the approached traffic (e.g., *Traffic Moving Well, Moving Slowly, or Very Slow*), to revise posted speed limits (e.g., use of variable speed limits), to estimate delay time through a work zone (e.g., *Expect 10 Min Delays*), to estimate the distance to slow-moving traffic ahead (e.g., *Slow Moving Traffic Next 5 Miles*), and to advise drivers that their speed exceeds an established limit (e.g., *Speed Limit 35 MPH, Your Speed XX*). Given the context of collision risk on approach to the tail of a traffic queue, a specific warning about either proximity to the tail or an excessive-speed warning seems most appropriate.

Information about the absolute distance to the tail of a traffic queue, although simple, may not be sufficiently informative to the driver to reflect the real danger in the situation. It does not take the closing speed of the approaching vehicle into account. Thus, the same display portraying a distance-to-queue-tail of 200 feet should be alarming at 75 mph and less worrisome at 25 mph. To use the sign, the driver must use the distance estimate (provided by the sign) and his or her knowledge of vehicle

speed to figure out the real urgency of the display. This may be unnecessarily complicated.

Rather than reporting the distance to the queue tail, we suggest that the sign deliver information about the driver's closing speed to the queue tail, indicating to drivers the direct urgency to slow down. (One way to do this, by modulating flash rate, is discussed below.) Thus, the magnitude of the warning would be directly related to the deceleration required to avoid a collision into the tail of the traffic queue. In some respects, it mimics an onboard collision warning system. But, like speed advisory signs, the message is shared across vehicles passing through each warning message's detection window.

Format of Warning

This section describes some attributes of a possible system of roadside signs to relay deceleration urgency to vehicles approaching a queue tail. This discussion assumes the existence of an effective detection system which can determine the speed and location of vehicles at the tail of a traffic queue and the closing rate of vehicles approaching the queue tail. It also assumes the existence of a functioning warning algorithm which can provide at least three levels of warning urgency to approaching vehicles based on their closing speed.

Sign Placement: Because the position and migration speed of a queue tail can change rapidly and cover a large distance, it is assumed that some form of queue-warning sign must be distributed with sufficient density on the roadway to ensure accuracy and reliable proximity to the queue tail. This density will likely exceed that commonly found in variable message sign placement, where three to four signs are often employed over a distance of three to four miles in a single direction (e.g., McCoy & Pesti, 2002; Tudor et al., 2003). As a guideline, we suggest spacing signs to be visible for at least 3 seconds at a speed of 75 mph: approximately 100 meters (about 16 posts every mile). To reduce cost, it may also be reasonable to reduce sign density at greater distances upstream of the work zone, although doing so could involve a tradeoff in safety.

Sign Format: As mentioned earlier, at least three levels of warning urgency are to be presented to drivers as they approach the tail of a traffic queue. The format of this warning should:

- clearly depict the urgency level in some fashion,

- attract a driver's attention to the potential hazard,
- be understandable with little prior experience,
- not be confused with other roadside warning systems,
- accomplish all of the above at very low cost.

Levels of urgency can be conveyed using a multi-element LED display in which more (or differently colored) elements are energized with increasing urgency (e.g., none, one, two, or three LEDs; none, yellow, orange, red), or by flashing LEDs at different frequencies to indicate urgency (e.g., 0 Hz-off, .5 Hz, 1 Hz, 2 Hz). Flash rate is preferred for several reasons. First, luminance transients from flashing lights are effective in automatically attracting an observer's attention (Theeuwes, 1995; Yantis & Jonides, 1984). And second, at large distances (100 m) visual acuity is insufficient to distinguish between multiple energized light elements unless they are separated by about 15 cm (i.e., 5 minutes of visual angle). If three lights are arranged linearly, they would extend about 30 cm. To help drivers understand the meaning of the warning, additional static signs may be used to advise drivers how to interpret the blinking signals. Issues related to cost and confusability may be examined as the design of the system is refined.

There are a few concerns related to the use of flashing lights on the roadway. Widespread proliferation of flashing lights could render them less effective in attracting driver attention. This has prompted some jurisdictions (e.g., Road & Traffic Authority, 2003) to regulate their use to reflect only dynamic situations (e.g., railroad crossings, active school zone) where flashing is temporary. In this application, we expect that the flash would be delivered only when a vehicle closes on a queue tail too quickly. Flashing lights direct attention to the location of the flash, not to the area of roadway concern (i.e., straight ahead). Arguably, this could delay detection of the stopped traffic ahead by directing attention away from an important area of the roadway. However, if the flash alerts a driver to the hazard before the stopped traffic ahead would normally be detected, then some advantage may remain even with a delay. Certain flash frequencies, known to instigate epileptic seizures, should also be avoided—typically frequencies above 2 Hz and below 55 Hz are avoided.

Credibility of Warning

Driver compliance with variable message signs that incorporate speed advisories appears to be especially strong when the advisory is combined with a display of the

driver's actual speed (Garber & Patel, 1994). It is unclear whether this occurs because the sign credibly reflects actual conditions, or because it demonstrates a speed monitoring capability that may concern the driver about its potential use in enforcement. The proposed warning system also monitors a driver's speed. Unlike speed advisory systems, the proposed QWS is active only to report excessive closing speed to the tail of a traffic queue and this is reported in discrete levels. It is plausible that this difference may obscure the fact that the system reflects actual driving conditions.

THIS PAGE WAS LEFT BLANK INTENTIONALLY

Pilot Simulator Study of Queue-warning Countermeasure

Overview

To further investigate the efficacy of a roadside queue-warning system, a simulation of one version of such a system was developed and tested on a sample of twelve drivers. The simulation attempted to capture key conditions like those that would be encountered by a driver, traveling along a limited access highway, in which stopped traffic is unexpectedly encountered. Thus, in the simulation, a driver initially proceeded along a clear, straight, two-lane roadway at the posted speed limit (45 mph and 60 mph) until the tail of a queue of stopped vehicles was reached. The location of the queue tail was uncertain; sight distance was artificially limited to150 meters forward of the driver's vehicle; and an adjacent and opposing two-lane roadway on the left was included in the simulation for added visual realism. This road carried light traffic and was separated from the experimental road by jersey barriers placed on the left.

Three roadway conditions were examined: a control condition, and two queue-warning conditions. In the control condition, a roadside warning sign was placed on the right side of the road, upstream of the queue tail to emulate the current sign placement practices for work zone areas. In the queue-warning conditions, a series of simple posts, topped by an amber/yellow light, were distributed along the roadway leading up to the stopped vehicles. The queue-warning system lights flashed if the deceleration required to avoid a collision with the queue tail exceeded a defined threshold. In the single-warning condition, one blink rate was used; in the three-level warning condition, three blink rates were used to indicate progressively greater decelerations required.

The objective of the study was to pilot a version of the warning system to see how it might influence drivers' braking performance on approach to a queue of stopped vehicles. Braking performance was evaluated using four performance metrics: maximum time to collision (TTC), peak deceleration, distance from the queue tail at peak deceleration, and the initial braking distance from the queue tail. These measures were chosen based on the plausible hypothesis that, if drivers are given advance warning that their speed is high as they approach a queue of stopped vehicles, they may regulate their speed to avoid dangerously low TTCs or aggressive

braking actions that would result in high peak deceleration. Furthermore, the location at which peak deceleration and brake initiation occurs might be expected to be further from the queue tail with an advanced warning.

Drivers were also asked to provide subjective opinions about the system by completing a short survey which solicited ratings about how helpful warning conditions were, how accurately they pinpointed to location of the queue tail, and how prepared to stop they felt when they encountered the queue tail.

Method

Simulator roadway environment

The simulator used in this study was a fixed-base high-fidelity simulator manufactured by DriveSafety of Orem, Utah. Road scenes were projected across three forward screens providing a 120 degree field of view. Resolution of each screen was 1024 x 760 pixels for a combined resolution of 3072 x 760.

Roadway with static signs. The simulation was conducted on a virtual limited-access straight section of roadway, 2.8 kilometers long and located in a rural setting populated by trees, hills, and small vegetation. The roadway layout for the control condition in which static road signs were positioned upstream of a targeted stopping location was loosely based on the MUTDC standards for warning sign placement for lane closures with a temporary traffic barrier (see figure 43, reproduced from the 2003 edition of the MUTDC standards). On expressways or freeways, the guideline recommends placement of a *Road Work Ahead* warning sign at 1550 m, a *Right Lane Closed Ahead* at 750 m, and a merge warning at 300 m upstream of the start of a taper. Because the study was primarily interested in drivers approaching a queue tail upstream of a lane closure, actual portrayal of a merge configuration at the point of lane closure was unnecessary. In the simulator, drivers approached stopped traffic (i.e., the queue tail) at one of three locations upstream of the virtual lane closure—50, 450, and 850 meters (see figure 44). Drivers were also given trials in which they encountered no stopped traffic at all. In this case, they continued driving for 500 meters past the virtual lane closure point.

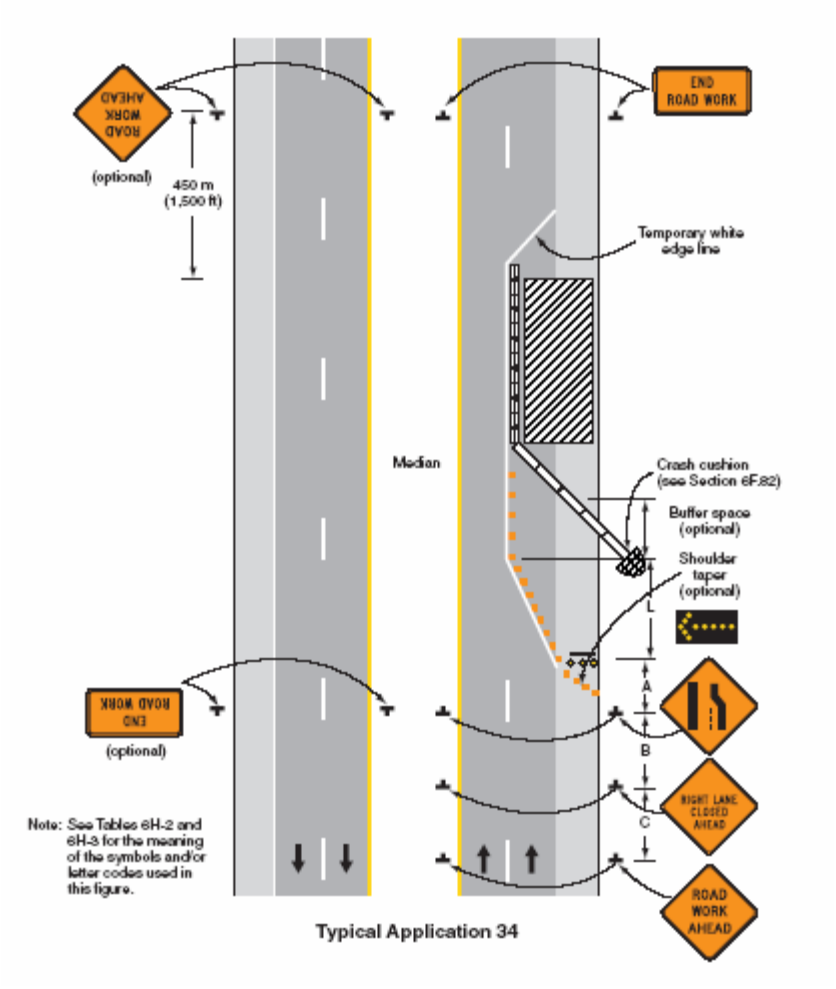

Figure 43. Illustration of lane closure configuration prescribed in the 2003 edition of the *Manual on Uniform Traffic Control Devices* (MUTCD). For expressway conditions, the distance A, B, and C are specified as 300, 450, and 800 meters, respectively.

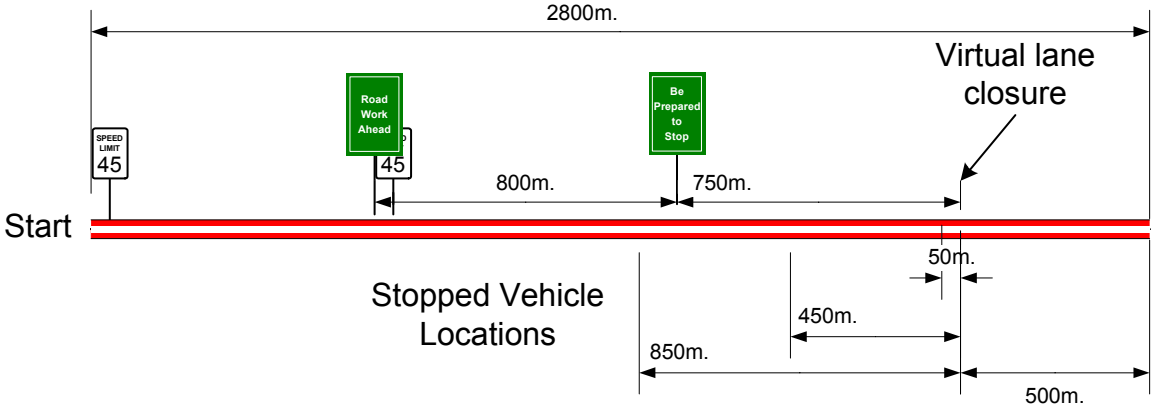

Figure 44. Simulator roadway layout in the static-road-sign condition. Sign locations are indicated above the roadway line; stopped vehicle locations are indicated below the line. The first sign encountered reads *Road Work Ahead*; the second sign reads *Be Prepared to Stop*.

Roadway with warning posts. A second roadway, similar to the static-sign condition, was used to investigate the effectiveness of post-mounted warning lights which signaled danger as drivers approached the tail of a traffic queue. Instead of the traditional static warning signs, this roadway was configured with an initial sign advising drivers to reduce their speed when the post-mounted lights are flashing (***Reduce Speed When Flashing***). Following this advisory sign, the roadway was configured with one-meter tall posts, topped with amber lights, and spaced along the roadway at 50-meter intervals. The tail of the queue of stopped vehicles was randomly placed in one of three locations along this roadway in a similar fashion to the control roadway. This is shown in figure 45.

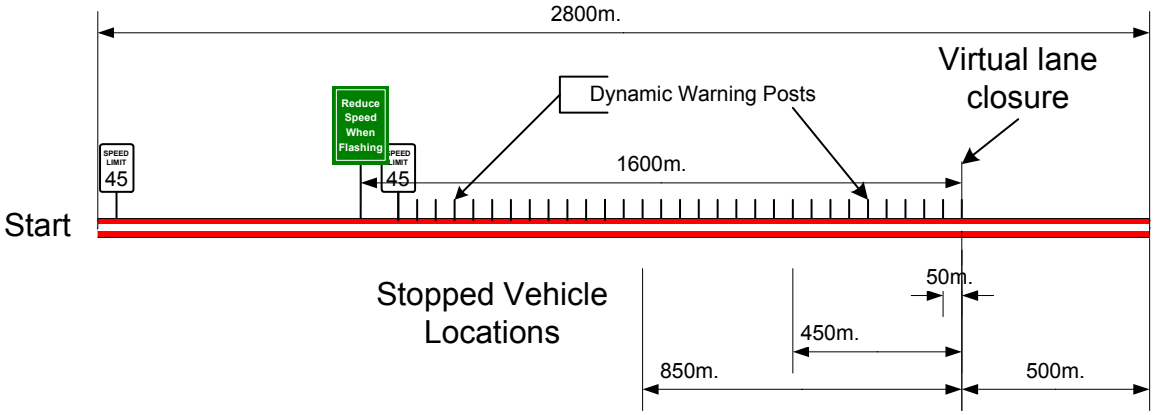

Figure 45. Simulator layout in the dynamic warning post conditions. Sign locations are indicated above the roadway line; stopped vehicle locations are indicated below the line. The first sign encountered reads *Reduce Speed When Flashing.*

Artificial sight distance limitation. Because the available roadway geometry in the simulator world was perfectly straight and unobstructed, sight-distance limits were unrealistically long and largely determined by the resolution of the display screen. In contrast, along a real-world roadway, grade changes, road curvature, the presence of overpasses, and other vehicular traffic naturally limit a driver's forward sight distance. With long sight distances, a driver would not need to rescan the roadway for new information as frequently as would be required for short sight distances. A warning system which advises drivers that they are rapidly approaching a stopped vehicle might arguably be superfluous if the tail of a queue of stopped vehicles were always clearly visible at a far distance. To better reflect sight distances in the real world and to encourage drivers' reliance on the roadside warnings, an artificial screen was used to impose a fixed sight distance limit. The screen extended across the roadway and measured 7 meters wide and 2 meters tall. It appeared at a fixed distance

of 150 meters ahead of the driver's vehicle position. The appearance of the screen on the simulator roadway is shown in figures 46 and 47.

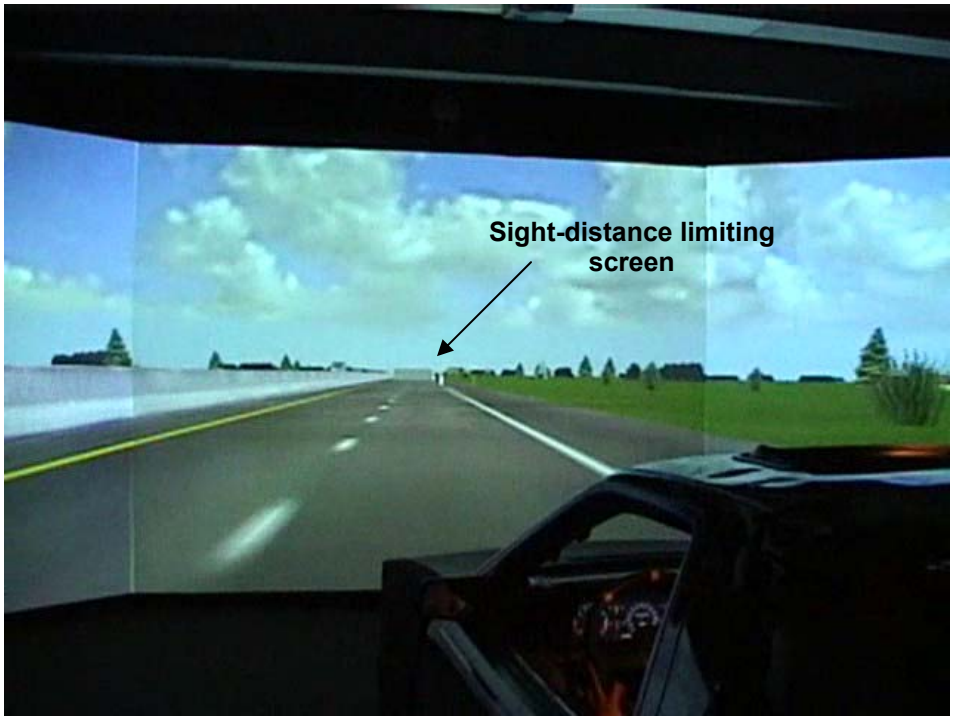

Figure 46. Simulator roadway with sight-distance-limiting screen positioned at 150 meters ahead of the vehicle.

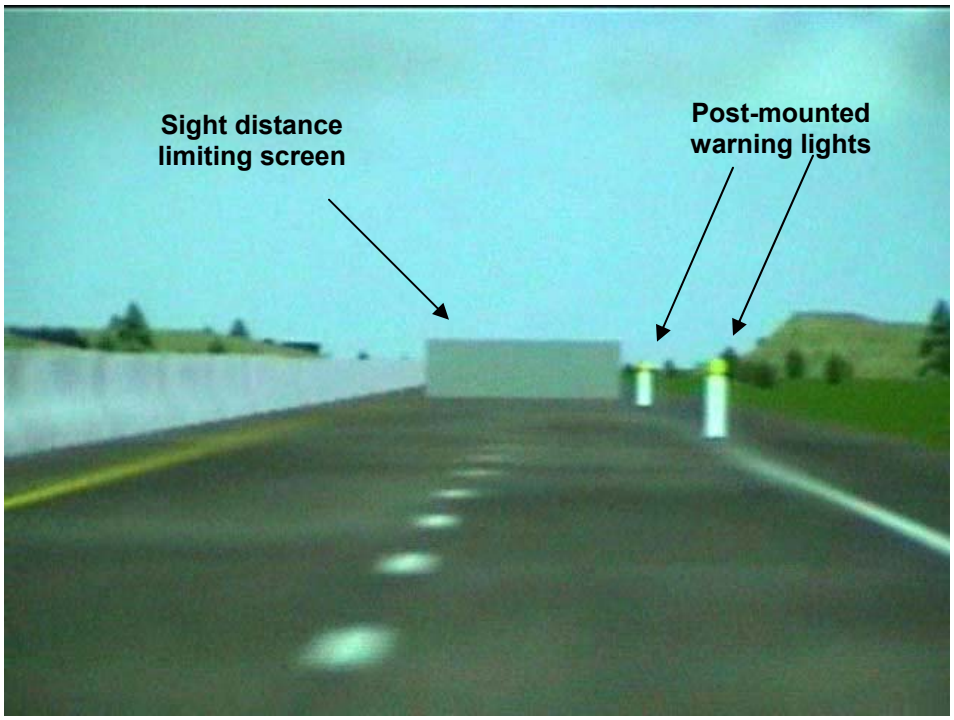

Figure 47. Detail of sight-distance-limiting screen and post-mounted warning lights.

Post Mounted Warning System Operation

Two warning conditions were examined in this study: a single-level warning and a three-level warning. In both warning conditions, a driver's approach speed and distance to the queue tail (stopped vehicles) were used to calculate a likely deceleration level required to stop the vehicle before reaching the tail of the queue. The calculation is based on equation 1 and simplified to account for a stopped vehicle on a level road at a fixed forward location as follows:

$$dec = 0.102\left(\frac{s^2}{2(d - s*t)}\right) \quad (5)$$

where:

dec	is the deceleration in gravitational units (g),
s	is the speed of the approaching vehicle in meters/sec,
d	is the distance between the approaching vehicle and the stopped vehicle,
t	is a constant representing the total lag time (in seconds) of both the driver to respond and the overall system delay (in this study a lag of 1.5 seconds was used), and
0.102	is a conversion constant for deceleration in g per m/s2.

In the single-level warning condition, a 1 Hz blink occurred when the required deceleration exceeded 0.05 g. In the three-level warning condition, three blink rates were used: 0.5 Hz above 0.05 g, 1 Hz above 0.1 g, and 2 Hz above 0.2 g. The selected blink rate was applied to all posts between the approaching vehicle and the queue tail. (The screen resolution limits of the simulator restricted the forward view to no more than three posts.)

In addition to the three roadway conditions examined (static-sign, one-level warning, three-level warning) and four queue tail locations (near, medium, far, none), two approach speeds were investigated—45 mph and 65 mph. This resulted in 24 different experimental conditions.

Subjects

Twelve paid subjects participated in this study, six male and six female. Within each gender, half of the subjects were older drivers (61-79 years) and half were younger drivers (22-26 years). All subjects were licensed drivers.

Procedure

Drivers in the study were first briefed about the general experiment and the overall driving task. Written consent was also obtained in accordance with policies concerning the use of human subjects in research. The experimental session began with a short (10 min) practice session in the simulator to familiarize drivers with the vehicle controls and to screen for motion sickness. Three drivers were excluded from the study due to motion sickness.

Experimental trials were blocked by roadway condition, with block order counterbalanced across drivers. Within each block, trials were randomized. Thus, the experimental session was divided into three blocks (static-sign, one-level, and three-level roadway conditions) of 8 trials (4 stopped vehicle distances by 2 approach speeds) within each block. Between blocks, participants were given a 10-minute break. Before the start of each block, the roadway warning condition for that block was described to drivers.

Drivers were instructed to accelerate and maintain the speed posted on the speed-limit signs placed 50 meters forward of the starting point. They were asked to maintain that speed as they would normally do on a roadway. They were also advised that, on some trials, they would be approaching the tail of a queue of stopped vehicles and to use the roadway signs for guidance to avoid a collision with the tail. Each driver's approach speed was checked over a 50-meter interval beginning at 650 meters into the drive, a location outside the stopped-vehicle warning area. If the approach speed deviated by more than 10 % of the posted speed within the check interval, the trial was restarted. After reaching the warning area, drivers were free to adjust their speed as they wished.

Each trial began at the same starting position on the roadway. Drivers accelerated to the posted speed limit and continued until they braked to a stop before the queue tail. In trials in which no stopped vehicle was present on the roadway, drivers continued along the roadway until they reached a large STOP billboard at the end of the roadway (500 meters past the virtual lane closure point; see figures 44 and 45). Because these trials did not include a stopping location defined by a queue tail, they were not included in the later analysis of stopping performance. The trials only served to add some uncertainty about stopping. That is, we intended that drivers be uncertain about *where* they should stop, and about *whether* they needed to stop at all.

After completing the experimental trials, drivers completed a brief survey that solicited opinions about how helpful, and accurate they found each system, and how well each system prepared them to avoid a collision with the queue tail. (The text of this survey is provided in appendix A).

Dependent Measures

Objective measures. Although the countermeasures investigated in this study are intended to reduce rear-end collisions into slowed or stopped vehicles in traffic queues, such collisions are unlikely to occur in a simulator. Consequently, surrogate measures that are plausible crash precursors were used in this study. The key measures included:

- *Minimum time to collision (TTC)*—calculated as the minimum time (in seconds) after the start of braking that the driver's vehicle would reach the queue tail, if the momentary vehicle speed was maintained. Short times to collision suggest greater likelihoods of collision.
- *Peak deceleration*—calculated as the maximum level of deceleration (in m/s^2) after the driver's first brake application. Aggressive braking is more likely to occur when a driver is surprised by a stopped vehicle.
- *Distance of peak deceleration*—the distance (in meters) from the stopped vehicle at which peak deceleration occurred.
- *Distance of first brake application*—the distance (in meters) from the stopped vehicle to the position of the approaching vehicle on first brake application.

Measures of braking performance were also recorded but are not included in this report because they were highly correlated with the deceleration measures and therefore redundant. For example, peak brake application is correlated with peak deceleration, as is the distance of peak application correlated with the distance of peak deceleration. In addition, because the brake measures represent a proportion of brake pedal depression (0 to 100 %), a driver could produce multiple peaks (100 % pedal depression) within a single trial, requiring braking analysis to also account for the duration of peak brake application.

Subjective measures. Answers to each of the three survey questions about each of three warning conditions were scored using 5-point Likert scales (see appendix A). Drivers were asked to report the degree to which each system was *helpful* using a scale by checking one of five boxes labeled as follows:

Very helpful	Helpful	Neither	Unhelpful	Very Unhelpful

Similarly, drivers reported the degree to which they were prepared to stop when they observed the queue tail, using a scale ranging from *Very prepared* to *Very unprepared*. They also rated the perceived accuracy of each warning system (*Very accurate* to *very inaccurate*).

Results

Trials in which no queue tail was present on the roadway were removed from the analysis. Without a queue tail as a reference point, measures of TTC cannot be sensibly made. The analysis examined three within-subjects factors: three roadway conditions (static-sign, one-level warning, and three-level warning), two approach speeds (45/72 and 65/105 mph/kph), and three stopping locations (50, 450, and 850 upstream of the virtual lane closure); and two between subjects variables: gender and age. A multi-way, repeated-measures analysis of variance (ANOVA) was performed on each measure; where applicable, results are reported with the Greenhouse-Geiser adjustment for violations of sphericity. An analysis of each dependent measure will be described in the following sections.

Minimum time to collision. A borderline main effect of roadway warning condition was observed for minimum TTC ($F_{(2,16)} = 4.37$, $p = 0.055$) and is illustrated in figure 48.

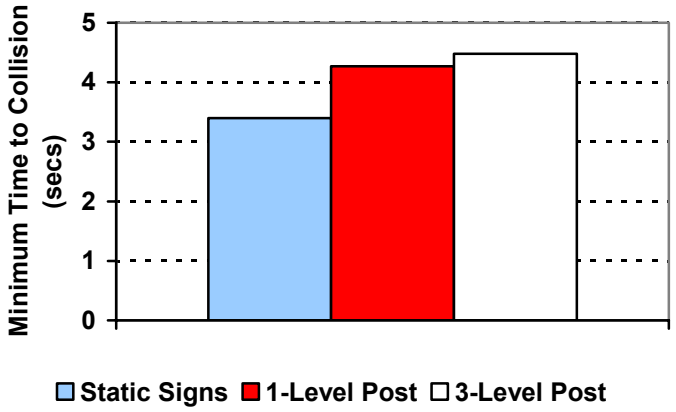

Figure 48. Minimum time to collision for each roadway condition.

Pair-wise comparisons of each condition type were not significant, although greater average differences were observed between the post-mounted warning conditions and the static-sign conditions (0.87 and 1.08 sec for one-level and three-level, respectively) than between the two post-mounted warning condition (0.22 seconds).

A main effect of speed was also observed for minimum TTC ($F_{(1,8)} = 42.54$, $p < 0.01$) and is illustrated in figure 49. At 65 mph (105 kph) minimum TTCs are about 1.3 seconds shorter than those at 45 mph (72 kph). An effect of speed is entirely expected since TTC is directly dependent on speed.

Figure 49. Minimum time to collision for each approach speed.

A three-way interaction between age, gender, and approach speed was also observed for minimum TTC ($F_{(1,8)} = 7.96$, $p = 0.022$). The minimum TTCs observed for young female drivers appeared to be less affected by approach speed than for the other drivers. This is shown in figure 50.

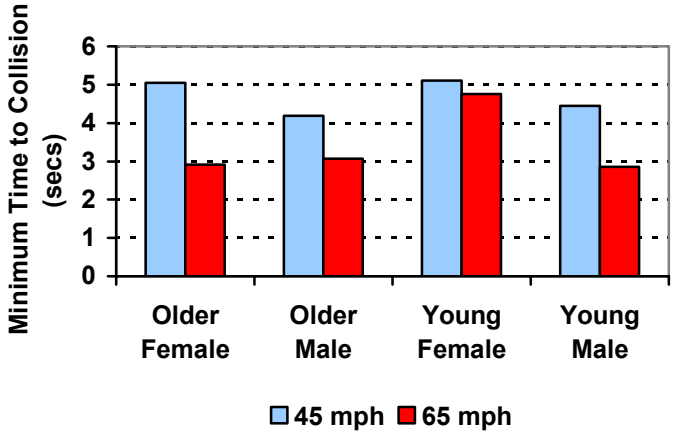

Figure 50. Three-way interaction observed between approach speed, gender, and age group.

Peak deceleration. A main effect of roadway warning condition was observed for peak deceleration ($F_{(2,16)} = 12.4$, $p = 0.001$) and is illustrated in figure 51. Pair-wise comparisons of each roadway warning condition showed significant differences between the static-sign condition and each of the post-mounted warning conditions (0.99 and 1.09 for one- and three-level warnings respectively, $p < 0.05$); but the post-mounted conditions did not differ from each other ($p = 1.00$). Not surprisingly, a main effect of speed was also found ($F_{(1,16)} = 47.4$, $p < 0.01$)—the mean difference between peak deceleration at 65 mph and 45 mph was 1.8 m/s^2 (not shown).

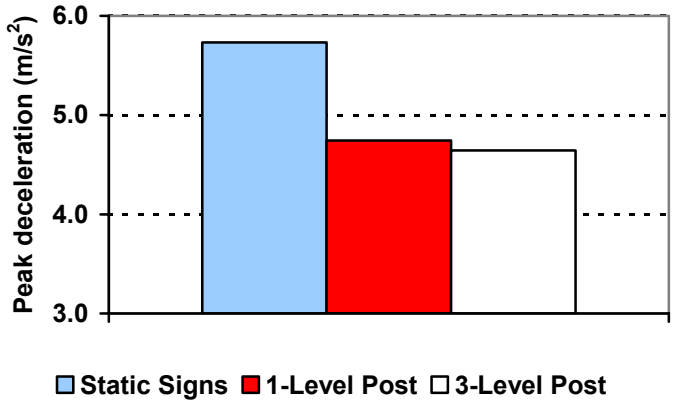

Figure 51. Peak deceleration for each roadway condition.

Main effects of stopped-vehicle distance and driver age group were also observed for peak decelerations. Stopped vehicles far upstream of the virtual lane closure resulted in higher peak decelerations (see figure 52), suggesting that drivers may have been less prepared to stop after a short cruise than after a longer cruise.

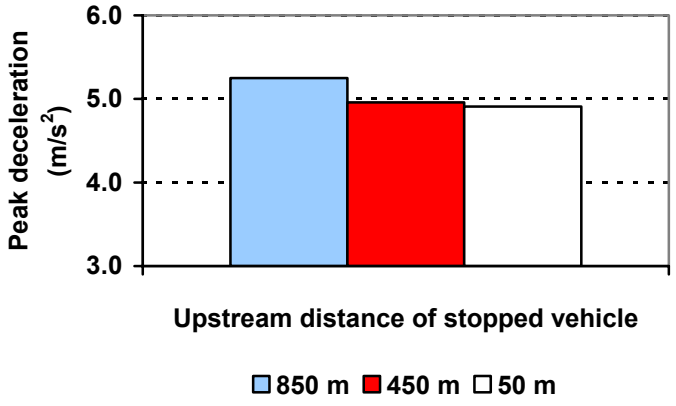

Figure 52. Main effect of upstream distance of stopped vehicle on peak deceleration.

Older drivers produced higher peak decelerations than younger drivers (see figure 53). One possible explanation for this might suggest that older drivers delay initiating braking and are thus required to apply more braking force to stop at a desired location. Unfortunately, there is no clear support for this hypothesis in the analysis of the distance from the stopped vehicle at which peak deceleration is reached ($F_{(1,8)}$ = 0.12, p = .740). It also could well be that older drivers may be more reliant on vestibular feedback from braking, which is absent in the simulator, and compensate by increasing brake pressure.

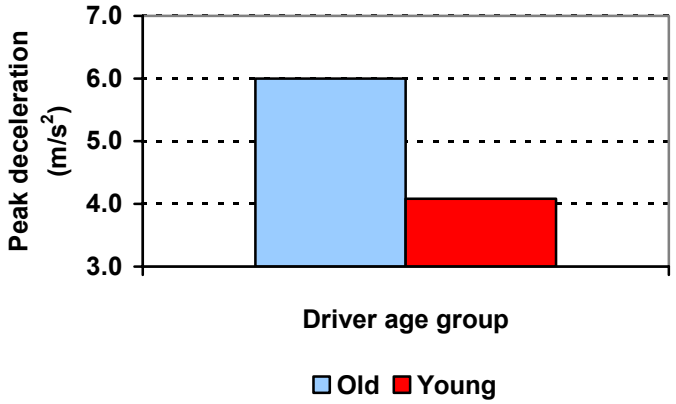

Figure 53. Main effect of driver age on observed peak deceleration.

An interaction between speed and roadway warning condition was also observed ($F_{(2,16)}$ = 7.54, p = 0.01). This is illustrated in figure 54 which shows a stronger influence of the warning conditions at higher approach speeds.

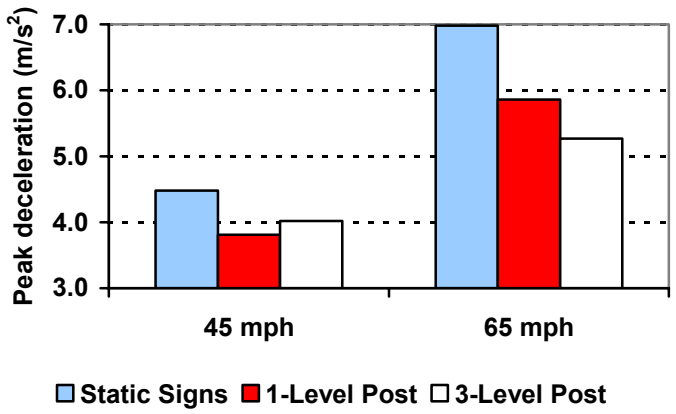

Figure 54. Two-way interaction of speed and roadway condition on peak deceleration.

Distance of peak deceleration and first brake application. Neither of these measures was systematically affected by the factors examined in this study.

Subjective data analysis. Subjective ratings were converted to an ordinal scale ranging from -2 (indicating *very unhelpful, unprepared,* or *inaccurate*) to +2 (indicating *very helpful, prepared,* or *accurate*). That is, positive scores indicated positive opinion, and negative scores indicated negative opinion. As figure 55 shows, drivers rated the three-level queue-warning condition consistently high, followed by the one-level condition and the static-sign condition. A repeated-measures analysis of variance found a main effect of roadway warning condition ($F_{(2,16)} = 6.25$, $p = .03$) suggesting that drivers rated the 1- and 3-level systems more positively than the static signs. However, a direct contrast between the two post-mounted warning conditions and the static-sign condition was marginally significant ($p = 0.06$). A two-way interaction between question type and roadway warning condition was also observed ($F_{(4,32)} = 3.47$, $p = 0.05$), suggesting that drivers' responses differentiated between the roadway conditions least when asked about the *helpfulness* of each warning condition, and most when asked about the *accuracy* of each condition.

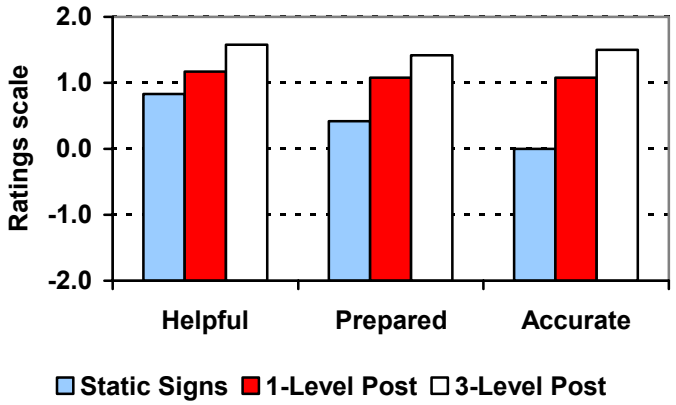

Figure 55. Average subjective rating by roadway condition for each of the three survey questions posed.

Discussion

The purpose of this study was to develop a rapid prototype of a queue-warning system which could be used to gather driving performance data and subjective opinion from drivers in order to evaluate the feasibility of a smart-barrel queue-warning system. In particular, we wanted to know whether a flashed warning would help prepare a driver to avoid a collision with the tail of a queue of stopped traffic.

We were also interested in whether drivers would regard such a warning as helpful, accurate, and effective in preparing them to stop. Finally, we examined the relative effectiveness of a three-level warning system, compared to a simpler, single-level, warning system.

In general, the objective results suggest that the warning systems were effective in both increasing the TTC on approach to a queue tail and in reducing a driver's peak deceleration. The effect on TTC implies that drivers would be more likely to avoid a collision with the tail of a queue of stopped vehicles. The reduction in peak deceleration implies a less aggressive braking regime as a consequence of clearer advance warning of an approach to a queue tail. It should be remembered, however, that the drivers in this study were fully briefed about the roadside warning systems and were also aware that their driving performance was being monitored. It remains to be seen whether these target systems would elicit similarly compliant and cooperative driving behavior from the general driving population. Nonetheless, the results are promising. The other recorded measures, offset from the stopped vehicle at first brake initiation and offset at peak deceleration, did not appear to be systematically affected by the warning systems.

The two-way interaction of speed and roadway condition on peak deceleration also suggests that the influence of the post-mounted warning systems is strongest at higher speeds. This is not surprising, given the nature of the measure. At lower speeds, the range of peak deceleration is compressed, perhaps reducing the size of differences between each warning condition.

Although a trend suggesting that the three-level warning system was more effective in increasing TTC than a one-level warning system, no statistical analysis found a reliable difference between these two systems. The observed difference was small (0.22 seconds), although the confidence interval for this difference was relatively large (-0.33 to +0.76 seconds). Informally, we also noted that some drivers, after learning the significance of each warning level in the three-level system, seemed to change their braking strategy. Instead of beginning braking on the earliest warnings, they withheld braking until the highest severity warning. Since exposure to the three-level system was quite limited (there were only 12 trials), there is little clear evidence for this trend. Nevertheless, we should be sensitive to possible strategies drivers might develop as they gain experience with these systems.

The subjective results also suggest that drivers regard the warning systems as helpful, accurate, and effective in preparing for an unexpected stop. Of course, this evaluation was made under the relatively ideal and uncluttered circumstances found in the simulator road environment—a perfectly straight roadway, clear of traffic, and containing few road signs made the overall driver workload unusually light in this study. It remains to be seen whether under heavier workloads or other sources of roadway distraction that the warning systems would be similarly rated.

THIS PAGE WAS LEFT BLANK INTENTIONALLY

Conclusions and Recommendations

This research project has developed the broad concept for a Work-Zone Safety ITS System that would provide a distributed, queue-warning system that automatically adapts to the current traffic-flow situation in and upstream of the work zone. The core element of the system would be a *smart barrel*—an ordinary appearing traffic-control barrel containing an inexpensive speed sensor and equipped with a simple, adjustable signaling system and the necessary equipment for communication to a central controller. The study has focused on initial investigations of two important elements of such a system: (1) an inexpensive, but sufficiently capable speed sensor and (2) a simple but effective signaling system. The following subsections briefly present conclusions and recommendations on these two subjects.

Speed-Senor Technologies

In this study, preliminary consideration was given to seven sensor technologies that might be used in developing an inexpensive vehicle speed sensor housed in a common traffic-control barrel. From the list of candidates, four technologies were initially chosen for evaluation. Of those, one was eliminated leaving three technologies to be examined experimentally:

- active infrared, optical sensors;
- passive infrared, pyroelectric sensors;
- magnetometers.

In the application of each of these sensor technologies, the basic approach was to mount two such sensors at diametrically opposed positions on a traffic-control barrel such that, with the barrel deployed at a work zone with the sensor spacing oriented in the direction of travel, each sensor would respond to a passing vehicle in a similar manner but at a spacing in time proportional to the vehicle's speed.

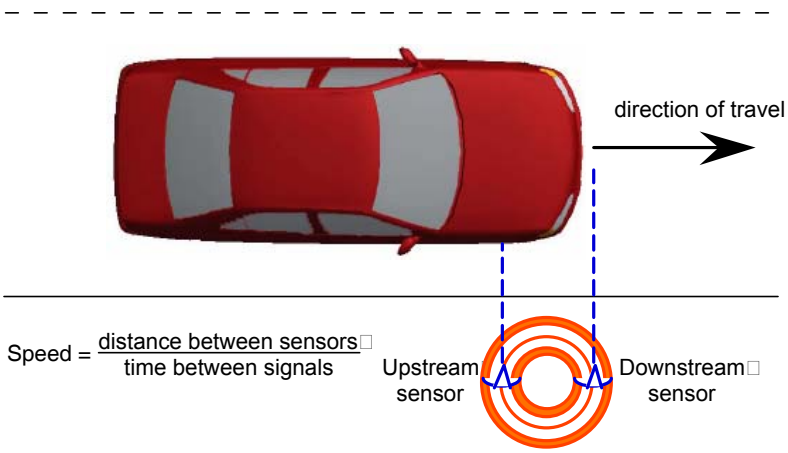

Figure 56. Vehicle speed is proportional to the time lag between signals from the upstream and downstream sensors

Following some preliminary development and experimentation, speed sensors based on these three technologies were evaluated in a limited field test. The three barrels containing the experimental sensors, plus additional barrels with radar speed sensor and video cameras were deployed at two sites. One site, located on a stretch of rural road, was dominated by traffic moving at relatively constant speeds and averaging about 50 mph. The other site was located upstream of a traffic-light controlled intersection on a busy urban parkway, and so had traffic moving from slow to moderate speeds but also slowing and queuing within the site.

Over a period of weeks, a total of some eighteen hours of data were gathered, the last nine hours of which were used for the basis of evaluation. The evaluation data included a total of 1627 vehicle passes through the two sites.

Of the three technologies examined in the field test, the active infrared, optical technology clearly performed the best in this limited test. The speed sensor based on this technology detected 97 % of the vehicles passing through the site and produced less than 4 % additional false detections. Two data processing methods developed for determining speed from the base sensor signals were about equally successful, one having a standard deviation of the errors of about 3.7 mph and the other 4.0 mph.

The speed sensor based on the passive infrared, pyroelectric technology performed nearly as well but required a computationally-expensive data processing method to do so. The standard deviation of the errors was about 4.2 mph with 96% of vehicles sensed. This method's biggest shortcoming was a false-positive rate approaching 20 %. It should be noted, however, that the pyroelectric sensors require appreciably

less power for operation than do the optical sensors, an important consideration for a battery-powered system.

Sensing speed with the magnetometers was the least successful. The best method investigated had a standard deviation of the errors of about 7 mph, a missed-vehicle rate of about 17 % and a false-positive rate of about 21 %.

In hindsight, it seems probable that the relative performance of these three approaches to speed sensing derives largely from the frequency response qualities of the three systems. Housing the two sensors in a single barrel establishes the maximum spacing between them at roughly 0.5 m. This, in turn, dictates that the system must distinguish time shifts between the two sensors with fidelity of at least 1-millisecond in order to achieve a reasonable quality of speed measurement at highway speeds. In the field test, the frequency response of all the systems was ultimately limited to 1 KHz as this was the sampling rate used for data acquisition. (This sampling rate limits the resolution of the system to about 3 mph for vehicles traveling at 60 mph.) Without detailed explanation, suffice it to say that the optical system was essentially limited only by the sampling rate, but that the pyroelectric system was further limited by the sensor properties and the magnetometers even more limited. This relationship is likely fundamental to the relative success of the three approaches in this test.

In counterpoint, however, it should be noted that in this initial program, none of the systems have been fully optimized. Improvements are likely possible through several approaches:

- Further development of the data processing algorithms could be expected to improve the performance of each system. This applies to the calculation of speed and also to reducing the rates of missed and false positive targets.
- The physical properties of the individual sensors can likely be improved. This is probably most applicable to the pyroelectric sensors. Those used in this study were assembled laboratory prototypes. Tightening the field of view and adjusting output gain appropriately may help raise the frequency response of this system.
- Higher data sampling rates can easily be achieved. In this program, the DAS simultaneously collected data from eight experimental sensors, a multi-target scanning radar and two video cameras. A system optimized for one pair of sensors should easily manage much higher sampling rates, or in some cases be interrupt driven.

Finally, we should consider the potential implications of what has not been learned in this brief study, namely the influences of a broad range of environmental conditions. Because the prototype barrels developed in this program were not autonomous (they required ancillary equipment including electric generator, data acquisition system, video cameras, etc.), they could only be deployed for relatively brief periods and in locations close to UMTRI. Thus, the majority of field data gathered in this study was taken during reasonable good, late autumn weather (although some was taken in what could be described as gray and drizzly Michigan weather). No data were recorded in the intense heat of a summer afternoon, nor in intense cold nor on snow-covered roads, nor on unlit rural roads at night, nor in the thick dust of a construction site. This is preamble to the comments that one of the attractive qualities of the magnetometer technology was its likely insensitivity to environmental conditions, and that potential difficulties with the other technologies include sensitivity to thermal conditions (the pyroelectric sensors) and to reduced visibility (both the pyroelectric and optical sensors). One other point of interest in this regard: the pyroelectric sensors have been seen in this project to respond to air turbulence around and, particularly, following a vehicle. This may have more important implications for large trucks than for passenger cars, but large trucks were somewhat rare at the test sites used in this study. There may well be more to learn in this regard.

Accordingly, regarding the pursuit of the speed-sensing smart barrel we would recommend:

- The potential improvements for each of the three technologies should be further evaluated through continued investigation and development of data reduction algorithms using the data already gathered in this study. In this regard we would have the greatest hope for reducing the rates of missed and false-positive targets, although some improvement in the basic speed measurement may also be achieved.
- In near-future studies involving more elaborate pilot field tests deploying greater numbers of smart barrels, both active (optical) and passive (pyroelectric) infrared technologies should be included as means for speed measurement.
- Future pilot field test should seek to gather data under as broad and representative a set of environmental conditions as is practicable.

Human Factors Conclusions

The pilot study which investigated the human factors issues associated with a queue-warning system sought to answer two basic questions:

- Would drivers regard such a system as helpful?
- Could a rudimentary version of such a warning system measurably alter driving performance?

For both questions, there appears to be some evidence for guarded optimism. As described in the pilot study results and discussion, drivers are both positively disposed to the queue-warning system relative to static road signs, and their driving performance changes in a way that suggests enhanced safety—minimum times to collision increase, peak decelerations decrease. Moreover, the interaction effect of approach speed and warning condition on peak deceleration suggests that the most dramatic differences occur at higher travel speeds.

Of course, we should also recognize that the simulator results require verification under more realistic roadway conditions, where drivers are not knowing participants in a study about a useful roadway warning system, and are subject to many more sources of distraction and substantially more uncertainty than is found in a tightly controlled experiment.

Finally, we note that by using a vehicle simulator, a functional version of a queue-warning system was quickly prototyped, reviewed, and adjusted independently of the availability of any of the sensor technologies currently under review. Many adjustments were inexpensive to make—especially compared to the likely cost of such changes to an actual system on a real roadway. Thus, for example, the density, height and blink rate of the post-mounted warning lights were adjusted several times during early piloting before settling on the values used in the study. However, it should also be recognized that use of a simulator imposes some limitations as well. For example, certain light configurations could not be examined with the simulator because of limited screen resolution, frame rate, and dynamic range of the display. The kinesthetic sensation of vehicle acceleration and deceleration was absent in the fixed based simulator used here—and some drivers found this disorienting. Finally, roadway geometry was far more schematic and predictable than would be seen on a real roadway. While a simulator may be of further use in prototyping, as development of a queue-warning system progresses, it will be necessary to examine many characteristics of the system on real roadways in real vehicles.

Based on results of the human factors study, we recommend that:

- Investigation of the barrel-based queue-warning system should be pursued with special focus on work zones in high-speed roadways. These roadways host the largest number and the most severe crashes, and the trends found in the human factors experiment suggests that the speed-warning system would be most influential under these conditions.
- Further research should also examine the driver's perception of the system under more complicated scenarios than observed in the pilot study, where a single vehicle approached stopped traffic. For example, because the warnings are targeted to the fastest moving traffic within a zone and not to a specific vehicle, some warnings will be seen by by some drivers for whom the warnings are not applicable. This could diminish the perceived accuracy of the displayed warnings. Conditions in which traffic queues span multiple lanes (and move at different rates within lanes) should likewise be investigated.
- Further work is likewise needed to successfully adapt the warning display to the work-zone environment. Our initial proposed format of the warning display—a flashing amber light—was developed to exploit the attention-getting properties of an onset transient, to be consistent with other roadside warnings (e.g., school-in-session, icy road conditions, animals detected), and to leverage use of the lighting device already mounted to roadside barrels. Normally, a barrel-mounted light functions as an auxiliary marker for the barrel and burns steadily at night; in some cases, it flashes to call attention to the location of specific hazard at night. Further human factors investigations will be needed to find an effective display solution that is both compatible with the nighttime barrel-marking/hazard-signaling functions, and a multi-level speed-differentiating warning system.

References

Chambless, J., Lindly, J. K., Ghadiali, A. M., & McFadden, J. (2002). Multistate work-zone crash characteristics. *ITE Journal, 72*(5), 46-50.

Fontaine, M. D., & Carlson, P. J. (2001). Evaluation of speed displays and rumble strips at rural-maintenance work zones. *Transportation Research Record, 1745*, 27-38.

Fum, D., & Tognoni, G. (1999). *Evaluating the effectiveness of road information and warning systems: The COMPANION experience.* Paper presented at the Intelligent Transport Systems, Sixth Annual World Congress, Orlando, FL.

Garber, N., & Patel, S. (1994). *Effectiveness of changeable message signs in controlling vehicles speeds in work zones* (Final Report FHWA/VA-95-R4). Richmond, VA: Virginia Department of Transportation.

Garber, N., & Patel, S. (1995). Control of vehicle speeds in temporary traffic control zones (work zones) using changable message signs with radar. *Transportation Research Record, 1509*, 73-81.

Garber, N., & Srinivasan, S. (1998). Influence of exposure duration on the effectiveness of changeable-message signs in controlling vehicle speeds at work zones. *Transportation Research Record, 1650*, 62-70.

Garber, N., & Zhao, M. (2002). Distribution and characteristics of crashes at different locations within work zone locations in Virginia. *Transportation Research Record, 1794*, 19-25.

Groves, C., Tarry, S., & Pyne, M. (2000). *COMPANION Stage 1 Final Report*. Hertfordshire, UK: Scottish Executive.

Hardie, C., Lavelle, S., & Fehl, K. (2001). *COMPANION Phase 3 - Trial of aid system*. Edinburgh.

Klassen, N., David, A., Whyte, D., Tarry, S., Pyne, M., Lerner, G., & Huber, W. (1998). *TABASCO - TR 1054 - Inter-Urban Corridors : Final Report* (TR1054 D7.5).

Klassen, N., Tarry, S., & Tognoni, G. (1997). *A new quality in roadside incident warning: a European approach within INFOTEN and TABASCO.* Paper presented at the Fourth ITS World Congress, Berlin.

Lerner, G., Huber, W., & Krause, G. (1997). *COMPANION development and field testing of a collective warning system.* Paper presented at the Fourth ITS World Congress, Berlin.

McCoy, P., & Pesti, G. (2002). Effectiveness of condition-responsive advisory speed messages in rural freeway work zones. *Transportation Research Record, 1794*.

Raub, R. A., Sawaya, O. B., Schofer, J. L., & Ziliaskopoulos, A. (2001). *Enhanced crash reporting to explore workzone crash patterns.* Paper presented at the Transportation Research Board 80th Annual Meeting, Washington, D.C.

Road & Traffic Authority. (2003). *Flashing lights at fixed locations in the road environment* [pdf]. Road Environment Safety Update No.18. Retrieved May 10, 2004, from the World Wide Web: http://www.rta.nsw.gov.au/roadsafety/downloads/roadenvironmentsafetyupdate_no18_nov2003.pdf

Schnell, T., Mohror, J., & Aktan, F. (2002). Evaluation of traffic flow analysis tools applied to work zones based on flow data collected in the field. *Transportation Research Record, 1811*, 57-66.

Summala, H., Lamble, D., & Laakso, M. (1998). Driving experience and perception of the lead car's braking when looking at in-car targets. *Accident Analysis & Prevention, 30*(4), 401-407.

Theeuwes, J. (1995). Abrupt luminance change pops out - abrupt color-change does not. *Perception & Psychophysics, 57*(5), 637-644.

Tudor, L., Meadors, A., & Plant, R. (2003). Deployment of smart work zone technology in Arkansas. *Transportation Research Record, 1824*, 3-14.

Wang, C., Dixon, K., & Jared, D. (2003). Evaluating speed-reduction strategies for highway work zones. *Transportation Research Record, 1824*, 44-53.

Wang, J., Hughes, W. E., Council, F. M., & Paniati, J. F. (1996). Investigation of highway work zone crashes: what we know and what we don't know. *Transportation Research Record, 1529*, 54-62.

Wiles, P. B., Cooner, S. A., Walters, C. H., & Pultorak, E. J. (2003). *Advance warning of stopped traffic on freeways: current practices and field studies of queue propagation* (Research report FHWA/TX-03/4413-1). Austin, TX: Texas Department of Transportation.

Yantis, S., & Jonides, J. (1984). Abrupt visual onsets and selective attention: evidence from visual search. *Journal of Experimental Psychology: Human Perception & Performance, 10*(5), 601-621.

Appendix A

Work Zone Questionnaire

Please provide the following information.

Driver ID:_____

Age:_____ Gender: (M F)

Instructions: We would like to know what your impressions are of each roadsign treatment—the fixed signs (*Road Work Ahead, Be Prepared to Stop*) and the post-mounted lights.

Please check one box:

1) Please rate the helpfulness of each road sign treatment:

	Very Helpful	Helpful	Neither	Unhelpful	Very Unhelpful
Signs					
Single Blink					
Multi Blink					

2) Please rate how prepared you were to stop for each roadsign treatment.

	Very Prepared	Prepared	Neither	Unprepared	Very Unprepared
Signs					
Single Blink					
Multi Blink					

3) How accurately did you think each road sign treatment pinpointed the location of stopped traffic?

	Very Accurate	Accurate	Neither	Inaccurate	Very Inaccurate
Signs					
Single Blink					
Multi Blink					

THIS PAGE WAS LEFT BLANK INTENTIONALLY

Appendix B

Review of Measured Speeds

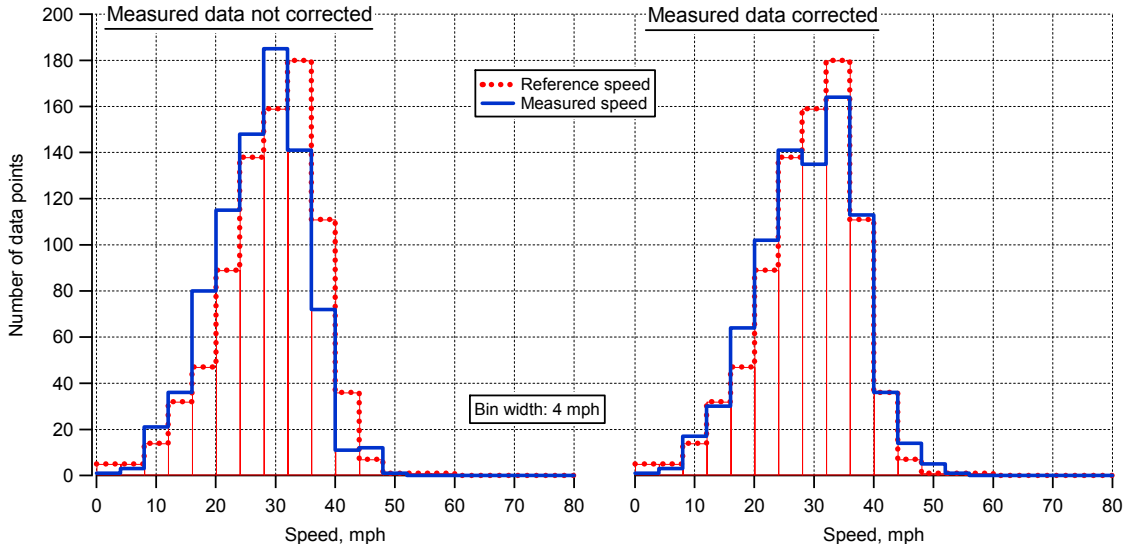

Active infrared; site 1 Huron Pkwy; first and last transition

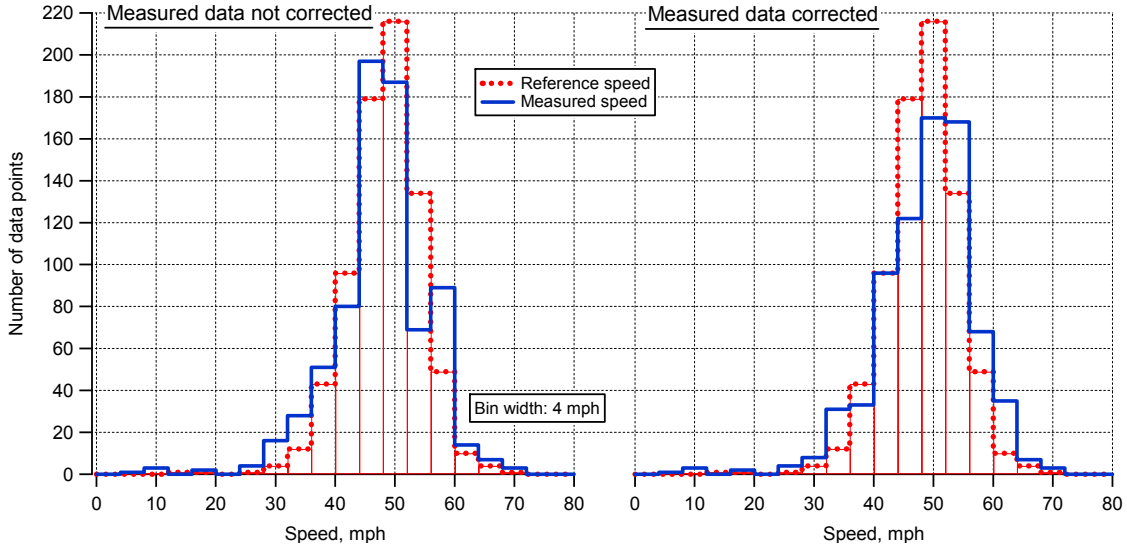

Active infrared; site 2 Earhart Rd.; first and last transition

Figure B1. Active infrared corrected and non-corrected results versus the reference speed for method 1, first and last transition

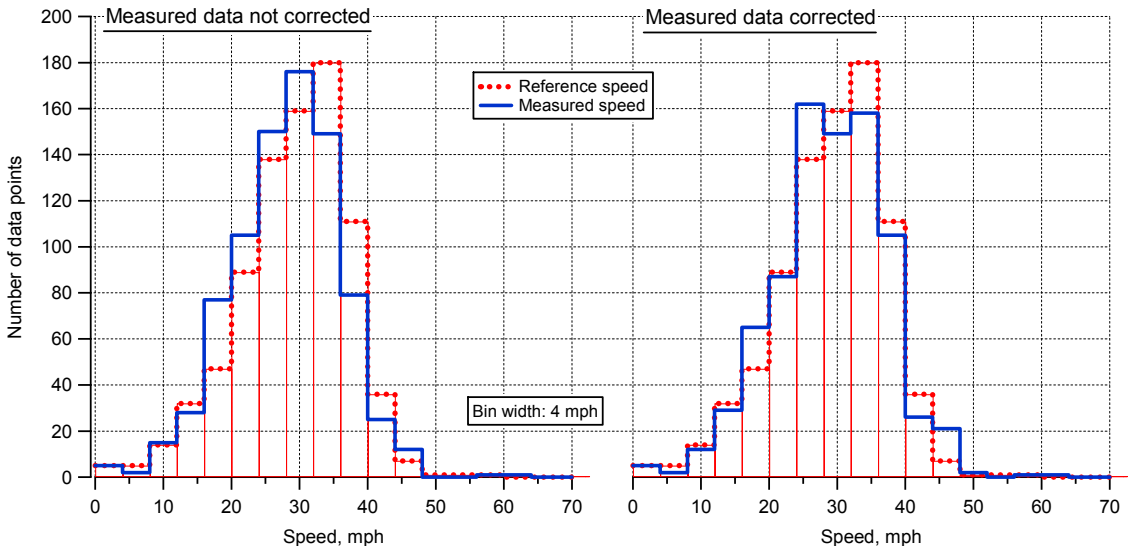

Active infrared; site 1 Huron Pkwy; all transitions

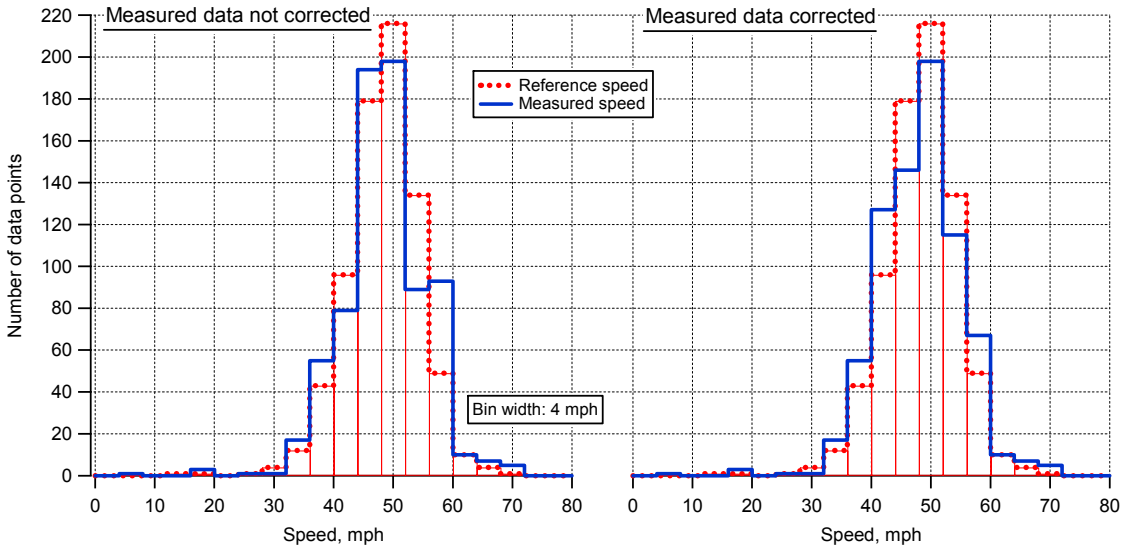

Active infrared (optical); site 2 Earhart Rd; all transitions

Figure B2. Active infrared corrected and non-corrected results versus the reference speed for method 2, all transitions

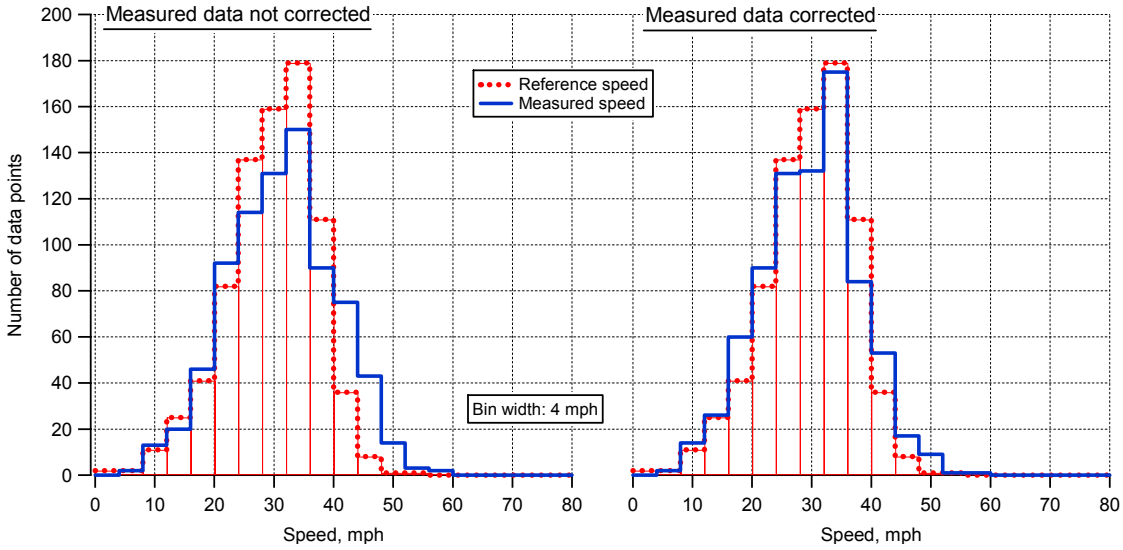

Passive infrared; site 1 Huron Pkwy; correlation

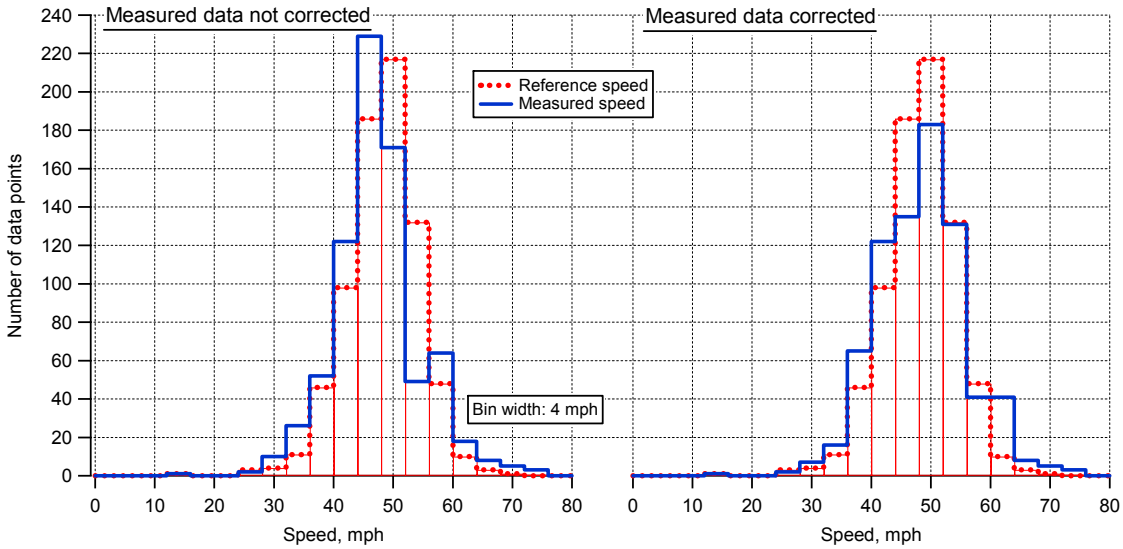

Passive infrared; site 2 Earhart Rd.; correlation

Figure B3. Passive infrared corrected and non-corrected results vs. the reference speed for correlation method

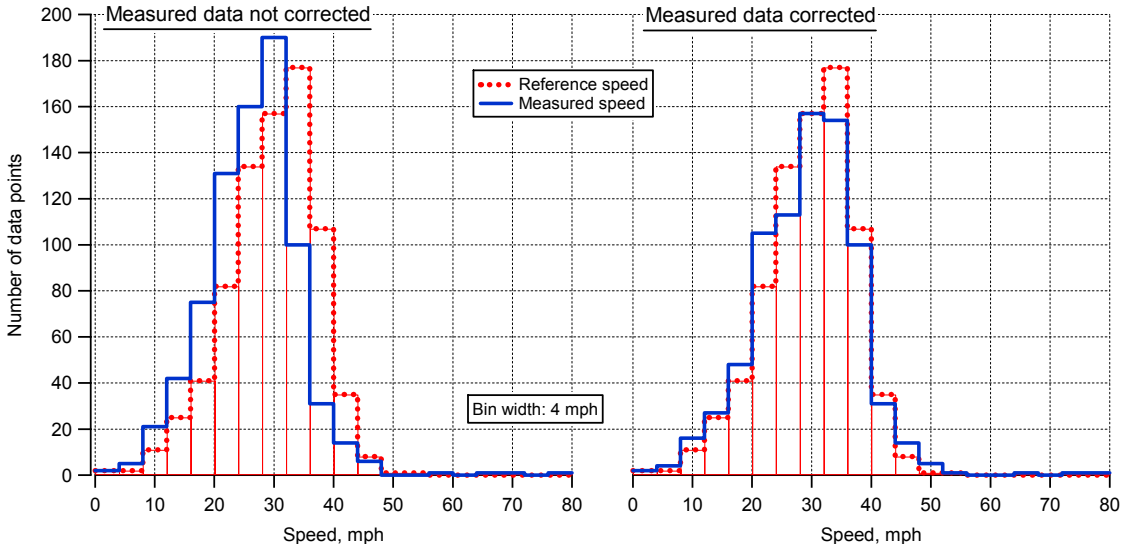

Passive infrared; site 1 Huron Pkwy; maximum slope

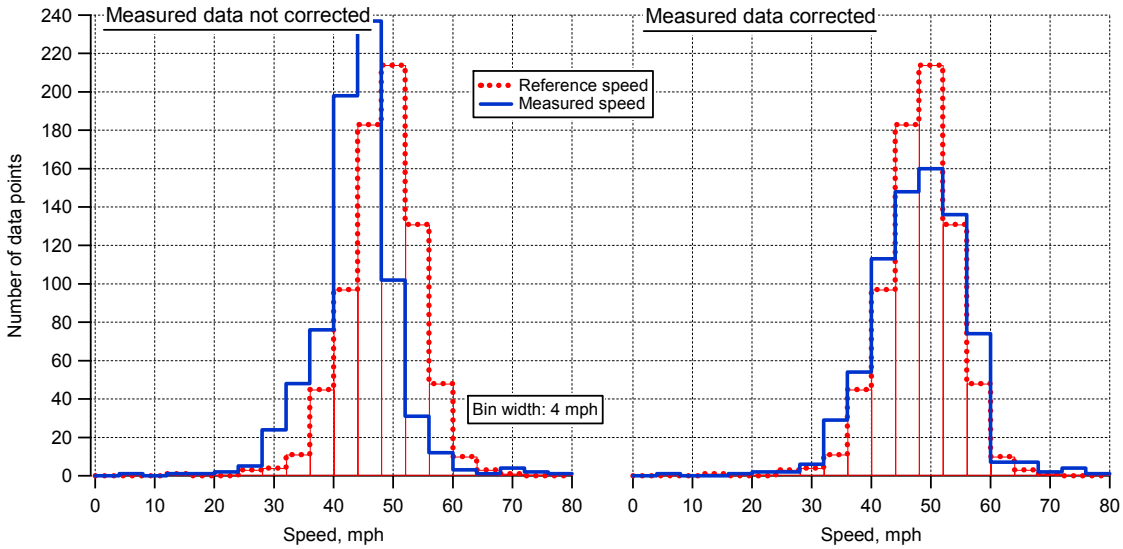

Passive infrared; site 2 Earhart Rd.; maximum slope

Figure B4. Passive infrared corrected and non-corrected results vs. the reference speed for maximum slope method

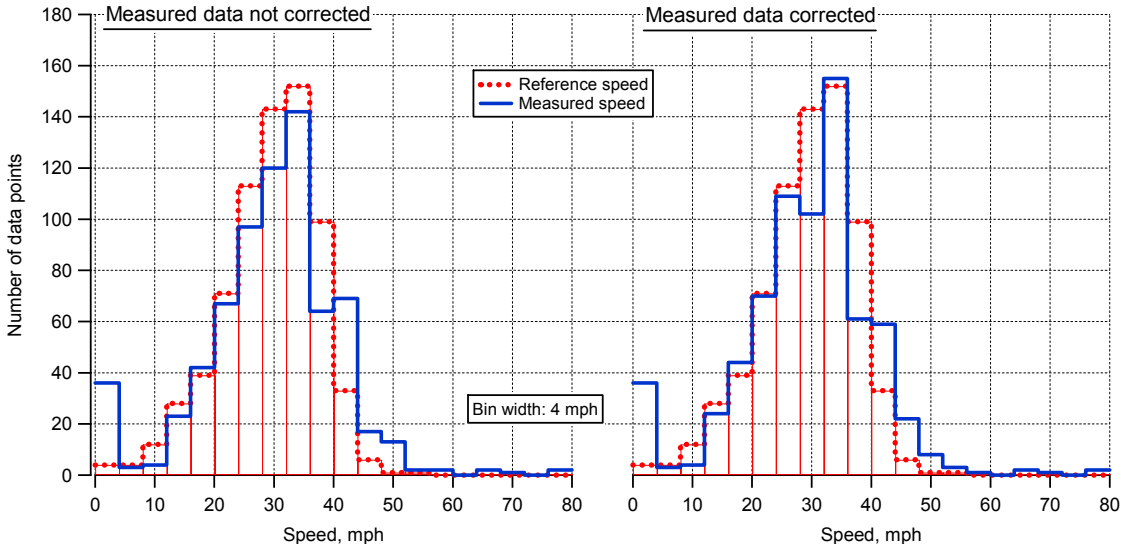

Magnetometer; site 1 Huron Pkwy; correlation, X signal

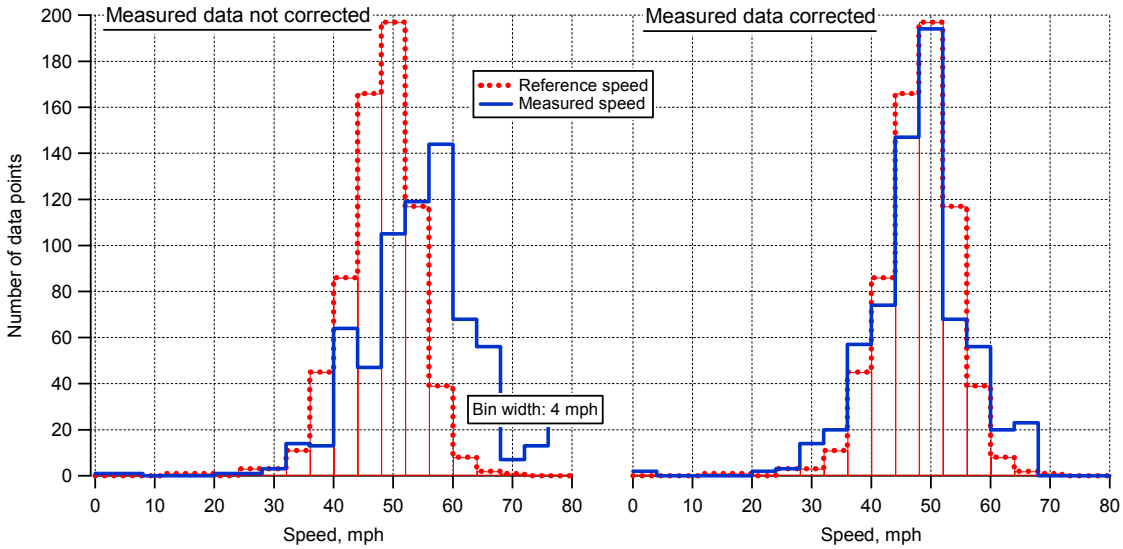

Magnetometer; site 2 Earhart Rd.; correlation, X signal

Figure B5. Magnetometer X signal corrected and non-corrected results vs. the reference speed

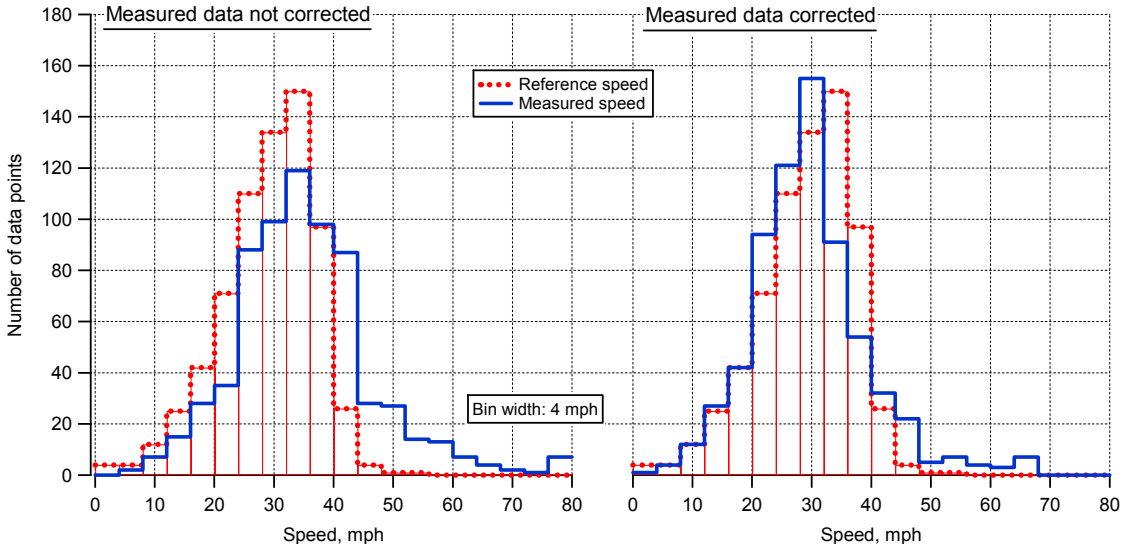

Magnetometer; site 1 Huron Pkwy; correlation, Y signal

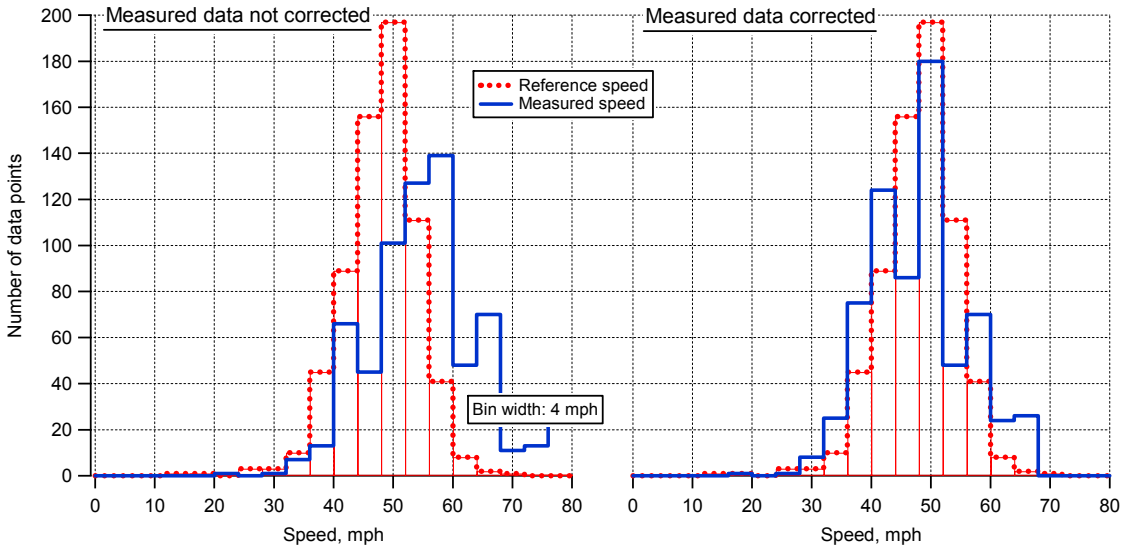

Magnetometer; site 2 Earhart Rd.; correlation, Y signal

Figure B6. Magnetometer Y signal corrected and non-corrected results vs. the reference speed

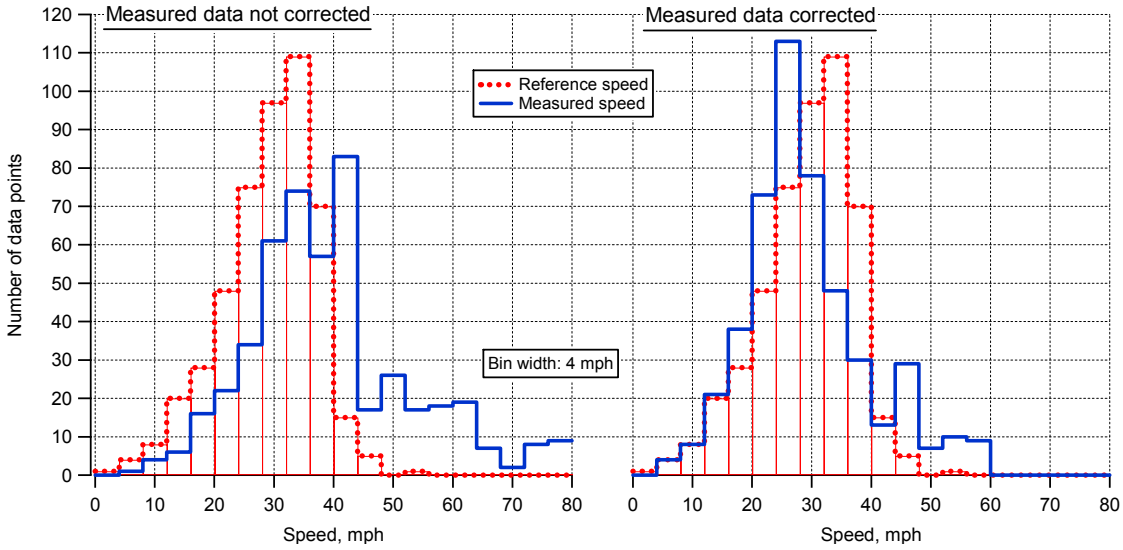

Magnetometer; site 1 Huron Pkwy; correlation, Z signal

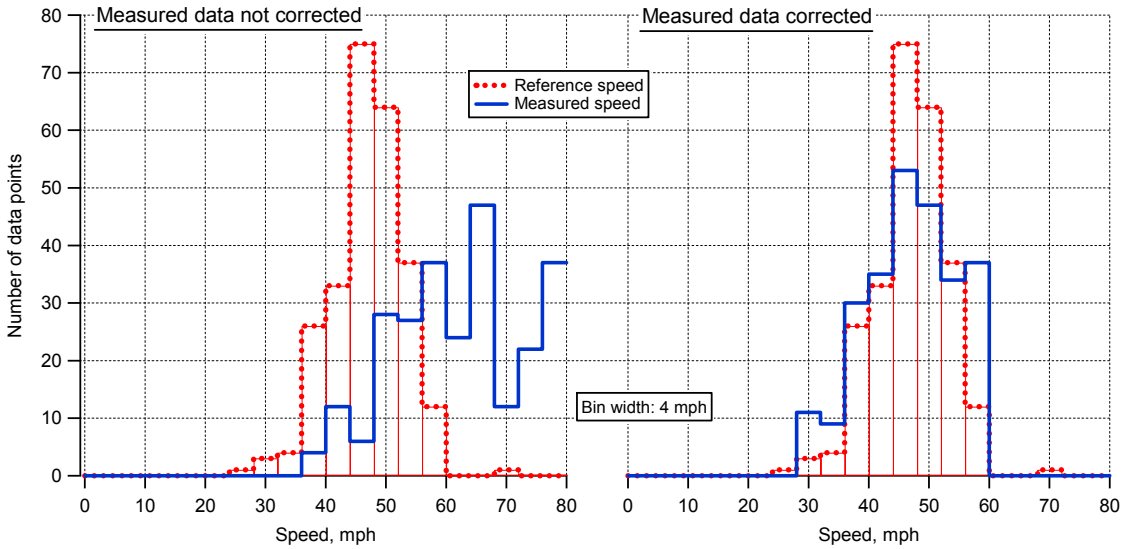

Magnetometer; site 2 Earhart Rd.; correlation, Z signal

Figure B7. Magnetometer Z signal corrected and non-corrected results vs. the reference speed

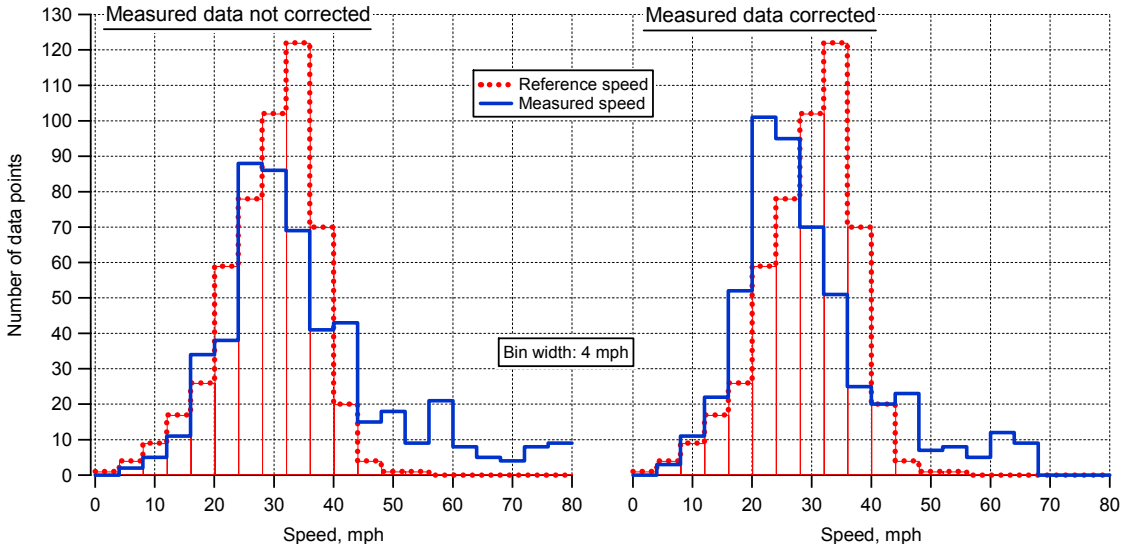

Magnetometer; site 1 Huron Pkwy; correlation, magnitude

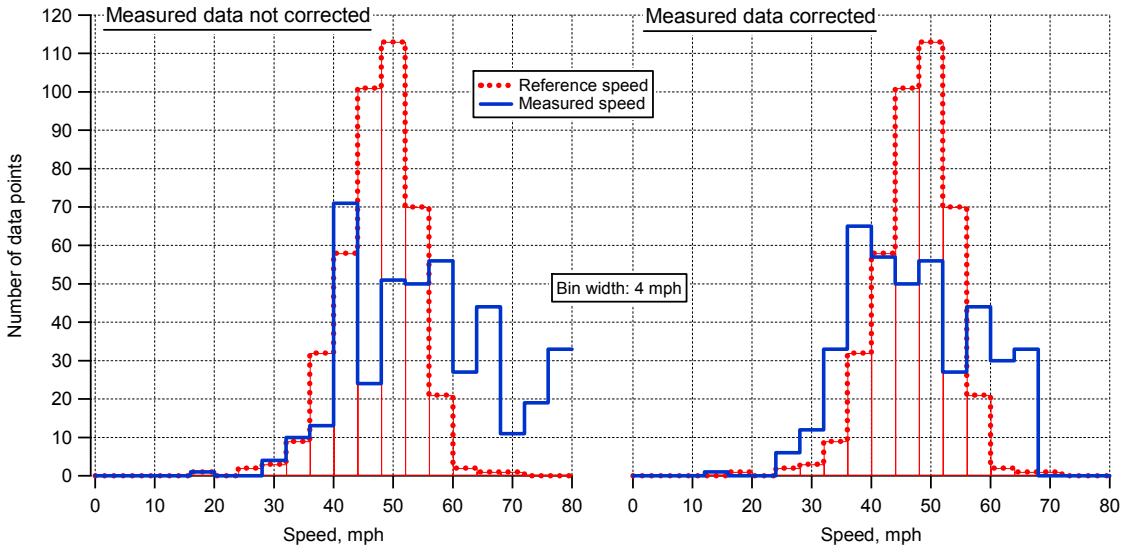

Magnetometer; site 2 Earhart Rd.; correlation, magnitude

Figure B8. Magnetometer magnitude signal corrected and non-corrected results vs. the reference speed